

Review Article

A review on CO₂ mitigation in the Iron and Steel industry through Power to X processes



Manuel Bailera ^{a,*}, Pilar Lisboa ^b, Begoña Peña ^a, Luis M. Romeo ^a

^a Escuela de Ingeniería y Arquitectura, Universidad de Zaragoza, Campus Río Ebro, María de Luna 3, 50018, Zaragoza, Spain
^b Fundación Agencia Aragonesa para la Investigación y el Desarrollo (ARAID), Zaragoza, Spain

ARTICLE INFO

Keywords:

Power-to-gas
Energy storage
Carbon capture
Iron and Steel
CO₂

ABSTRACT

In this paper we present the first systematic review of Power to X processes applied to the iron and steel industry. These processes convert renewable electricity into valuable chemicals through an electrolysis stage that produces the final product or a necessary intermediate. We have classified them in five categories (Power to Iron, Power to Hydrogen, Power to Syngas, Power to Methane and Power to Methanol) to compare the results of the different studies published so far, gathering specific energy consumption, electrolysis power capacity, CO₂ emissions, and technology readiness level. We also present, for the first time, novel concepts that integrate oxy-fuel ironmaking and Power to Gas. Lastly, we round the review off with a summary of the most important research projects on the topic, including relevant data on the largest pilot facilities (2–6 MW).

1. Introduction

Global warming is already unequivocal and extensively endorsed by scientific community. As agreed at the United Nations Climate Change Conference in 2015, CO₂ atmospheric concentration must be kept below 450 ppm by the year 2100 in order to limit the global temperature increase below 2 °C (compared to pre-industrial levels) [1]. According to the International Energy Agency, such mitigation target relies on decarbonizing electricity generation and industry [2]. For this reason, the European policy framework for the period 2020–2030 promotes

increasing the share of renewable energy in the electricity sector to 45 % by 2030 (so far, a 30.8 % share has been reached [3]), while considers carbon capture as the only feasible option to reduce industrial emissions at the large scale needed [4]. Among carbon intensive industries, Iron and Steel is one of the biggest CO₂ emitters, accounting for the 7–9 % of the total CO₂ emissions worldwide [5]. Since iron and steelmaking processes are based on the reduction of iron ore, which is a process not directly electrifiable at large scale yet, and it is fed mainly by coal and other fossil fuels, significant amounts of CO₂ emissions are released to the atmosphere [6].

Abbreviations: ACCAR, Allis-Chalmers Controlled Atmosphere Reactor; AFT, Adiabatic flame temperature; AISI, American Iron and Steel Institute; ANR, Agence Nationale de la Recherche (French National Research Agency); ARA, Auxiliary reduction agent; ASCOPE, Acier sans CO₂ par électrolyse (Steel without CO₂ by electrolysis); BF, Blast furnace; BF-BOF, Blast furnace - basic oxygen furnace; BFG, Blast furnace gas; BOF, Basic oxygen furnace; BOFG, Basic oxygen furnace gas; CAPEX, Capital expenditure; CCU, Carbon capture and utilization; CFE, Carbon-free electricity; COG, Coke oven gas; CS, Crude steel; DR, Direct reduction / direct reduced; DRC, Direct Reduction Corporation process; DRI, Direct reduced iron; EAF, Electric arc furnace; EPC, Electric power consumption; EUM, European Union electricity mix; FOBF, Full oxygen blast furnace; FP6, Sixth framework programme; GHG, Greenhouse gas; GHSV, Gas hourly space velocity; HBI, Hot briquetted iron; HDRI, Direct reduction of iron by hydrogen; HDRI-BF, Direct reduction of iron by hydrogen followed by a blast furnace; HDRI-EAF, Direct reduction of iron by hydrogen followed by an electric arc furnace; HM, Hot metal; HTGR, High-temperature gas-cooled nuclear reactor; IERO, Iron production by electrochemical reduction of its oxide for high CO₂ mitigation; IR, Indirect reduction; LHV, Lower heating value; LS, Liquid steel; MIT, Massachusetts Institute of Technology; Mit; CO₂, Mitigated CO₂; MOE, Molten oxide electrolysis; NG, Natural gas; NG-DRI-EAF, Natural gas based direct reduced iron in electric arc furnace; NGSR, Natural gas steam reforming; OHF, Open hearth furnace; OPEX, Operational expenditures; PC, Pulverized coal; PEM, Polymer electrolyte membrane / proton exchange membrane; PMDR, Point of minimum direct reduction; PSA, Pressure swing adsorption; PSR, Partial Smelting Reduction; PtG, Power to Gas; PtH₂, Power to Hydrogen; PtX, Power to X; P2G, Power to Gas; RA, Reducing agent; RFCS, Research Fund for Coal and Steel; RWGS, Reverse water-gas shift; Scrap-EAF, Electric arc furnace supplied with scrap; SEC, Specific energy consumption; SF, Shaft furnace; SNG, Synthetic natural gas; SOEC, Solid oxide electrolyzer cell; TGRBF, Top gas recycling blast furnace; TGR-OBF, Top gas recycling oxygen blast furnace; TRL, Technology Readiness Level; ULCOLYSIS, High-temperature molten oxide electrolysis steel-making; ULCOS, Ultra-Low CO₂ steelmaking; ULCOWIN, Low-temperature electrowinning for steelmaking; VPSA, Vacuum pressure swing adsorption.

* Corresponding author.

E-mail addresses: mbailera@unizar.es (M. Bailera), pilarlm@unizar.es (P. Lisboa).

<https://doi.org/10.1016/j.jcou.2021.101456>

Received 3 November 2020; Received in revised form 8 January 2021; Accepted 18 January 2021

Available online 16 February 2021

2212-9820/© 2021 The Authors. Published by Elsevier Ltd. This is an open access article under the CC BY-NC-ND license

(<http://creativecommons.org/licenses/by-nc-nd/4.0/>).

In the Iron and Steel industry, the majority of the research to mitigate CO₂ emissions focuses on applying post combustion capture to the blast furnace (i.e., applying mature carbon capture to the largest emitting source of the plant) [7]. One of the best options within this topic is to combine vacuum pressure swing adsorption (VPSA) with top gas recycling oxygen blast furnace (TGR-OBF). In the TGR-OBF process, the remaining flue from top gas after carbon capture is recycled into the blast furnace, and oxygen is used instead of air during combustion [8]. The recycled gas, which has a high CO content, can act as a reducing agent in the furnace thus allowing to slightly reduce the necessity of coke input, while the oxy-fuel combustion leads to higher CO₂ concentrations in the top gas. Under this configuration, CO₂ emissions can be reduced between 56 % and 84 % with respect to conventional blast furnaces [8,9], with a capture cost in the range 39–58 €/tCO₂ [8,10]. Another potential option is to apply post combustion amine capture to the flue gas resulting from burning the blast furnace top gas in a power plant, what leads to 50–75 % emission reduction in the steel plant [11] at a cost of 84–114 €/tCO₂ [12]. However, from the perspective of business, carbon capture is just an additional process that increases consumption about 1.9 MJ kg of hot rolled coil [13] without providing any economic income. For this reason, companies prefer to pay for carbon allowances, which are currently cheaper than capture costs, at 25 €/tCO₂ in the carbon emission trading [14].

Aiming for solutions that substantially reduce CO₂ emissions while providing additional benefits, Power to X (PtX) stands out as a promising candidate. The Power to X concept includes all those processes that converts renewable electricity into valuable products, using an electrolysis stage to obtain either the final product or an intermediate product [15]. The technology is already mature within the field of energy storage [16], and its application to different industries, such as pulp industry [17] and chemical plants [18], has been evaluated lately showing profitable scenarios. In the case of the Iron and Steel industry, it can be performed electrolysis of iron oxides to directly dissociate the O₂ and Fe (Power to Iron), electrolysis of the emitted CO₂ to obtain syngas (Power to Syngas) or electrolysis of water to produce H₂ (Power to Hydrogen). Moreover, both the syngas and the hydrogen can be used in a methanation process to obtain methane (Power to Methane), and the three of them are useful as reducing agents in the blast furnace to diminish the coke consumption (Fig. 1). Additionally, the hydrogen can be used in a methanol synthesis process to consume the top gas emitted by the blast furnace.

The key of applying Power to X to the Iron and Steel industry is that, whatever the route used, there is always a benefit accompanying the additional energy consumption, contrarily to what happens in the case

of conventional carbon capture. In most cases, the benefit is the reduction of fuel input, which is actually substituted by renewable energy either directly (as in Power to Steel and Power to Hydrogen) or indirectly through a carbon closed loop (as in Power to Syngas and Power to Methane). The other potential benefit is the production of valuable products for sale, as in Power to Methanol.

To the best of authors knowledge, this concept has not been properly contextualized nor reviewed in literature. Therefore, the objective of this paper is to review those studies related to the utilization of Power to X routes within the Iron and Steel Industry (other reviews addressed low carbon ironmaking without deepening in the PtX routes [19,20]). The relevance lies in presenting a global picture that helps identifying synergies between the different routes, and establishing a clear classification for future research. Besides, research groups may notice other groups with common objectives, thus promoting potential collaborations. The review follows a systematic approach, limited to studies presented in scientific journals and conferences. Additionally, the most important research projects that started within the last five years are described. The paper also includes the proposal of novel integrations of Power to X processes with oxy-fuel processes, not found in literature, for the Iron and Steel industry.

2. Methodology of systematic review

A systematic methodology was followed to find the most relevant literature to the topic. First, Web of Science was selected as the search engine for this review because of its advanced search capabilities and wide range of databases. Then, several databases were selected to establish the scope of the search (see Appendix A). A set of 18 searches were performed, returning a total of 485 entries (Table 1). Each search combined a term related to the Iron and Steel process and another term concerning Power to X concept, appearing in the title or the abstract. The hits returned from the search were screened by reading the abstract, and selected for reviewing when some of the following criteria was fulfilled:

- Appeared to apply Power to X processes directly on the Iron and Steel industry.
- Appeared to relate Power to X processes indirectly to the Iron and Steel industry.
- Appeared to contain information on CCU processes related to the Iron and Steel industry, which might be reinterpreted as Power to X concepts or used to contextualize the utilization of carbon dioxide in the Iron and Steel industry.

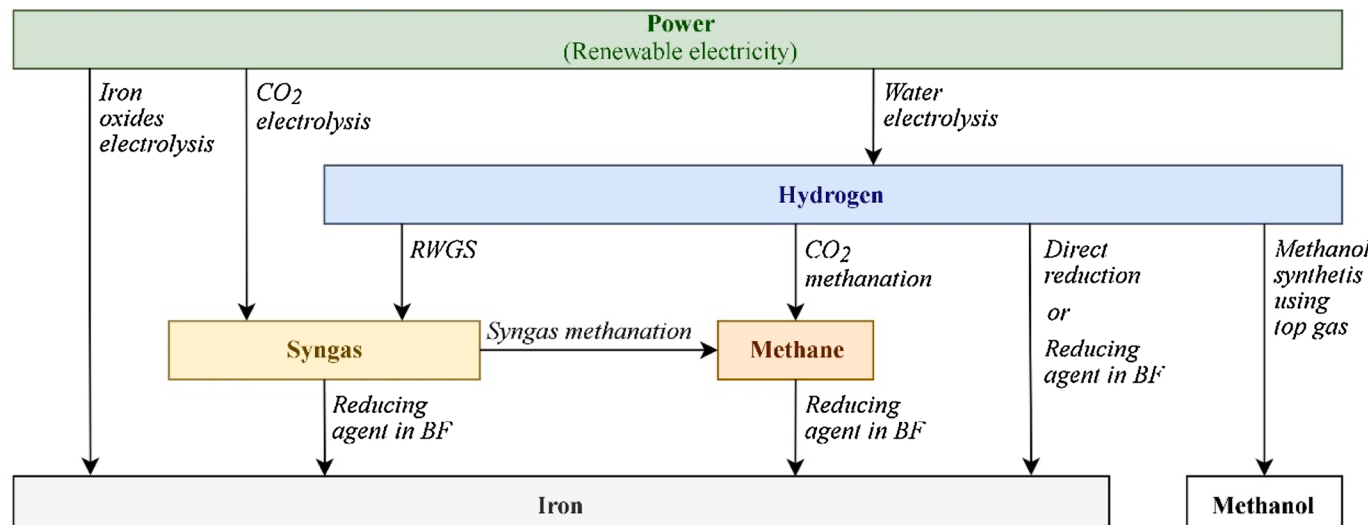


Fig. 1. Power to X routes in the Iron and Steel industry.

Table 1

Search terms, number of hits returned and number of papers reviewed.

nº	Search term	Hits	Reviewed
1	("Iron plant" OR "Iron industry" OR "Ironworks" OR "Ironmaking" OR "Iron production" OR "Iron refining") AND ("Power to Gas" OR "Power to X" OR "PtG" OR "P2G" OR "PtX" OR "electrolysis")	27	17
2	("Steel plant" OR "Steel industry" OR "Steelworks" OR "Steelmaking" OR "Steel production" OR "Steel refining") AND ("Power to Gas" OR "Power to X" OR "PtG" OR "P2G" OR "PtX" OR "electrolysis")	51	10
3	("Blast furnace" OR "Basic oxygen furnace") AND ("Power to Gas" OR "Power to X" OR "PtG" OR "P2G" OR "PtX" OR "electrolysis")	32	4
4	("Electric arc furnace" OR "Steel scrap") AND ("Power to Gas" OR "Power to X" OR "PtG" OR "P2G" OR "PtX" OR "electrolysis")	10	0
5	("Smelting" OR "Foundry") AND ("Power to Gas" OR "Power to X" OR "PtG" OR "P2G" OR "PtX" OR "electrolysis")	107	0
6	("Direct iron reduction" OR "Direct reduced iron" OR "Sponge iron") AND ("Power to Gas" OR "Power to X" OR "PtG" OR "P2G" OR "PtX" OR "electrolysis")	7	1
7	("Iron plant" OR "Iron industry" OR "Ironworks" OR "Ironmaking" OR "Iron production" OR "Iron refining") AND ("Methanation" OR "synthetic methane" OR "synthetic natural gas" OR "SNG" OR "Methanol" OR "syngas")	24	2
8	("Steel plant" OR "Steel industry" OR "Steelworks" OR "Steelmaking" OR "Steel production" OR "Steel refining") AND ("Methanation" OR "synthetic methane" OR "synthetic natural gas" OR "SNG" OR "Methanol" OR "syngas")	68	13
9	("Blast furnace" OR "Basic oxygen furnace") AND ("Methanation" OR "synthetic methane" OR "synthetic natural gas" OR "SNG" OR "Methanol" OR "syngas")	84	7
10	("Electric arc furnace" OR "Steel scrap") AND ("Methanation" OR "synthetic methane" OR "synthetic natural gas" OR "SNG" OR "Methanol" OR "syngas")	6	0
11	("Smelting" OR "Foundry") AND ("Methanation" OR "synthetic methane" OR "synthetic natural gas" OR "SNG" OR "Methanol" OR "syngas")	14	0
12	("Direct iron reduction" OR "Direct reduced iron" OR "Sponge iron") AND ("Methanation" OR "synthetic methane" OR "synthetic natural gas" OR "SNG" OR "Methanol" OR "syngas")	16	1
13	("Iron plant" OR "Iron industry" OR "Ironworks" OR "Ironmaking" OR "Iron production" OR "Iron refining") AND ("Carbon capture and utilization" OR "CCU" OR "Carbon recycling")	13	5
14	("Steel plant" OR "Steel industry" OR "Steelworks" OR "Steelmaking" OR "Steel production" OR "Steel refining") AND ("Carbon capture and utilization" OR "CCU" OR "Carbon recycling")	14	3
15	("Blast furnace" OR "Basic oxygen furnace") AND ("Carbon capture and utilization" OR "CCU" OR "Carbon recycling")	10	0
16	("Electric arc furnace" OR "Steel scrap") AND ("Carbon capture and utilization" OR "CCU" OR "Carbon recycling")	0	0
17	("Smelting" OR "Foundry") AND ("Carbon capture and utilization" OR "CCU" OR "Carbon recycling")	2	0
18	("Direct iron reduction" OR "Direct reduced iron" OR "Sponge iron") AND ("Carbon capture and utilization" OR "CCU" OR "Carbon recycling")	0	0
	Total	485	63

A total of 63 research articles were reviewed and classified in five different topics according to the type of Power to X process involved. The topics correspond to the subsections of Section 4 in this manuscript.

3. Current Iron & Steel production

The total production of crude steel achieved 1869 Mt in 2019 including carbon steel, stainless steel and other alloys [21]. The metallic inputs of steelmaking are around 70 % iron ore (primary production) and 30 % recycled steel scrap (secondary production). The related global final energy consumption accounted for 845 Mtoe in 2019, equivalent to 20 % of industrial energy need and 8 % of total final energy use. In terms of energy resources, it accounted for the 15 % of global coal demand, 2.5 % of global natural gas demand and 5.5 % of global electricity demand [21]. Consequently, the steel sector is responsible for 2.6 Gt of direct CO₂ emissions and 1.1 Gt of indirect CO₂ emissions [21], representing the 7–9 % of the total global CO₂ emissions [5].

Currently, the main steel manufacturing routes are the blast furnace in combination with basic oxygen furnaces (BF-BOF) and the electric arc furnace route (EAF). The EAF plants use scrap or direct reduced iron (DRI), mainly produced with natural gas (NG). Other steelmaking processes, which contribute in a minor share to the total amount of produced steel, include the open hearth furnaces (OHF) and others such as direct reduction of iron or smelting reduction. The Table 2 summarizes the figures of net energy consumptions and specific carbon emissions per crude steel (CS) for the three main production routes, including agglomeration & coke production, ironmaking & steelmaking, and casting. Indirect emissions are related to electricity and imported heat generation. In average, this industrial sector has an energy intensity of

19.8 GJ/t [22].

The OHF process is highly energy intensive which also use hot metal from BFs as the main material. Given its environmental and economic limitations, the OHF process only contributes to the global production in about 0.3 % and its application is in clear decline [21]. Hence, in the following subsections, the basic oxygen furnace technology and the electric arc furnace are described to settle the basis of the reference situation defined by these conventional steel manufacturing routes.

3.1. Blast furnace-basic oxygen furnace route

The most spread manufacturing route for crude iron is the reduction of iron ores with coke in a blast furnace at temperatures beyond 2000 °C. This process which directly generates liquid metal through a carbo-thermic reduction is highly carbon-intense; up to 2000 kgCO₂/t_{pig} iron are reported [23,24]. Initially, the iron ore is pretreated in a pellet or sinter plant where limestone and dolomite are added to the mixture that is known as the burden. The burden, which contains Fe₂O₃ and Fe₃O₄ together with the additives, is fed into the blast furnace where the iron is reduced and melted. The typical reduction agents used to separate the iron and the oxygen are coke and pulverized coal (PC). The burden and coke are introduced through the upper part of the blast furnace while pulverized coal and oxygen enriched air are fed in counterbalance through the bottom. The reduction of iron ore (Fe₂O₃) to pig iron, directly with coke (Eq. 1) produces CO₂ emissions related to the reaction. The specific emissions related to the reduction reaction of iron are typically 588 kgCO₂/t_{pig} iron [25]. The reducing agents also react with the oxygen to produce carbon monoxide which is later converted to carbon dioxide after reducing the iron ore to metal iron (Eq. 2).

Table 2

Conventional technologies in steel manufacturing plants (data for 2019) [21].

Production route	Share of total production	Net energy consumption (GJ/t _{CS})	Direct CO ₂ emissions (kgCO ₂ /t _{CS})	Indirect CO ₂ emissions (kgCO ₂ /t _{CS})
BF-BOF	72 %	21–23	1200	1000
NG-DRI-EAF	28 %	17–22	1000	400
Scrap-EAF		2.1–5.2	40	300



The gas leaves the blast furnace through the upper side, while the molten metal and slag are discharged through the bottom. The pressurized gas (1.2–3.5 bar) from the blast furnace is expanded in a gas turbine to produce electrical power. The flue gas stream from the turbine is split; a small fraction is used to preheat the input air to the blast furnace, but the main fraction is integrated into other processes of the steelmaking process. The gross energy demand of a blast furnace is strongly reduced after integration of the BF gas (4.719 GJ/t_{pig iron}) and the net energy demand in this equipment represents near a 70 % of the gross energy demand. The net energy figure, presented in Table 2, includes the power demand of the air unit separation for the oxygen provision. However, coke and burden production represent additional processes whose energy consumption should be further accounted.

This manufacturing process is highly carbon intensive; its CO₂ emissions comes from the combustion of a share of the blast furnace gas (90 % of CO₂ emissions) for preheating the air and from the electrical demand of the air separation unit that supply the required O₂ (10 % carbon emissions). When the CO₂ content of the exported blast furnace gas (21 %vol) is accounted as emissions of the manufacturing process, the specific carbon emissions of this production route achieve average values of 1099 kgCO₂/t_{pig iron} [25].

3.2. Electric arc furnace routes

Over the 28 % of carbon and alloy steels in the world is produced via the electric arc furnace routes recycling ferrous scrap as main raw material and using electricity as primary source of energy. Depending on the availability of steel scrap and the plant configuration, other sources of metallic, such as direct reduced iron or hot metal, can be used in the EAF route.

Direct reduction (DR) processes produce different types of reduced solid iron, such as sponge iron (DRI) or hot briquetted iron (HBI). The annual production is less than a hundred of million tons (86 Mt in 2017 [26]), but it is an attractive option to reduce CO₂ intensity with promising prospective [21]. More than 80 % of the direct reduced iron is produced in vertical countercurrent shaft furnaces, which uses syngas from natural gas reforming as reducing agent. Two commercial technologies dominate the current market: Midrex process (65 %) and Energiron process (17 %) [26]. Pellets and lump ore are fed from the top of the shaft furnace and descend by gravity, while the reducing agent flows upwards. Three main sections are distinguished: reduction zone in the upper part where reduction takes place at temperatures above 900 °C, a cooling section in the lower part where the solid product is cooled down up to 50 °C before being discharged, and a transition zone between them to isolate both sections from each other [26,27]. The Midrex process uses an external natural gas reformer, while Energiron uses in-situ natural gas reforming and CO₂ capture in the flue gases [28]. The remaining 18 % of direct reduced iron is produced through coal-based reducing agents in rotary kilns (ACCAR, DRC and Krupp Rein processes) or rotary hearth furnaces (Fastmet process) [29].

The scrap and DR iron are loaded in the cylindrical refractory lined electric arc furnace. The melting begins when electrical energy is supplied to the carbon electrodes. Oxy-fuel burners (fed by natural gas) and oxygen lances may also be used to supply chemical energy [30]. As the hot waste gases leave the EAF, combustion air is introduced to the pipe to convert the existing CO into CO₂ (post-combustion CO control). Emissions of CO₂ are also generated in the oxy-fuel burners. These burners raise the capacity of the furnace by increasing the speed of the melting process and reducing the consumption of electricity and electrode material. These burners are often designed to minimize NO_x emissions operating the burners below their nominal combustion efficiency. This practice increases CO emissions to some extent but also

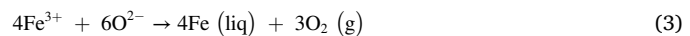
lowers carbon emissions [30]. Downstream processes, such as casting, reheating and rolling, are similar to those in the BF–BOF route.

4. Power to Iron

Direct iron production at molten metal state from iron oxides by the sole application of electrical energy, so called power to iron technology, could represent a potential route to decarbonize steel industry in the long-term [31]. However, it must be highlighted the current limited practical application of Power to Iron technology. Its embryonic research level makes it not realistic beyond TRL 3-4.

Crude iron is traditionally manufactured through carbo-thermic reduction in a blast furnace (section 3.1). Since this energy intensive technique produces large carbon and Sulphur dioxide emissions and undesired byproducts, a cleaner alternative for fast iron production might be the electrolysis of iron ore in aqueous, molten salts or oxide based electrolytes [32]. Molten salts or oxide based electrolytes are mainly used in high temperature electrolyte cells; while aqueous electrolytes are found in low temperature electrolyte cells.

The electrolysis produces liquid metal, through the reduction of iron oxide dissolved in the solvent melt which has been adequately designed according to Eq. 3 [33].



The oxidation reaction to compensate iron reduction in molten oxide electrolysis is the generation of oxygen in the inert anode. Although this redox reaction is chemically simple, it is hard to implement given the multiple valence states of iron and the required operating temperature above the iron melting point [34]. The first constraint leads to a low faradaic yield and the second one requires highly demanding properties for the cell materials. Hence, Power to Iron is still in its infancy and further technological development must be done to address issues such as anode material development, electrolyte properties improvement or optimized electrolysis conditions for both high temperature molten cell electrolytes and low temperature alkaline cell electrolytes.

4.1. Challenges for the development of Power to Iron electrolyte cells

4.1.1. High temperature molten electrolyte cells

The challenges for iron production by means of Power to Iron related to the demanding properties of the cell materials are (i) the operating temperature of the cell over 1538 °C, (ii) the corrosion of most metals in such operating conditions under anodic polarization and (iii) the spontaneous reduction of iron oxides in contact with refractory metals and carbon [35].

Power to Iron in molten oxide electrolyte has been demonstrated using consumable (graphite for use with ferro-alloys and titanium) or unaffordable (iridium or platinum for use with iron) anode materials [35]. The Power to Iron process requires an anode material that resists depletion while sustaining oxygen evolution. The development of the inert anode is quite complex due to the ultrahigh temperatures, the high solubilizing power of a multicomponent oxide melt and the evolution of pure oxygen gas at atmospheric pressure [36].

The suitability of iridium as anode material in Power to Iron cells operated in alkaline cell electrolytes was assessed by Kim et al. [36]. Beside its unaffordable cost, iridium appeared to be an unsuitable candidate material as oxygen-evolving anode for alkaline electrolytic iron deposition. Promising results on improved anode material which could make feasible large-scale molten oxide electrolysis for the production of steel were obtained by Allanore et al. [35]. They found an anode material containing chromium-based alloys which exhibit limited consumption during iron extraction and oxygen evolution. These findings lead to a principal consequence, the successful extraction of iron using an affordable alloy-based anode material at lab-scale.

The design of an effective Power to Iron process requires a good

understanding of the electrochemical properties of iron ions in molten salt and oxide electrolytes [37]. Judge et al. represented the conditions of frozen electrolyte sidewall and molten oxide electrolyte in the electrolysis cell for two high temperature isotherms (1200 and 1600 °C). These results provide information to improve the design of the electrolyte to maximize current efficiency [33]. Several studies address thermodynamic considerations to find adequate solutions for Power to Iron limitations related to high temperature and low faradic yield. Their main objectives were to prove the faradic reduction of iron at high temperatures, to find proper electrolyte and electrode materials and to determine the electrode kinetics and the reaction mechanism of iron production identifying the electrochemical processes at each electrode [32,34].

Wiencke et al. implemented the redox reaction of Power to Iron at steady state in a small lab-scale facility. An electrolyte composed of molten oxides (SiO₂ 66 %w, Al₂O₃ 20 %w, MgO 14 %w) where Fe₃O₄ dissolved as source of iron was derived from thermodynamic considerations and used in the experimentation. They obtained liquid iron at liquid state only applying an electrical voltage over the minimum thermodynamic requirement. The faradaic character of the cathodic reaction was checked by following the accompanying anodic oxygen gas evolution [34].

Also focused on the characterization of iron ions and iron reduction at temperatures above 1400 °C, Kvalheim et al. performed lab-scale experiments in molten oxide electrolyte (SiO₂ 50 %w, MgO 20 %w, Al₂O₃ 20 %w and CaO 10 %w) where Fe₂O₃ dissolved as source of iron (0.1–10 %w). Platinum was used as the anode material due to oxygen evolving anode at such high temperatures. However, this unaffordable material must be substituted by the development of an inexpensive inert anode for oxygen evolution. Iron was successfully extracted through deposition in molybdenum cathode at very low current efficiency at 1510 °C [32].

Gao et al. constructed an integrated three-electrode cell with an assembly of magnesia-stabilized zirconia | Pt | O₂ tube, acting as the container of the molten slag, as reference electrode and also counter electrode. Their findings confirm that zirconia-based solid electrolytes can play an important role in electrochemical research in high temperature molten oxide electrolytes [37].

In 2010, Licht and Wang explored lithium carbonate as electrolyte and reported a great change of the free energy and solubility product of Fe₂O₃ at elevated temperatures, opening a new carbon free route to iron production [38]. The resulting process could produce iron metal in molten media at high rate and low electrolysis energy which could be provided by conventional as well as renewable energy sources [39]. The most common impurities found in iron ores, silicate and aluminate, were found to be also soluble in molten lithium carbonate and do not adversely affect the electrolytic iron deposition [40]. Once the process was proven, Li et al. modified the electrolytic iron deposition conditions in molten lithium carbonate to control the particle size of the product and to reduce the amount of electrolyte extracted with the final product. Pure iron metal was formed at high current efficiency, and the

electrolysis potential observed diminished with (i) a decreasing current density, (ii) the addition of lithium oxide, (iii) an increase of anode surface, and (iv) an increasing temperature [41].

A summary of the most representative operating conditions of the different Power to Iron processes is presented in Table 3. It includes the material of the electrolyte and electrodes, source of iron, temperature, voltage and current/current density.

4.1.2. Low temperature alkaline electrolyte cells

A novel and more environmentally friendly electrochemical reduction of iron compounds for iron metal deposition occurs at a low temperature of 110 °C in alkaline solution. Feynerol et al. compared the reactivity of hematite, magnetite and goethite suspensions during their reduction into iron through electrolysis using a laboratory cell alkaline electrolyte model [31].

Wang et al. successfully designed, constructed and operated an electrical-ionic conductive colloidal electrode containing the active iron compound (Fe₂O₃ particles), the liquid electrolyte (NaOH solution), and a percolating electrical conductor (carbon) to generate iron metal [24]. The simultaneous percolation of electrons and ions effectively increased the current collector surface and enables the process to work at higher rates. A uniformly dispersed colloid of hematite with high ionic conductivity and electronic conductivity was the source of iron in their experiments. To enhance the faradaic efficiency and energy efficiency in the electrolysis, a titanium plate with low catalytic activity toward H₂, was used as cathode current collector, and platinum foil, with high catalytic activity toward O₂, was selected as anode. The experimental results confirmed the complete reduction of hematite to iron metal and Fe₃O₄.

In view to design large scale iron production by electrolytic reduction of hematite particles suspended in a strong alkaline medium, the performance of various cell configurations was investigated by Allanore et al. [42]. The horizontal parallel plates configuration is the most promising one with energy consumption below 10.8 GJ t_{Fe}⁻¹. After correction to account for the cost of iron ore preprocessing (grinding and melting), the total energy requirement rises up to 13.0 GJ t_{Fe}⁻¹. This value is potentially lower than current most efficient iron production routes based on the blast furnace [22].

4.2. Potential integration of the Power to Iron process

Parkinson et al. [43] proposed the coupling of iron ore reduction with the partial oxidation of light hydrocarbons to produce iron and organic chemicals. First, the iron oxides react with hydrogen chloride and the resulting iron chlorides are then reduced to the iron metal product by electrolysis. The oxidized iron chlorides are also used for reaction with methane to produce the methyl-chloride intermediates which are eventually converted to hydrocarbons (Fig. 2). The process integration potentially removes major costs for both conventional processes, improving overall efficiency and process profitability. The application of a liquid metal halide (FeCl₃) as oxidizing agent instead of

Table 3

Representative operating conditions of the different Power to Iron processes reviewed.

Type	Electrolyte	Electrodes	Fe source	T (°C)	V (V)	I (A or A/cm ²)	Ref.
Molten oxide	Al ₂ O ₃ 47%w, MgO 6%w, CaO 47%w	Cr _{1-x} Fe _x	Fe ₃ O ₄	1565	3.8	2 A/cm ²	[35]
Molten oxide	Al ₂ O ₃ 20%w, MgO 14%w SiO ₂ 66%w	Pt _{1-x} Rh _x	Fe ₃ O ₄	1550	3.0	0.08 A	[34]
Molten oxide	Al ₂ O ₃ 20%w, MgO 16%w, SiO ₂ 46%w, CaO 18%w	Mo / Ir	Fe ₂ O ₃	1550	4	3.5 A	[36]
Molten oxide	Al ₂ O ₃ 20%w, MgO 20%w, SiO ₂ 50%w, CaO 10%w	Pt _{1-x} Rh _x / Mo	Fe ₂ O ₃	1510	8 – 12	0.05 A	[32]
Molten oxide	Al ₂ O ₃ 9%w, MgO 16%w, SiO ₂ 47%w, CaO 28%w	Ir / Pt	FeO	1450	n/a	n/a	[37]
Molten oxide	Li ₂ CO ₃	Pt / Ni / Fe	Fe ₂ O ₃	800	1.7	0.05 A	[38]
Molten oxide	Li ₂ CO ₃	Fe / Ni	Fe ₂ O ₃	950	0.7	0.5 A/cm ²	[39]
Molten oxide	Li ₂ CO ₃ 91.7%w, Li ₂ O 8.3%w	Fe / Ni	Fe ₂ O ₃	730	1.2 – 3.1	0.1 – 5.0 A	[41]
Alkaline	NaOH solution	Graphite / Ni	α-Fe ₂ O ₃	110	1.7	0.11 A/cm ²	[31]
Alkaline	45 %w NaOH solution	Ti / Pt	Fe ₂ O ₃	110	1.7	0.02 A/cm ²	[24]
Alkaline	50 %w NaOH solution	Graphite / Ni	Fe ₂ O ₃	110	1.24	0.1 A/cm ²	[42]

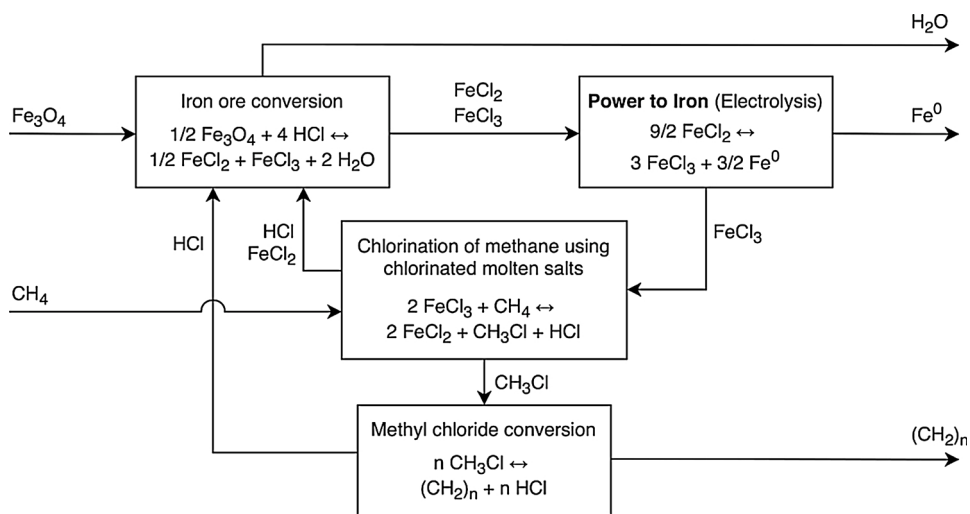


Fig. 2. Conceptual diagram of the integration of Power to Iron with hydrocarbon production, proposed by Parkinson et al. [43].

using a pure halogen allows for an advantageous management of the exothermic heat load. Furthermore, leaching iron ore with the inorganic acid (HCl) generated as a by-product creates a higher value iron feedstock to an electrolyser. Finally, the regeneration of the iron chloride through the electrolytic reduction to iron eliminates the great cost of halogen regeneration.

The carbon-free production of iron through upgrading the iron oxide ore for electrolysis using a by-product of hydrocarbon partial oxidation can reduce environmental effects of conventional manufacturing processes and minimize the economic impacts of carbon prices. The economic feasibility of the integrated process is highly dependent on the availability of affordable hydrocarbons and electricity. The demonstration of technical feasibility and improvement of economic estimations are still needed to ensure the deployment of this process. The open research lines include investigations on the rate of chlorination of ferric chloride-sodium chloride eutectic molten salt mixtures; analysis of the impact of iron ore impurities on overall reaction products and rate of iron ore reduction; and increase of the purity of reduced iron under system conditions.

4.3. Techno-economic analysis and technological maturity

Two of the main worldwide programmes focused on carbon reduction in steelmaking industry include Power to Iron among the breakthrough technologies for the future of iron and steel industry: the European Ultra Low CO₂ Steelmaking (ULCOS) programme in Europe and the American Iron and Steel Institute (AISI) CO₂ Breakthrough Program in the United States. The forth leg of ULCOS Programme relates to the development of Power to Iron technology (ULCOWIN and ULCOLYSIS) and has been granted through the following programmes: FP6 ULCOS, RFCS IERO, ANR ASCOPE and Autothermal Cell. The main advantages of Power to Iron compared to conventional technologies is that probably no carbon will be needed in the production process. Although no major drawbacks have been pointed out so far, the embryonic phase of development makes quite improbable its practical implementation in the mid-term. According to the AISI CO₂ Breakthrough Program, one of the two innovative technologies identified to cut carbon emissions in iron and steel production is the high temperature molten oxide electrolysis (MOE) which has been examined at Massachusetts Institute of Technology (MIT). The concept was validated at lab-scale in 2011 with sound electrochemical mechanism, suitable anode electrode material and potentially feasible economics. The prediction on the technological maturity foresees a pilot phase demonstrator of Power to Iron by 2030 although no larger scale demonstration

facilities have been presented so far [6].

Fischbeck et al. [44] assessed the techno-economic aspects of some innovative steel production technologies under three energy scenarios for different development of future assumptions. Among these technologies, direct reduction of iron ore through electrolysis appeared as the most material and energy efficient route with very limited CO₂ emission; especially under a mainly renewable electricity system. Considering economic feasibility, direct iron ore electrolytic reduction showed a great potential to achieve economically viable carbon emission reduction along the next 50 years. This economic feasibility is mainly based on the foreseen increment of fossil fuel prices and the significant decrease in electricity cost, related to the expected higher shares of renewable energy sources in the energy system of the next decades. Under an ambitious renewable energy sources scenario, direct reduction of iron ore is predicted to outperform the coal based routes in the 2030–2040 period and will become a leader technology past 2050. However, under a most conservative energy scenario this technology appears not to be relevant before 2100 and higher CO₂ prices and lower CAPEX would be required. The conclusions of the study recommended (i) steel producers to invest into direct electrolysis of iron ore to reach industrial maturity by 2030–2040 and (ii) policy makers to provide a consistent and secure climate policy for industry.

A multi criteria analysis including numerous criteria from technology, society & politics, economics, safety, and ecology was developed by Weigel et al. to further assess these innovative technologies of iron production [45]. The criteria were valued based on quantitative or qualitative data from techno-economic models, literature review or expert judgement. In order to integrate the unique perspectives of different stakeholder groups, different sets of weighting factors were used in this study. Power to Iron, with slight economical disadvantages, was considered to present a high innovative potential that might enable this route to become suitable when the research period is over, if technical maturity is reached.

5. Power to H₂

Hydrogen is an energy carrier that can contribute to significantly reduce CO₂ emissions of iron and steel industries. According to the International Energy Agency, green hydrogen could reduce up to 2.3 GtCO₂e/y. Nevertheless, the actual amount of avoided GHG and the ‘green’ title will depend on the hydrogen generation process, as it could be produced from water electrolysis powered by renewable resources, but also from natural gas steam reforming and coal gasification. The use of hydrogen as reducing agent in ironmaking processes has been

Table 4
Hydrogen-based routes for ironmaking.

Production route	Technology	Related process	Previous studies
Direct reduction of iron ore	Fixed bed	Jaleel-Hyl	[46]
	Fluidized bed	Finmet / Circored	[25,44,45]
	Shaft furnace	Midrex / Energiron	[6,47,48,49]
	Flash furnace	FIT	[50]
	Rotary furnace	SL-RN / ACCAR/ Fastmet	
Direct injection into BF	Blast furnace		[51]

Table 5
Ironmaking plants based on hydrogen from natural gas reforming.

HDRI plant	Ironmaking process	Production (t _{DRI} /day)	Metallization (%)	Ref.
Outokumpu (Point Lisas, Trinidad)	Circored	1560	95	[52]
Hylsa (Monterrey, Mexico)	Energiron	36	94–96	[54]
Arcelormittal (Hamburg, Germany)	Midrex	n/a	n/a	[55]

investigated according to two main routes (Table 4): direct reduction of iron ore (full or partial use of hydrogen) and direct injection of hydrogen in a blast furnace. In the former case it is obtained direct reduced iron (DRI) in the form of sponge iron or hot briquetted iron (HBI), while in the latter it is obtained molten iron (crude iron) with higher carbon content.

So far, commercial status in hydrogen-based ironmaking has been reached only by plants that use fossil hydrogen (i.e., hydrogen from natural gas reforming). The first steelmaking unit was commissioned in 1999 in Trinidad, based on the direct reduction of iron ore by hydrogen (HDRI) using the Circored process, with a production of 65 t_{HBI}/h and 95 % metallization rate (Table 5) [52]. Because of the fluidized bed problems and the lower production rate than the expected, this plant was shut down in 2001 [53]. The second facility is the Hylsa demonstration plant of the commercial supplier Energiron with a production rate of 1.5 t_{DRI}/h and metallization of 94–96% [54]. Also, Arcelormittal recently commissioned Midrex to design a demonstration plant for hydrogen-based steel production in Hamburg [55,56]. In this case, the hydrogen production could turn green in the future since Arcelormittal participates in the project ‘Gigawatt Electrolysis plant’, which aims to develop a 1 GW electrolyzer in Zeeland (Netherlands) [57].

In the recent years, hydrogen routes have attracted much attention from the steelmakers in Europe and USA, promoted by R&D programmes and policies against Climate Change and the expansion of renewable energies in the power sector. A significant number of research projects involving steelmakers aims to develop hydrogen-based technologies using renewable electricity, through the well-known water electrolysis, for free-carbon iron and steelmaking (see section 10). In the following subsections, the status of water electrolysis technology is briefly summarized, and the studies found in literature about PtH₂-based concepts for ironmaking and steelmaking are reviewed.

5.1. Water electrolysis status

Power to H₂ concept stores electricity in the form of chemical energy

by means of oxidation-reduction reactions in an electrolyzer. The most mature technologies are: Alkaline, PEM and SOEC (solid oxide electrolyzer cell) [58]. Alkaline electrolyzers reach efficiencies of 62–71 % (LHV basis) under operating conditions of 1–60 bar and 40–90 °C. Load may be varied from 20 to 150 % nominal value, as overload is possible. The largest projected capacity so far is 610 MW to be started in 2022, although the current typical capacities are of several megawatts. For PEM electrolyzers, efficiencies range from 58 to 68 % (LHV basis), while typical operating temperatures and pressures are 20–100 °C and 1–100 bar, respectively. In spite of higher economic costs, PEM technology is attracting the interest in the context of steelmaking because the lower minimum load (5%) and shorter start-up times, which increase flexibility. Current capacities are around megawatt; however, Air Liquid and H-TEC System plan to reach 10 and 20 MW, respectively. SOEC technology is still under research. Higher efficiencies (76–86 %) can be reached if heat integration is considered. Operating conditions are 1–20 bar and 600–1000 °C, while load can be varied from 50 to 120 %. Maximum current capacities are of 150 kW (Sunfire). Further details can be found in [58].

5.2. Hydrogen injection in blast furnaces

The indirect reduction of iron ore in blast furnaces involves the intermediate reactions of carbon monoxide and hydrogen gathered in Table 6. The global reaction for CO is exothermic while is endothermic for H₂. This fact must be taken into account in the energy balances.

The benefit of pure hydrogen injection into a blast furnace as auxiliary reduction agent (ARA) has been simulated in several works mainly focused in the reduction of coke [60,61]. However, to the authors' knowledge, the study of Yilmaz et al. [51] is the only research published so far combining PtH₂ and blast furnace. Furthermore, this paper presents the first systematic analysis of the influence of both mass rate and temperature of the injected hydrogen on energy demand, coke rate and adiabatic flame temperature (AFT). The concept is shown in Fig. 3. Electricity is used to dissociate water in hydrogen and oxygen in a

Table 6
CO and H₂ based indirect reduction (IR) reactions [59].

CO-based IR	T (°C)	Δh° ₂₉₈ (kJ/mol)	H ₂ -based IR	T (°C)	Δh° ₂₉₈ (kJ/mol)
3Fe ₂ O ₃ + CO ⇌ 2Fe ₃ O ₄ + CO ₂		−25.2	3Fe ₂ O ₃ + H ₂ ⇌ 2Fe ₃ O ₄ + H ₂ O		16.1
Fe ₃ O ₄ + 4CO ⇌ 3Fe + 4CO ₂	≤ 570	−16.4	Fe ₃ O ₄ + 4 H ₂ ⇌ 3Fe + 4 H ₂ O	≤ 570	148.4
Fe ₃ O ₄ + CO ⇌ 3FeO + CO ₂	≥ 570	22.3	Fe ₃ O ₄ + H ₂ ⇌ 3FeO + H ₂ O	≥ 570	63.5
FeO + CO ⇌ Fe + CO ₂	≥ 570	−12.9	FeO + H ₂ ⇌ Fe + H ₂ O	≥ 570	28.3

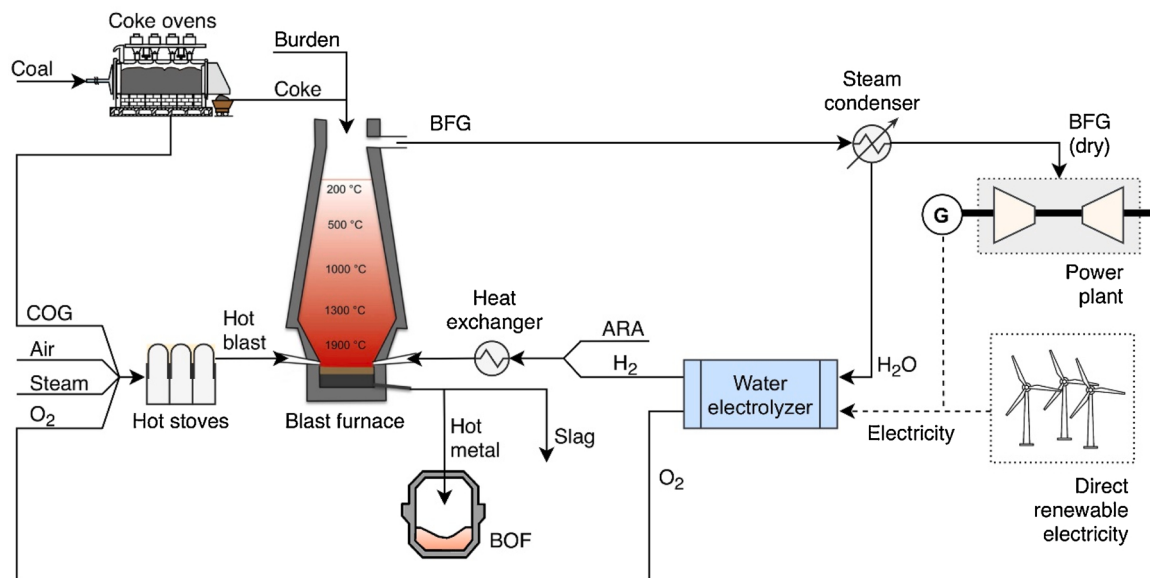


Fig. 3. Conceptual diagram of the integration of Power to H₂ and blast furnace ironmaking through hydrogen injection, studied by Yilmaz et al. [51].

low temperature electrolyzer (efficiency of 58.8 %, LHV basis, and specific energy consumption of 5.1 kW h/Nm³H₂). The produced oxygen and air are heated in the hot stoves. Auxiliary reducing agents (ARA, including H₂) and the hot blast are injected from the bottom according to the counter-current operation of the reactor. The coke and the burden are discharged from the top of the blast furnace in alternating layers. Pulverized coal is injected in the lower furnace under conventional operation and the hot metal and the slag are separated by gravity in the lower part. The top gas leaves the blast furnace from above and is used for electricity and steam generation in the power plant (50 %), for heating the blast in hot stoves (35 %), and for coke ovens (15 %).

This work is mainly focused in the simulation of the blast furnace. The steady-state operation of this system has been modelled in ASPEN Plus coupled to the FactSage and ChemApp thermodynamic databases and equilibrium calculations. The model consists in a heat exchanger (pre-heating zone), four isothermal equilibrium reactors (upper furnace, lower furnace and hearth) and an adiabatic equilibrium reactor (combustion/raceway zone). The coke rate is adjusted to keep constant carbon content in the hot metal of 4.6 wt%; and the oxygen enrichment to maintain an AFT of 2150 °C. The reference case involving 120 kg of pulverized coal per ton of hot metal (kgPC/t_{HM}) and 498 kg coke/t_{HM} with no ARA is compared to two different ARA compositions: pure hydrogen and hydrogen with pulverized coal.

In the former case, the relation between coke rate and the specific mass flow of hydrogen is shown in Fig. 4 for different injection temperatures of hydrogen. As H₂ injection rate increases, an initial sharp

decrease is observed in the required coke, but it increases again after a minimum for low injection temperatures and slows down above 1000 °C. The optimal operating condition corresponds to 1200 °C and hydrogen rate around 30 kgH₂/t_{HM}, as a result of two effects. On the one hand, the high specific heat of hydrogen reduces the adiabatic flame temperature. To maintain the established set point, a higher oxygen mass flow is required, what increases the consumption of coke to keep the thermal state of the furnace. On the other hand, this effect is partially compensated if hydrogen is pre-heated, being hydrogen a heat source. Additionally, hydrogen content and the lower heating value (LHV) of the dry top gas increase proportionally to the injected H₂ mass flow, revealing that hydrogen is only consumed below 950 °C because of thermodynamic constrains related to the water-gas shift reaction [61]. Under the optimal operating conditions (27.5 kgH₂/t_{HM}), the CO₂ emissions decrease 21.4 % with respect to the reference case. Besides, the utilization fraction of hydrogen is maximized and the specific hydrogen demand per mitigated ton of CO₂ is minimized (44 % and 95 kgH₂/t_{mit;CO₂}, respectively). The oxygen requirements can be covered by the electrolysis under this hydrogen rate, avoiding the expensive air separation unit.

In the latter case of combined injection of hydrogen and pulverized coal as ARA, higher injected amounts of PC give rise to lower combined replacement ratios of coke by PC and hydrogen. The best replacement ratio is achieved for 30 kgH₂/t_{HM} and 60 kgPC/t_{HM}. As for the specific reduction of the coke rate by hydrogen, low amounts of PC are preferred because it is associated to higher oxygen requirements to maintain the AFT, which in turn reduces hot blast heat. Specific CO₂ emissions are quite similar for the PC rates tested. The minimum specific H₂ demand per mitigated ton of CO₂ corresponds to 10 kgH₂/t_{HM} and 60 kgPC/t_{HM}, being 3.3 % higher than pure hydrogen case.

Regarding the overall process, the HDRI-BF process has been compared to the conventional BF operation with PC injection. Total energy demand increases in 1.5 % (up to 16.42 GJ/t_{HM}) with respect to the reference case, while coke energy demand and the output top gas energy increase in 4.2 % and 4.7 %, respectively. In summary, the furnace operation is not changed significantly when operating with hydrogen injection. As for CO₂ emissions, savings above 20 % could be reached if carbon-free electricity is used. Nevertheless, considering the current emissions related to the EU mix (295 kgCO₂/MWh [62]), the emissions associated to hydrogen production from electricity are about 469 kgCO₂/t_{HM}, meaning a 13 % increase with respect to the reference case (1353 kgCO₂/t_{HM}).

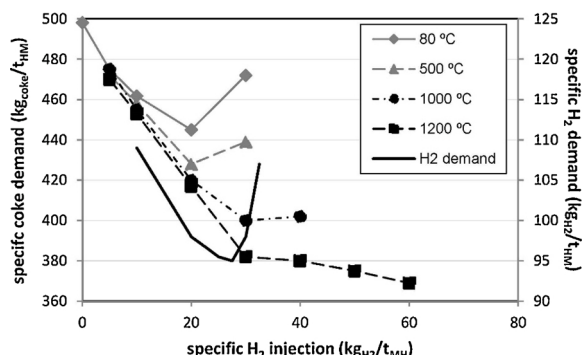


Fig. 4. Simulation results for H₂ as ARA in a blast furnace (data from [51]).

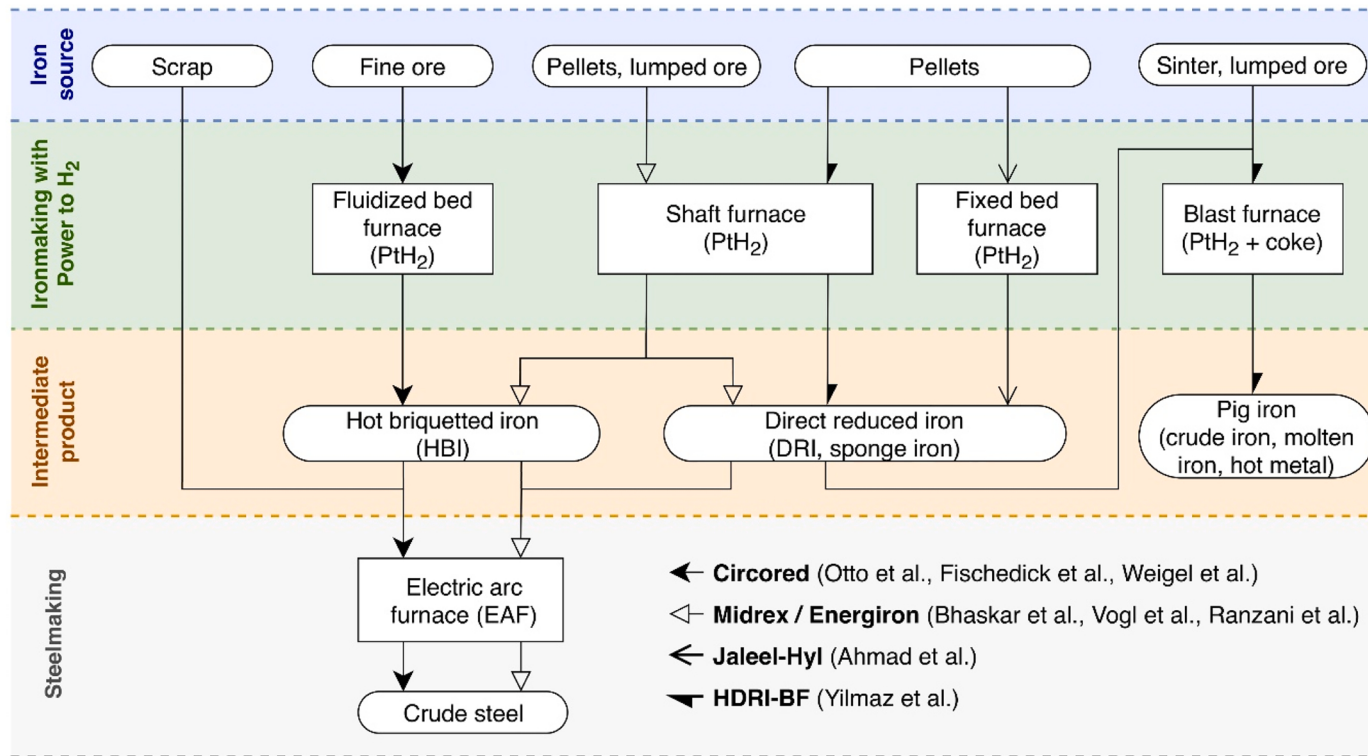


Fig. 5. Summary of PtH₂-based DRI routes investigated so far.

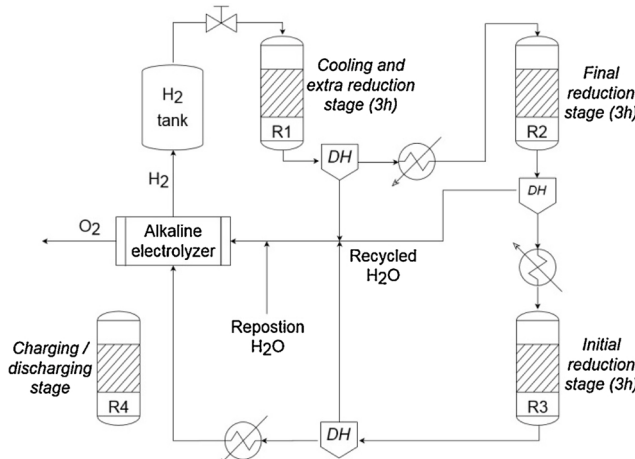


Fig. 6. The experimental facility presented in [46] for HDRI in batch mode.

5.3. Hydrogen as direct reducing agent

Energiron and Midrex are so far the most commonly used processes (79 %) for direct reduction (DR) of iron in form of pellets and lump ore. Both technologies use natural gas steam reforming to generate the gaseous reducing agent (CO+H₂), while another 21 % is produced from

coal-based processes. Unlike Midrex process, Hyl-Energiron includes internal NG reformer and CO₂ capture in the flue gas before reinjection. The final product is hot briquetted iron (HBI) in Midrex, while sponge iron (direct reduced iron, DRI) is obtained in Energiron process with similar metallization grade and higher carbon content. Conventional DR processes are performed in a shaft furnace, consisting in a counter-current moving bed. The studies about hydrogen direct reduced iron (HDRI) in the context of PtH₂ have explored various alternatives which are summarized in Fig. 5, and reviewed in the present section.

The first study was developed in a Hyl-based facility consisting of an electrolyzer and four identical fixed bed reactors operating in batch mode [46]. The pilot plant (Fig. 6) produces 50 kg_{DRI} per cycle of 9 h, excluding charging and discharging. Hydrogen is stored at 4 atm to be used for both DRI process and heating of hydrogen. Dehumidification of the reducing gas is performed after each reactor and the water is recirculated towards the electrolyzer. The non-consumed H₂ is also recovered. The batch mode operation with rotation periods of 3 h is as follows. After charged with iron pellets, the initial reduction stage takes place for 3 h as hydrogen pass through the reactor. After that, the final reduction occurs for three more hours and, afterwards, the DRI process is completed in the cooling extra reduction stage (3 h). Finally, the sponge iron is discharged and the reactor is charged with fresh pellets for the next reduction cycle (R4). Hydrogen runs through the reactors in reverse order. Firstly, hydrogen is pre-heated by cooling the reactor that is in the last stage of DRI process from 1000 °C to 50 °C (R1). After dehumidification and re-heating up to 1050 °C, hydrogen enters the final (R2) and

Table 7

Comparative study performed for different reducing agents (RA). Data from [46].

Source RA	RA demand (kg/t _{DRI})	LHV (MJ/kg)	Energy RA (MJ/t _{DRI})	Emissions (kgCO ₂ /t _{DRI})	Water (kgH ₂ O/t _{DRI})
CH ₄	107	50	5350	300	289
Coke	205	295	6048	600	246
PtH ₂	54	120	6446	0	484

the initial reduction (R3) reactors successively before recirculation.

The experimental tests proved the concept with a metallization of 90 %. The comparative study presented in that work with respect to conventional technologies is summarized in Table 7. For comparison purposes, the data presented in [46] have been standardized in terms of specific demand of reducing agent (kg per ton of DRI), specific energy demand (MJ per ton of DRI), specific CO₂ equivalent emissions associated to the reducing agent (kg per ton of DRI) and specific demand of water (kg per ton of DRI). Calculated from the energy content of the consumed H₂, the specific energy demand for PtH₂ case is slightly higher than for conventional reducing agents. If the reported electricity consumption is considered (4.3 MW h/t_{DRI}), the specific energy demand is 15.5 GJ/t_{DRI} and the corresponding CO₂ emissions rise up to 1268 kgCO₂/t_{DRI}, considering the current energy mix in EU-28 (295 kgCO₂/MWh [62]). The fuel demand is quite higher than that reported in conventional technologies based in shaft furnaces (~ 125 GJ/t_{DRI} and 400–500 kgCO₂/t_{DRI} [28]). It has to be noticed that the efficiency of that electrolysis (80 kW h/kgH₂) is quite lower than for the current PEM and Alkaline technologies (45–65 kW h/kgH₂). Regularizing the values to an efficiency of 70 % (LHV basis), energy demand and emissions could be reduced up to 9.3 GJ/t_{DRI} and 759 kgCO₂/t_{DRI}, respectively.

Pure hydrogen as reducing agent in a direct reduction shaft furnace was investigated in the ULCOS project from the experimental and theoretical point of view [6,47]. Specifically, a 2D axisymmetric and steady-state model, using finite volume method, was developed to solve the local mass, energy and momentum balances and to simulate the kinetic mechanisms involved in the reduction process (hematite to magnetite to wüstite to iron). The concept was sketched in Fig. 5: hydrogen is produced from electricity in an electrolyzer and injected in a shaft furnace to reduce hematite pellets. The carbon-free DRI is finally converted into liquid steel in an electric arc furnace and, finally, further processed to hot rolled coil. Standardized experiments were performed to clarify the kinetic mechanisms. The modelled shaft furnace, similar to a Midrex one, is a counter-current moving bed reactor of 9 m height and 6.6 m diameter where the reducing gas (H₂, H₂O and N₂) is mainly (98 %) injected laterally near the bottom of the reactor. Different conditions were simulated [47], including the Midrex conditions as reference state. Both experiments and simulations established that 800 °C is the optimum temperature to reduce hematite cubes by hydrogen. Pellet size is another influent parameter: 2 and 4 m of the reactor height are necessary for the complete reduction of 6 and 12 mm diameter pellets, respectively. With 24 mm diameters only conversions of 75 % are obtained. According to such results, mathematical simulations based in kinetics experiments of a shorter shaft furnace (6 m height) were also published [63]. Full metallization was reached at 3.4 m 800 °C, which could be comparable to 10 m reduction zone of a Midrex shaft. Above 900 °C, 100 % reduction is obtained in less than 2 m, allowing smaller reactors than the current DR shafts. Neither energy demand nor specific emissions can be computed from the data provided in these works.

Results of HYBRIT project for a similar concept were presented in [48]. Pre-heated hematite pellets are reduced at 800 °C in a shaft furnace (SF) and later compacted to HBI. The reducing agent is pure hydrogen generated in an electrolyzer of features similar to that of alkaline and PEM technologies (70 °C and efficiency of 72 %, LHV basis). The hydrogen with 50 % oversupply ($\lambda = 1.5$) is pre-heated with the output gas of the SF in a condenser of 70 % efficiency, where H₂ surplus is separated from the water. Both water and not consumed hydrogen are recirculated. Finally, HBI and scrap with 50 % share are melted and converted to liquid steel (LS) in an electric arc furnace. The input rates per ton of LS are: 738 kg_{pellets}, 536 kg_{scrap} and 25 kgH₂. The approach is performed through a mechanistic process model based in mass and energy balances. Assumptions about the operating parameters for each sub-system are made from bibliographic data according to the Midrex process and detailed reactions are not considered for SF and EAF. The specific energy consumption is 3.48 MW h/t_{LS} and 0.753 MW h/t_{LS} for the extreme cases of 100 % HBI and 100 % scrap, respectively. About

two thirds of the energy is consumed in the electrolyzer. SEC increases 41 kW h/t_{LS} per unit risen in λ , concluding that $\lambda = 1.5$ is an optimum value. Re-heating of the HBI involves an additional consumption of 159 kW h/t_{LS}. Regarding CO₂ emissions, the equivalent electricity rate to equal the current level of BF-BOF (1870 kgCO₂/MWh) were established in 532 kgCO₂/MWh for 100 % HBI, the less favorable ratio. According to this result, HDRI-EAF technology reduces emissions in almost all European countries. Even considering carbon-free electricity, the steel-making process is not carbon-free, although emissions would be as low as 53 kgCO₂/t_{LS} (2.8 % of the BF-BOF emissions). The economic analysis shows CAPEX 30 % higher than for BF-BOF while OPEX strongly dependent on the scrap share and prices of electricity and CO₂ emissions. They concluded that HDRI-based steel production could be competitive for 40 €/MWh and 62 €/tCO₂. Finally, some advantages such as oxygen production and flexibility for grid balancing are pointed out.

Recently, Bhaskar et al. [49] developed a model based in open-source software (Phyton) to simulate the hydrogen direct reduction in a shaft furnace couple to an electric arc furnace (HDRI-EAF). The concept is very similar to the described above [48]. Iron pellets are pre-heated up to 800 °C before discharging in the shaft furnace where DRI of 94 % metallization is obtained. The DRI is converted into liquid steel in an EAF operating at 1650 °C with efficiency of 60 %. The outlet gases of the shaft furnace at 250 °C are driven to a waste gas separation unit to recover the unreacted hydrogen. The additional required hydrogen is generated in an alkaline electrolyzer operating at 90 °C. The oxygen produced by electrolysis is used for CO production in the EAF, where 10 kg/t_{LS} of carbon and 50 kg/t_{LS} of lime and MgO are added. Hydrogen is mixed with the recycled hydrogen and heated up to 500 °C before entering to the shaft furnace. Energy required for pelletizing is not considered in the model. Only electric energy demand is considered, resulting in a total amount of 3.72 MWh/t_{LS} ($\lambda = 1.5$). The 70 % approximately is consumed in the electrolyzer. Porosity, sizing and geometry of pellets influence the reaction kinetics. The presence of impurities increases the energy consumption in the EAF in a proportional amount. CO₂ emissions are also calculated according to different electricity mixes.

The Circored process was also assessed in [25] considering hydrogen from electrolysis as reduced agent in the direct reduction of iron. Fine ores are dried and pre-heated up to 850–900 °C through NG combustion and are converted into HBI of 95 % metallization. Given the carbon-free nature of such HBI, coal must be injected in the EAF stage in amounts depending on the scrap share to achieve a carbon content of 2% in the final product. The specific energy consumption is 19.96 GJ/t_{LS} from which 12.5 GJ/t_{LS} are from electricity and 5.6 GJ/t_{LS} from NG. The specific CO₂ emissions results in 2407 kgCO₂/t_{LS}, assuming the German electricity mix of 2012 (160 kgCO₂/GJ). These figures are higher than that obtained for the conventional Circored process in which hydrogen is produced from external NGSR: 18.3 GJ/t_{LS} and 1206 kgCO₂/t_{LS}.

A general assessment about HDRI, among other technologies, was performed in [44,45]. The Circored process was modelled through a simplified approach based in mass and energy balances. Details about the process simulation are scarce, as the papers were focused in the

Table 8

Comparative study for two Midrex-DRI and two Energiron-HBI. Data from [46].

	Units	DRI4.0	DRI2.0	HBI1.5	HBI0.5
Fe total	wt%	87.3	89.3	88.2	90.2
C in DRI	kg/t _{DRI}	40	20	15	5
Total Energy demand	GJ/t _{DRI}	12.5	11.9	12.5	11.1
Mass of H ₂	kg/t _{DRI}	0	67.1	0	68.9
H ₂ energy consumption	GJ/t _{DRI}	0	8.06	0	8.27
Mass of CH ₄	kg/t _{DRI}	199	26.6	199	6.60
CH ₄ energy consumption	GJ/t _{DRI}	10.0	1.34	10.0	0.335
CO ₂ emissions (NG)	kg/t _{DRI}	413	6.60	497	1.50
Electrolysis demand (H ₂)	MWh/t _{DRI}	0	3.76	0	3.87
CO ₂ emissions (NG+ H ₂)	kgCO ₂ /t _{DRI}	413	1117	497	1141

definition of different criteria, regarding technology, society, safety, economy and environment, and the establishment of future scenarios with comparison purposes. The obtained consumptions per ton of liquid steel were 13.1 GJ/t_{LS} (only electricity), 1500 kg of fine ore, 325 kg of scrap, while the specific CO₂ emissions considering carbon-free electricity were 339 kgCO₂/t_{LS}. From the economic point of view, HDR is not profitable until 2030 or 2040, depending of the analyzed scenario. This technology is very sensitive to electricity prices, but takes advantage over BF-BOF at rising prices of carbon allowances. The considered CAPEX was 874 €/t capacity, considering 414 €/t for HDR-EAF, 450 €/t for H₂ electrolyser (650 €/kW_{el}) and 80 % of cheap peak electricity [44]. Considering environmental, safety and social aspects, HDR is the best option in the long term (2050) for the four weighting distributions investigated to emulate different stakeholder perspectives [45].

5.4. Hybrid solution: HDRI in blast furnace

Given the long period obtained for the hydrogen-based DRI technologies to be profitable, the possibility of using HDRI in blast furnaces (Fig. 5) has been also investigated. Midrex and Energiron DRI forms are used commercially in blast furnaces since 1989 with the aim of reducing fuel consumption and increasing productivity [64]. Yilmaz & Turek [28] studied the use of pure hydrogen to produce DRI and compared the benefits of introducing in a blast furnace four different DRI with metallization of 96 %: two Midrex HBI and two Energiron DRI. Regarding the DRI production, the results are summarized in Table 8, considering 96 % metallization and 2.5 GJ/t_{DRI} consumed in auxiliaries. Electricity is considered carbon-free in [46] and the efficiency of the electrolyzer was assumed to be 58.8 % (LHV basis) equivalent to 5.1 kW h/Nm³. Under these hypotheses, the substitution of NG by H₂ reduces direct CO₂ emissions in almost 100 % and energy consumption in 6–14 % with respect to conventional processes. However, if specific emissions related to electricity generation (295 kg/MWh in the EU mix [62]) are taken into account, HDRI production could triple the specific CO₂ emissions with respect to NG-based processes (last two rows in Table 8). To reach 400 kgCO₂/t_{DRI}, the CO₂ intensity of the electricity mix should be around 100 kg/MWh.

The global process resulting from the injection of these DRIs as part of the burden into a blast furnace was also assessed in terms of CO₂ emissions and energy demand, by using the model explained in Section 5.2 [51]. A 6.4–7.3 % decrease of fuel consumption for each 10 % metallization of the burden was obtained, in agreement with the literature. This fuel reduction slows down as the DRI carbon content decreases, specially above 30 % metallization. The positive effects of DRI are damped as burden metallization increases, because coke mass decreases faster than top gas mass, causing insufficient heat supply. The increase in DRI carbon content can balance this effect. Considering a constant rate of 40 kg_{PC}/t_{HM}, the point of minimum direct reduction (PMDR, bending point) varies from 356.5 to 433.4 kg_{DRI}/t_{HM}, depending on the type of the DRI, while coke rate decreases from 344.7 to 306.2 kg/t_{HM}, respectively. The effects on CO₂ emissions were analyzed for a constant coke rate of 300 kg/t_{HM}. On-site emissions decrease as DRI share is increased up to 400 kg_{DRI}/t_{HM} (PMDR), specially for DRI2.0 and HBI0.5 as expected. Then the positive effects are gradually lost, causing even increase in CO₂ emissions for DRI4.0 and HBI1.5. The origin of this

Table 10

Figures related to H₂ uses in the BF-BOF route (4.2 kWh/Nm³ H₂).

Units	H ₂ -BF	Energiron [46]		Midrex [46]	
	[51]	DRI4.0	DRI2.0	HBI1.5	HBI0.5
Mass of H ₂	kg//t _{LS}	27.5	0	26.8	0
SEC	MWh/t _{LS}	486	4.46	4.81	4.55
CO ₂ - CFE	kgCO ₂ /t _{LS}	1031	1138	972	1171
CO ₂ - EUM	kgCO ₂ /t _{LS}	1408	1138	1331	1171
					1340

behavior is the diminution of the top gas energy which must be compensated with additional fuel. The optimal specific DRI demand per mitigated ton of on-site CO₂ emissions is reached near PMDR: 1.12 t_{DRI}/t_{mit;CO2} for HBI0.5 and DRI2.0, 2.11 t_{DRI}/t_{mit;CO2} for HBI1.5 and 2.55 t_{DRI}/t_{mit;CO2} for DRI4.0 (always under the assumption of carbon-free electricity). The minimum emissions ranges from 970 to 1191 kgCO₂/t_{HM}, corresponding to 28 and 12 % decrease with respect to the reference case (1353 t_{CO2}/t_{HM}). Compared to direct H₂ injection in the BF (95 kgH₂/t_{mit;CO2}) [51], a lower minimum specific hydrogen demand per mitigated ton of CO₂ is obtained: 76 kgH₂/t_{mit;CO2}. As for energy demand, a 4.5 % decrease is obtained in the best case (15.7 GJ/t_{HM} for HBI0.5). The main differences are related to the substitution of NG by H₂ in an equivalent amount and the reduction of the energy of top gas excess in one third, what has to be into account in the integrated steel mill.

5.5. Discussion about PtH₂ in steelmaking

Different concepts to integrate PtH₂ in iron and steelmaking have been evaluated as potential routes to mitigate CO₂ emissions. According to the reviewed literature, the specific energy consumption (SEC) is not significantly affected with respect to conventional processes, while significant CO₂ emissions could be reduced if carbon-free electricity (CFE) is considered. Nevertheless, such results have been obtained under different assumptions that make difficult to reach conclusions about the real benefits. For the sake of comparison, the results reviewed above have been regularized to 70 % efficiency in electrolyzer (LHV basis) and specific CO₂ emissions of the current EU electricity mix (EUM, 295 kgCO₂/MWh in 2016 [62]). Tables 9 and 10 summarizes the results of these previous works together with the corresponding average values of current global steelmaking [25].

Quite similar hydrogen rates have been used in DRI processes, but some differences are observed in SEC and emissions. The specific energy consumption calculated from [25] is very similar to the current average value in the steelmaking industry, but specific emissions are quite lower, even including that associated to electricity. Very similar emissions are derived from [44,45]. However, there is a discrepancy in SEC. The former work takes into account the energy for pre-heating the pellets with natural gas, while the two latter present little details about their hypotheses. For the studies associated to shaft furnaces, SECs and emissions are about 35 % lower than the reference case. Notwithstanding, it has to be noted that pelletizing was not considered in [48, 49] what could involve about 2.2 GJ/t_{LS} [48]. As Midrex and Energiron processes are completely electrified, very low CO₂ emissions are obtained under CFE assumption. Emissions due to carbon use in EAF,

Table 9

Figures related to HDRI-EAF (4.2 kWh/Nm³ H₂).

Units	Global average [25]	Circored		Midrex / Energiron	
		[25]	[44,45]	[48]	[49]
Mass of H ₂	kg//t _{LS}	58.1	61.8	51.0	59.6
SEC	MWh/t _{LS}	5.55	5.54	3.64	3.48
CO ₂ - CFE	kgCO ₂ /t _{LS}	409	339	53	0
CO ₂ - EUM	kgCO ₂ /t _{LS}	1800	1433	1412	1086
					1197

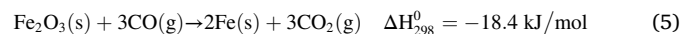
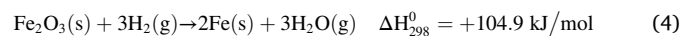
consumption of graphite electrodes and lime calcination were taken into account by Vogl [48], but not in [49].

Regarding the use of hydrogen in the conventional BF-BOF route, a rate of 950 kg_{HM}/t_{LS} has been considered for comparison purposes, as well as additional amounts energy and emissions corresponding to the BOF stage (1 G J/t_{LS} and 31 kg_{CO2}/t_{LS} [65]). Similar amounts of hydrogen were used in both concepts, direct use as reducing agent and to produce DRI to be injected the BF. SEC is quite similar in all cases and 15 % lower than the reference case. The higher savings are obtained for the conventional DRIs (DRI4.0 and HBI1.5), which also present the lower CO₂ emissions if EU mix is considered. Under CFE, emissions decrease in almost 50 % for DRI2.0 and HBI0.5, and 25 % for EUM scenario.

According to these figures, the use of hydrogen in iron and steelmaking could help to reduce CO₂ emissions under scenarios with high penetration of renewable power generation. The low carbon content in HDRI is not a technical problem to be used in both BF and EAF. Although hydrogen based technologies are not profitable at current prices of carbon emissions (too low) and electricity (too high), the presented studies suggests that HDR-EAF is the most promising steelmaking route in the long term from the economic, environmental, safety and social point of view [45].

6. Power to syngas

Syngas is a synthetically produced fuel gas mixture, typically consisting of carbon monoxide, hydrogen and carbon dioxide. Its composition makes syngas a valuable product in the ironmaking processes as reducing agent for the blast furnace. The reduction of Fe₂O₃ by the hydrogen contained in the syngas is endothermic and follows Eq. (4), while the reduction by CO is exothermic and follows Eq. (5) [66].



Power to Syngas reuses carbon cyclically by regenerating the CO₂ emitted by the blast furnace in syngas through a non-emitting source of energy (renewable energy or nuclear power). The integration of this concept in the Iron and Steel industry can be performed through two possible routes, which differ in the process used to reduce the CO₂: (i)

electrolysis of CO₂ or (ii) reverse water-gas shift reaction (see Fig. 1). Both routes were firstly proposed by Kato in 2010 [67].

6.1. CO₂ electrolysis route

The first Power to Syngas route uses CO₂ electrolysis to reduce CO₂ in syngas. The conceptual diagram of its integration in the ironmaking process is presented in Fig. 7. In this concept, the source of CO₂ is the effluent gas emitted by the blast furnace (BF gas). It can be used the CO₂ captured from the blast furnace gas or the BF gas itself in the electrolysis process. In the former case, the produced syngas would not have hydrogen content, whereas in the latter case it would contain the H₂ that was already present in the BF gas. The electrolysis process should be supplied with energy from non-emitting energy sources in order to avoid secondary emissions. The produced syngas is then used as reducing agent in the blast furnace, thus diminishing the initial coke input. Moreover, there is available O₂ as byproduct from the CO₂ electrolysis that can be used in the blast furnace, the basic oxygen furnace or other processes.

When integrating Power to Syngas technology, it is clear that the input flows of the blast furnace change. So, in order to maintain the original operating conditions in the iron and steel plant, some operating parameters have to be adjusted [68]. For example, the composition of the syngas introduced in the blast furnace may affect the final carbon content in the hot metal, which subsequently modifies the melting point. In this situation, the coke input should be adjusted accordingly. Also, the

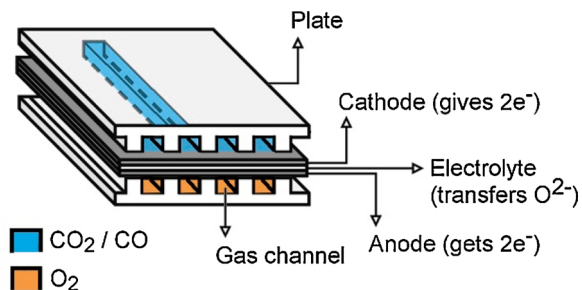


Fig. 8. Schematic diagram of a solid oxide electrolysis cell.

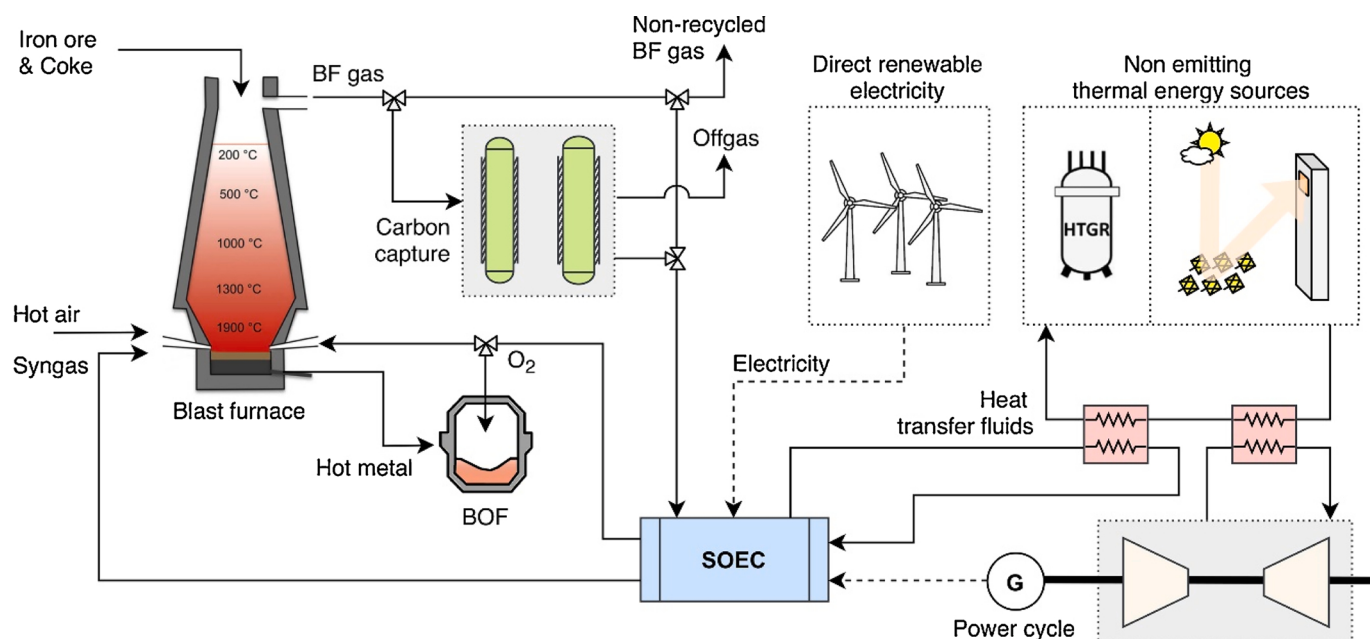
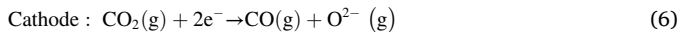


Fig. 7. Conceptual diagram of the integration of Power to Syngas (SOEC) in the Iron and Steel industry.

temperature profile along the furnace can be affected, which may result in incomplete reduction of iron ore. In this case, the flow rate of enriched O₂ and hot air entering the furnace, as well as the temperature of the circulated syngas, are adjusted to keep the heat flux ratio and the raceway temperature within suitable values.

6.1.1. Solid oxide electrolyzer cells

So far, the only technology for CO₂ electrolysis that is close to commercialization (TRL8) and has demonstrated long-term durability beyond a year is the high-temperature solid oxide electrolyzer cell (SOEC). These cells have two electrodes in contact with a solid ceramic electrolyte, which above 600 °C can conduct ions and remain impermeable to electrons and gaseous oxygen (for a detailed state-of-the-art review on CO₂ electrolysis technologies, please see the work of Küngas [69]). The inlet flow of CO₂ is fed to gas channels that are in contact with the cathode. The CO₂ diffuses through the cathode material to reach the cathode-electrolyte interface, where it gets decomposed to CO and O²⁻ by the interaction with electrons (Eq. 6). The CO produced in the cathode side is collected at the outlet of the gas channel, while the O²⁻ ions travels through the electrolyte to the anode side. At the anode-electrolyte interface, the ions lose their charge and recombine thus obtaining O₂ (Eq. 7), which is collected in the gas channels of the anode side. Lastly, the electrons enter to the electric circuit through the anode (Fig. 8) [70].



Among the common figures of merit for characterizing SOECs, the electric power consumption (EPC) is the most useful parameter from an industrial point of view. The EPC represents the amount of electricity that is required for obtaining 1 Nm³ of CO [69]. It will also give a reference parameter when comparing different studies of integration of the Power to Syngas concept in the Iron and Steel industry. The EPC is computed by Eq. (8),

$$EPC \left[\frac{\text{kWh}}{\text{Nm}^3} \right] = \frac{E[\text{V}] \cdot n[-] \cdot F \left[\frac{\text{C}}{\text{mol}} \right]}{\eta_F[-] \cdot V_m \left[\frac{\text{Nm}^3}{\text{mol}} \right] \cdot 3600 \left[\frac{\text{s}}{\text{h}} \right] \cdot 1000 \left[\frac{\text{W}}{\text{kW}} \right]} \quad (8)$$

where E is the cell voltage (voltage difference between the cathode and the anode), n is the number of transferred electrons ($n = 2$ in the reduction of CO₂ to CO), F is the Faraday's constant (96485.34 C/mol), η_F is the Faradaic efficiency (very close to 1 in SOEC) and V_m is the volume of 1 mol of ideal gas under normal conditions (i.e., 0.0224 Nm³/mol). Typical values for EPC in high-temperature solid electrolyzer cells vary between 2.4 and 3.4 kW h/Nm³ [69]. It must be pointed out that, as the overall CO₂ electrolysis reaction is endothermic, there must be an additional input of thermal energy to the SOEC (for further details, see Appendix C). To avoid secondary emissions, both the electric and the thermal supply should come from a non-emitting energy source (e.g., renewable energy or nuclear power). Additionally, industrial high-temperature waste heat can be used as thermal energy source to increase the overall efficiency of the system.

6.1.2. Studies on the concept of Power to Syngas using SOEC

Several authors have studied this potential integration. The different studies are compared in Table 11. The order of presentation in the table and in the following paragraphs is in ascending order of complexity (from overall energy and mass balances to detailed simulation), and therefore in order of better approach to the real system.

Kato et al. [71] were the first research group that studied this integration. They considered that the electricity and heat supply for the CO₂ electrolyzer came from a high-temperature gas-cooled nuclear reactor (HTGR). The energy from the nuclear reactor is recovered from its

helium coolant at 850 °C. Two potential scenarios were analyzed, corresponding to CO₂ electrolysis at high temperature (EPC = 2.6 kWh/Nm³) and at ambient temperature (EPC = 3.5 kWh/Nm³). In the first scenario, part of the sensible heat of the coolant (from 850 °C to 808 °C) is used to preheat the electrolyzer. The rest is used in a gas turbine (45 % efficiency) to supply electricity to the electrolyzer. In the second scenario (ambient temperature SOEC), the helium coolant is used only for power generation in the gas turbine, diminishing its temperature from 850 °C to 587 °C. The overall concept was sized to completely consume the CO₂ emissions of an average blast furnace in Japan, which are 129.6 kgCO₂/s. Thus, the required available thermal output from the HTGR should be 1.73 GWt in the first scenario, and 1.86 GWt in the second scenario. This corresponds to about three units of the nuclear reactor model GTHTR300, designed by JAERI, which has a power output of 600 MWt. Regarding the cell surface area, they estimated that 29.7 km² would be required even in the best case, concluding that the reactivity of the cell should be improved. The latter was calculated through experiments on a high-temperature tubular SOEC with zirconia Y₂O₃-ZrO₂ electrolyte, comparing three different electrode materials (perovskite La_{0.8}Sr_{0.2}MnO₃, platinum and a mixture of both) [70]. They also studied the possibility of using a cathode made of Ni mixed with perovskite, and an anode mixing zirconia and perovskite, aiming for cheaper SOECs by avoiding noble metals. However, the current density was higher and therefore the consumption [72].

Fujii et al. [73] also studied the integration of the Power to Syngas concept using a high-temperature gas-cooled nuclear reactor as energy source. The sensible heat of the cooling fluid from the HTGR was used to provide thermal energy in the SOEC (from 850 °C to 827.3 °C) and then diverted to a gas turbine for power generation (from 827.3 °C and 5.1 MPa to 561.0 °C and 2.55 MPa). The system was sized to convert 15.6 kgCO₂/s, corresponding to 30 % of the CO₂ emissions of a blast furnace emitting 4.5 ktCO₂/day. To determine the required cell surface area and the electric power consumption of the SOEC, they performed experiments on an electrolyzer with Ni-YSZ cathode, YSZ electrolyte and La_{0.6}Sr_{0.4}Co_{0.2}Fe_{0.8}O_{3-δ} anode. The estimated surface area for the analyzed system amounted to about 0.1 km². The EPC of the electrolyzer was 5.91 kWh/Nm³. Besides, they assumed in their calculations that the Joule heating was not used in the reaction (see Appendix C), therefore they also needed 1.3 kWh_t/Nm³ from an external source. To provide both electric and heat consumptions, it was enough with 493 MWt from the HTGR (i.e., less than one unit of the nuclear reactor model GTHTR300, which can provide up to 600 MWt).

Since the studies mentioned above concluded that SOECs would require large cell surface areas to reach significant CO₂ recycling, Numata et al. [74] developed a metal-supported SOEC for which large cell structures are easier to create. The configuration of integration was the same as that of the previous researchers (HTGR and combined cycle). In this case, the 50 % of the blast furnace gas was diverted to the electrolyzer, and 60 % of this inlet was reduced (i.e., it is recycled the 30 % of the CO₂ emitted by the furnace). The materials of the cathode, electrolyte, and anode were the same as in the experiments of Fujii et al. [73]. Due to gas leaks in the cell, the faradaic efficiency diminished to $\eta_F = 48$ %. Therefore, the electrical consumption of the concept remarkable increased in comparison with previous studies (the EPC was 14.11 kWh/Nm³). The CO₂ conversion capacity was 16.4 kgCO₂/s, and the required cell surface area 0.083 km². If a Faradaic efficiency close to 1 had been achieved, the cell surface would have decreased by 52 % [74].

Suzuki et al. [68] studied the Power to Syngas concept with and without CO₂ separation before diverting the effluent gas to the electrolyzer. For the former case, mono-ethanol amine capture was chosen. The analysis was much greater in detail than the already mentioned studies, as it comprised the modelling of the heat transfer and chemical reactions taking place in the blast furnace. The simulation was performed in Aspen Plus software, separating the blast furnace in five sub-processes (low-, middle- and high-temperature equilibrium

Table 11Studies on Power to Syngas integration in the Iron and Steel industry, using the CO₂ electrolysis route.

Study	Configuration analyzed	Experimental data in analysis	CO ₂ recycled (%)	SOEC (MWe)	Specific consumption (MJ/kgCO ₂ recycled)
Kato et al. 2011 [71]	Thermal source: HTGR 850 °C Electrical source: Gas-turbine ($\eta = 45.0\%$) supplied by HTGR SOEC: 25 °C, E = 1.48 V, EPC = 3.5 kWh/Nm ³ Blast furnace: 11.2 kt _{CO₂} /day Thermal source: HTGR 850 °C Electrical source: Gas-turbine ($\eta = 43.3\%$) supplied by HTGR	No	100	840	Heat: 0 Electricity: 6.5
Kato 2014 [81]	SOEC: 800 °C, E = 1.09 V, EPC = 2.6 kWh/Nm ³ Blast furnace: 8.6 kt _{pig iron} /day, 6.3 kt _{CO₂} /day Thermal source: HTGR 850 °C Electrical source: Gas-turbine ($\eta = 42.7\%$) supplied by HTGR	No	100	351	Heat: 2.1 Electricity: 4.8
Kato et al. 2011 [71](a) Dipu et al. 2012 [70] (b) Dipu et al. 2014 [72](c)	(a), (b), (c): 800 °C, E = 1.09 V, SOEC: EPC = 2.6 kWh/Nm ³ (b): 0.60 μ mol/(min·cm ²), 29.7 km ² cell area (c): 0.41 μ mol/(min·cm ²), 43.3 km ² cell area Blast furnace: 11.2 kt _{CO₂} /day Thermal source: HTGR 850 °C Electrical source: Gas-turbine ($\eta = 42.5\%$) supplied by HTGR	a): No (b), (c): SOEC cell surface area	100	621	Heat: 2.1 Electricity: 4.8
Fujii et al. 2015 [73]	SOEC: 800 °C, E = 2.47 V, EPC = 5.91 kWh/Nm ³ , 0.098 km ² cell area Blast furnace: 6.8 kt _{pig iron} /day, 4.5 kt _{CO₂} /day Thermal source: HTGR 850 °C Electrical source: Gas-turbine ($\eta = 45.0\%$) supplied by HTGR	SOEC cell surface area and electric consumption	30	171	Heat: 2.4 Electricity: 10.8
Numata et al. 2019 [74]	SOEC: 800 °C, E = 2.83 V, EPC = 14.11 kWh/Nm ³ , 0.083 km ² cell area Blast furnace: 6.8 kt _{pig iron} /day, 4.7 kt _{CO₂} /day Thermal source: HTGR 850 °C Electrical source: Technology not specified ($\eta = 45.0\%$) supplied by HTGR	SOEC characterization at laboratory scale	30	423	Heat: 1.5 Electricity: 25.8
Suzuki et al. 2015 [68]	Technology not specified ($\eta = 48.1\%$) supplied by HTGR SOEC: 800 °C, E = 1.30 V, EPC = 3.11 kWh/Nm ³ Blast furnace: 10.5 kt _{pig iron} /day, 9.2 kt _{CO₂} /day Thermal source: HTGR 850 °C Electrical source: Technology not specified ($\eta = 48.1\%$) supplied by HTGR	BF and SOEC models verified with actual operational data	18	109	Heat: 1.1 Electricity: 5.7
Suzuki et al. 2015 [68]	SOEC: 800 °C, E = 1.30 V, EPC = 3.11 kWh/Nm ³ Blast furnace: 10.5 kt _{pig iron} /day, 9.1 kt _{CO₂} /day Carbon capture: mono-ethanol amine process after BF, 4 GJ/tCO ₂ , $\eta = 90\%$ Thermal source: HTGR 950 °C Electrical source: Gas turbine ($\eta = 48.1\%$) supplied by HTGR	BF and SOEC models verified with actual operation data	16	97	Heat: 7.8 (including carbon capture) Electricity: 5.7
Hayashi et al. 2015 [77]	SOEC: 800 °C, E = 1.32 V, EPC = 3.16 kWh/Nm ³ Blast furnace: 10.5 kt _{pig iron} /day, 9.0 kt _{CO₂} /day Carbon capture: mono-ethanol amine process after BF, 4 GJ/tCO ₂ , $\eta = 90\%$ Thermal source: HTGR or Renewable energy (Not specified) Electrical source: Technology not specified ($\eta = 45.4\%$)	BF and SOEC models verified with actual operation data	16	98	Heat: 7.7 (including carbon capture) Electricity: 5.8
Hisashige et al. 2019 [78]	SOEC: 800 °C, E = 1.30 V, EPC = 3.11 kWh/Nm ³ Shaft furnace (PSR): n/a Carbon capture: CO-specific PSA after SOEC, $\eta = 80\%$	Shaft furnace (PSR) and SOEC models verified with actual operation data	n/a	n/a	Heat: n/a Electricity: n/a

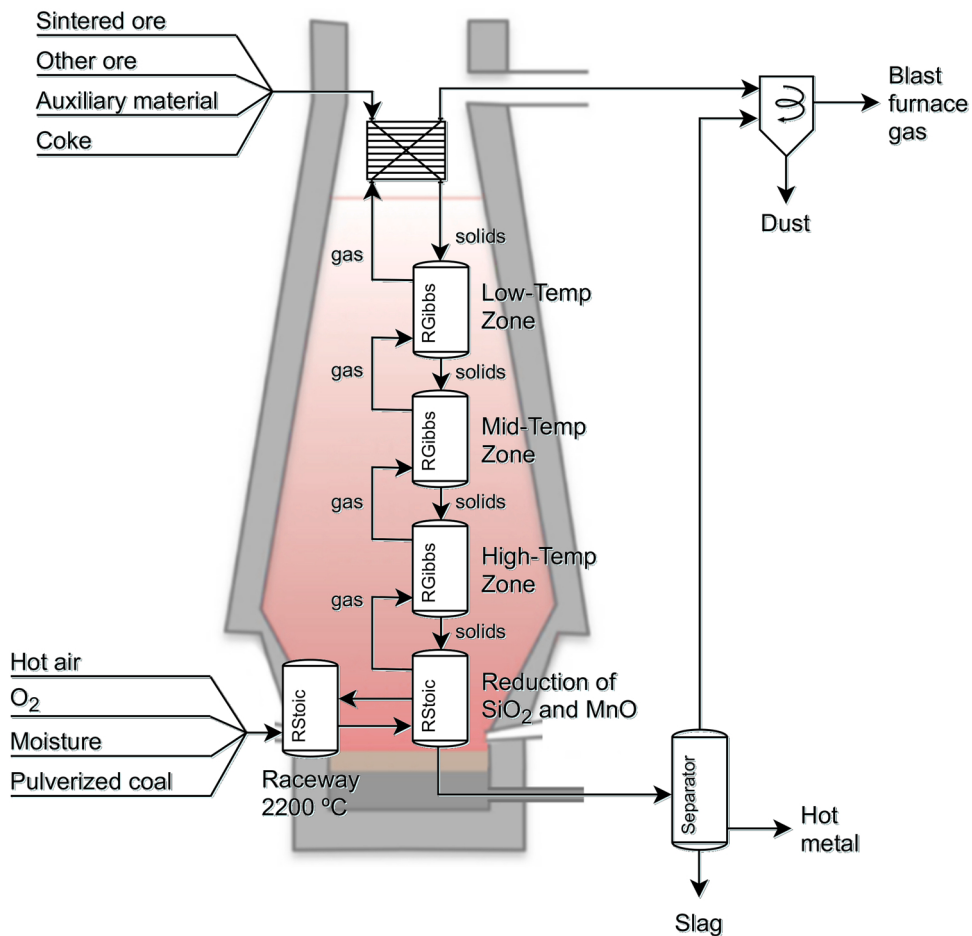
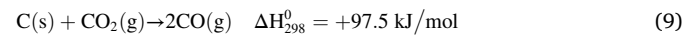


Fig. 9. Simplified schematic diagram of the blast furnace model developed by Suzuki et al. in Aspen Plus [68].

reactors, reduction of SiO₂ and MnO, and partial oxidation of pulverized coal in the raceways) (Fig. 9). Regarding the SOEC, the EPC was 3.11 kWh/Nm³, with a CO₂ conversion of 60 %. Assuming adiabatic SOEC (i.e., the joule heating is used in the reaction), the external thermal input required in the SOEC is 0.6 kWh/Nm³. The source of energy was also a high-temperature gas-cooled nuclear reactor, as in the previous studies. The blast furnace model was validated with real data from [75], and the SOEC model was designed using the experimental performance of Wang et al. [76]. The simulation results were within 5% error compared to actual operation.

In the scenario without carbon capture, the 30 % of the effluent gas from the blast furnace is diverted directly to the electrolyzer. Since it converts the 60 % of CO₂, the recycled fraction of CO₂ is 18 %, corresponding to 19.1 kgCO₂/s [68]. It must be noted that, compared to conventional ironmaking, the fact of recirculating gases makes BF gas flow to increase. Therefore, the actual CO₂ emission reduction compared to conventional process is 11.4 % (instead of the 18 % recycled fraction of the Power to Syngas configuration). In the second scenario (i.e., with amine carbon capture), the fraction of CO₂ emitted by the blast furnace that is recycled is 16.2 %, corresponding to 17.1 kgCO₂/s. Compared to conventional iron and steel plants, the CO₂ is reduced only by 3.4 %. This reduction is lower than in the case without carbon capture, since the latter also recirculates H₂ (originally present in the BF gas) to the blast furnace. This hydrogen acts as reducing agent and additionally diminishes the required coke input. With carbon capture, only a syngas composed of CO and CO₂ is recirculated, as CO₂ was separated from the rest of the components before entering the SOEC. Besides, the external heat demanded by the overall system increases to 4.24 kWh/Nm³ in the case with carbon capture, due to the CO₂ desorption process. In both

cases (with and without carbon capture), the energy demand from the HTGR is about 300 MWt, therefore one unit of the model GTHTR300 (600 MWt output) would be enough. Regarding the temperature of the blast furnace, Suzuki et al. showed that overall drops about 100 °C may take place in both scenarios. The presence of additional CO₂ in the recycled gas promotes the carbon solution reaction, which is endothermic (Eq. 9), thus reducing the temperature inside the furnace.



Hayashi et al. [77] continued the research of Suzuki et al. [68] to also quantify the effects of Power to Syngas on the reduction of coke consumption. In this case, only the scenario that includes carbon capture was considered. The energy source (HTGR), the size of the blast furnace (10.5 kt pig iron/day) and the percentage of BF processed (30 % diverted, 90 % captured, and 60 % converted) were the same. As novelty, this study incorporated detailed models in Aspen Plus for the high-temperature gas-cooled reactor, the gas turbine (power producer), and the SOEC. They showed that the coke input is reduced a 4.3 % using this concept, compared to conventional blast furnaces.

In contrast to previous research, Hisashige et al. [78] applied Power to Syngas to the “Packed bed type Partial Smelting Reduction process” (PSR). This process concurrently smelts scrap and reduces iron ore in a low shaft furnace. Iron scrap is useful in the sense that it is already in the reduced state and thus can be regenerated to steel with less energy consumption and CO₂ emissions. However, iron ore is still necessary to dilute the tramp elements present in scrap, which would otherwise degrade the quality of the final steel. The integrated plant was modelled in Aspen Plus, by modifying the process flow diagram from Hayashi et al. [77]. The new model comprises shaft furnace, SOEC, pressure

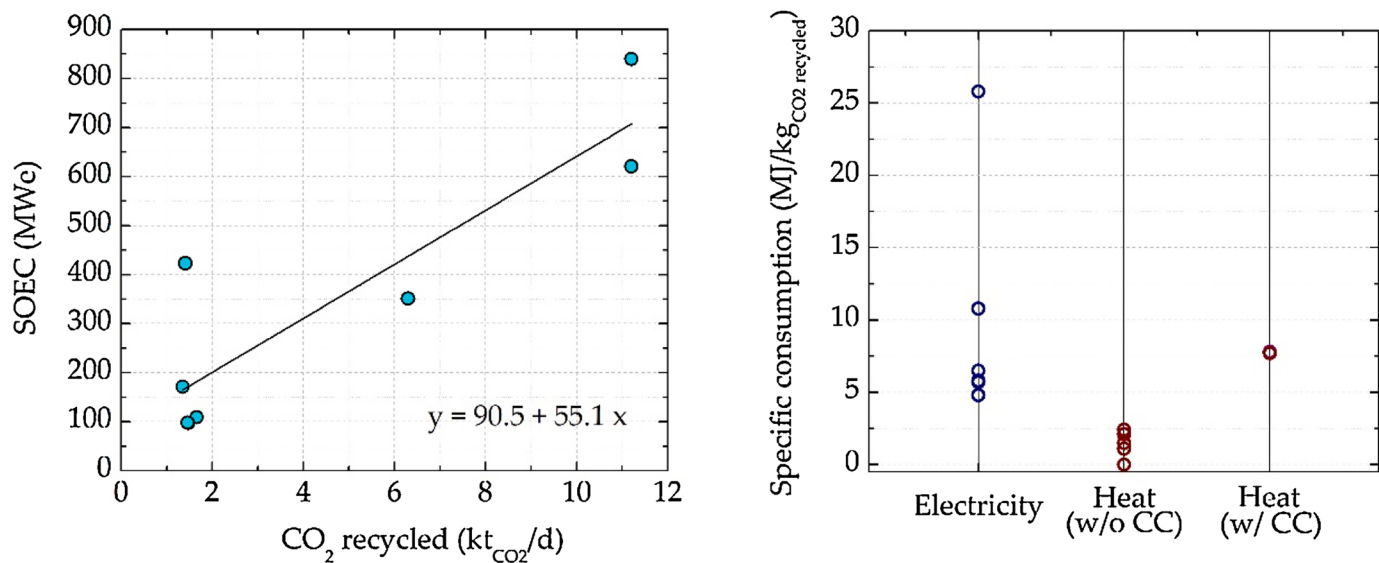


Fig. 10. SOEC power capacity vs. CO₂ recycled, and Electrical and thermal (w/ and w/o CCS) specific consumptions. Data computed from the papers reviewed concerning Power to Syngas integration.

swing adsorption (PSA) for CO separation, and auxiliary systems. The PSR gas is burned to obtain a high concentration CO₂ gas before SOEC. Since CO₂ conversion in the SOEC is assumed 70 %, CO-specific PSA (80 % recovery) is used at the outlet in order to divert a pure stream of CO to the shaft furnace. The new operating conditions in the furnace were predicted by the Rist model [79], and validated with empirical results from a small furnace demonstration [80]. A maximum of 10 % scrap ratio (percentage of iron provided in the form of scrap with respect to the total input of iron) was considered in the furnace to avoid excessive drops in temperature. Moreover, the recirculation of PSR gas was limited to 70 % (i.e., reintroduction of 428.7 kg_{CO}/t_{pig iron} in the furnace) since the rest of the gas is used as fuel for other sub-processes. Under this scenario, the CO₂ emissions were reduced a 22 % compared with conventional blast furnaces [78]. Data in 11 could not be computed from the data provided in the article.

6.1.3. Discussion on the concept of Power to Syngas using SOEC

From the review and analysis of the different studies presented here,

some conclusions can be drawn. First of all is that, despite some optimistic studies ideally consider 100 % CO₂ recycling, more reasonable analyses conclude that potential reductions of CO₂ emission with respect to conventional blast furnaces would lie between 11 % and 22 %.

Data show that the specific electricity consumption, in terms of electricity required per kilogram of CO₂ recycled, usually ranges between 4.8 MJ/kg_{CO₂} and 10.8 MJ/kg_{CO₂}. The typical thermal energy consumption varies from 1 to 2.5 MJ/kg_{CO₂} for configurations in which carbon capture is not used. If CO₂ is separated from the blast furnace gas before introduced in the SOEC, the overall thermal consumption increases to 7.8 MJ/kg_{CO₂}. In terms of the required power capacity, the SOEC seems to follow a linear trend with the amount of CO₂ recycled, according to the results of the different studies (Fig. 10).

As none of the reviewed papers deal with economics, categorical conclusions cannot be drawn in this issue. From a technical point of view, carbon capture may be necessary to guarantee good operation conditions in some SOEC (technical limitations). However, in the global picture, it would be preferable to supply the BF gas directly to the SOEC

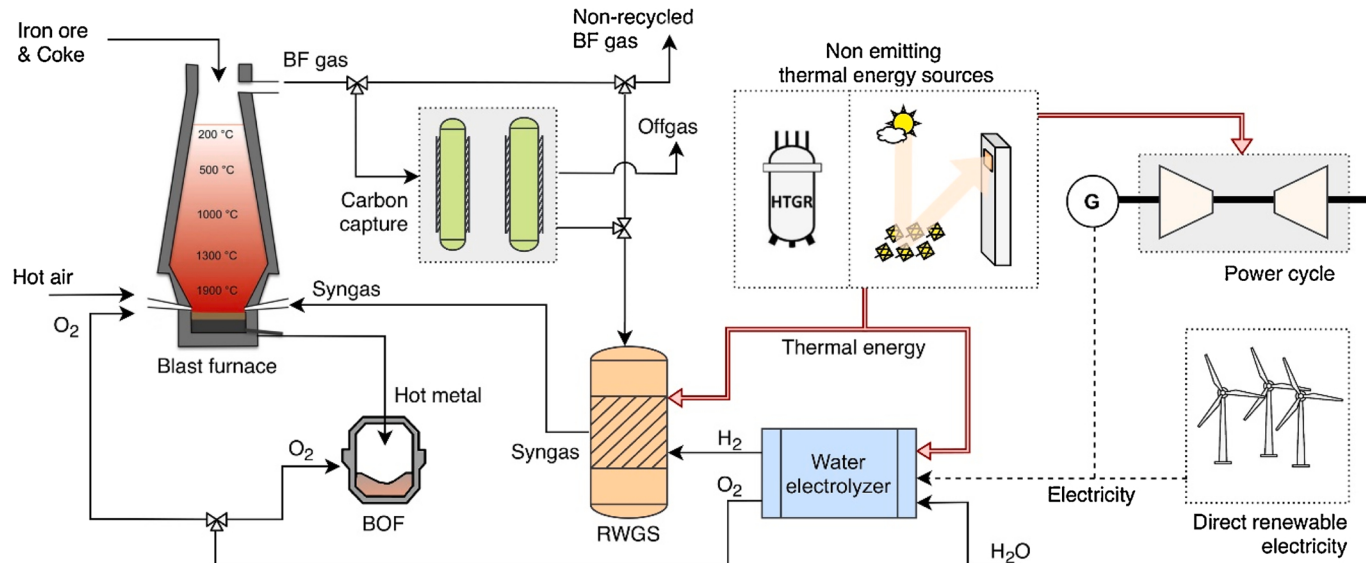


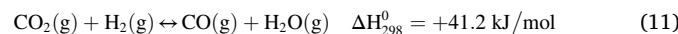
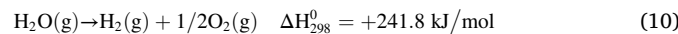
Fig. 11. Conceptual diagram of the integration of Power to Syngas (RWGS) in the Iron and Steel industry.

if possible (without a previous carbon capture stage). This is because, in this way, the H₂ that is initially present in the BF gas will be reintroduced in the furnace after passing through the SOEC, thus reducing the coke demand in the blast furnace. Additionally, if carbon capture is not used, the thermal energy requirement of the system diminishes.

From a qualitative point of view, it must be mentioned that all research so far in the topic of Power to Syngas have considered nuclear power as the energy source for the integration. There is a lack of studies in literature analyzing the effects of integrating variable power sources such as solar or wind power. The main reason for this is that all studies were focused on Japan. Also, despite several authors stated that the O₂ by-produced in the SOEC can be used in other processes to increase the overall efficiency of the plant, its integration has not been thoroughly analyzed. Other important point to mention is that all studies considered chemical equilibrium in the simulations, so detailed analyses using rate-based models could still improve the knowledge on the topic.

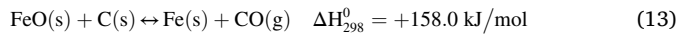
6.2. Water electrolysis and RWGS route

The other possible route for Power to Syngas integration is by using water electrolysis. This produces H₂ as intermediate product to subsequently reduce CO₂ through the reverse water-gas shift reaction (Eqs. 10 and 11).



Since RWGS is endothermic, thermal energy from a non-emitting source should be supplied to the reactor (Fig. 11). If a high-temperature SOEC is used for water electrolysis, heat will be also necessary. The conceptual diagram is quite similar to that presented in Fig. 7, with the difference that there is an additional input of water to the system, required by the electrolyzer.

As in the previous integration route, Power to Syngas affects blast furnace operation because of the recirculation of gas. In this case, the necessity of adjusting the coke input to account for the carbon content of the syngas is still present. In contrast, the temperature inside the blast furnace is less affected when using the RWGS route [68]. The unreacted hydrogen remaining in syngas will reduce iron oxides inside the blast furnace (Eq. 12), replacing solid carbon as reducing agent (Eq. 13). Thus, in practice, the overall process becomes less endothermic.

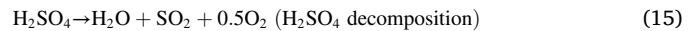
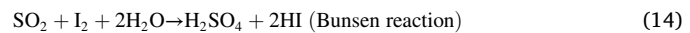


This palliate the energy consumption of the side-reaction related to the additional CO₂ presence (Eq. 9), which tends to reduce the temperature in excess. Suzuki et al. [68] estimated that the temperature inside the blast furnace may decrease 45 °C when using the RWGS route, instead of about 100 °C as is the case for the CO₂ electrolysis route.

6.2.1. Studies on the concept of Power to Syngas using RWGS

Among the reviewed papers, only Kato [81] studied the Power to Syngas route based on water electrolysis and RWGS reaction. Aiming for comparison, he used the same configuration than he analyzed for the CO₂ electrolysis route. Nuclear power (HTGR model GTHTR300) supplies the thermal energy required for heating and electricity production. Part of the sensible heat from the helium coolant (from 850 °C to 828 °C) is used to preheat the water electrolyzer, while other part for the RWGS reactor (from 828 °C to 810 °C). The rest is used in a gas turbine (43.3% efficiency) to supply electricity to the electrolyzer. He assumed a SOEC electrolyzer for water electrolysis, with an electric consumption of 2.7 kWh/Nm³H₂ and a thermal energy consumption of 0.6 kWh/Nm³H₂. The blast furnace is assumed to produce 8.6 kt_{pig} iron/day, emitting 6.3 ktCO₂/day. Thus, to process the 100 % of the CO₂ emissions, an electrolyzer of 359.6 MWe would be required. Moreover, the thermal necessities for the electrolyzer and the endothermic RWGS are 80.2 MWt and 68.8 MWt, respectively. The overall electric and thermal specific consumptions of the concept, per kilogram of CO₂ recycled, are 4.9 MJe/kgCO₂ and 2.0 MJt/kgCO₂.

A similar concept to the Power to Syngas route based on RWGS was studied by both Suzuki et al. [68] and Hayashi et al. [77]. The difference lies in the hydrogen production technology. Instead of water electrolysis, they used an iodine-sulfur process, which is a thermochemical water splitting process comprising three reactions (Eqs. 14–16) [77].



According to the criterion of this review, this cannot be considered as

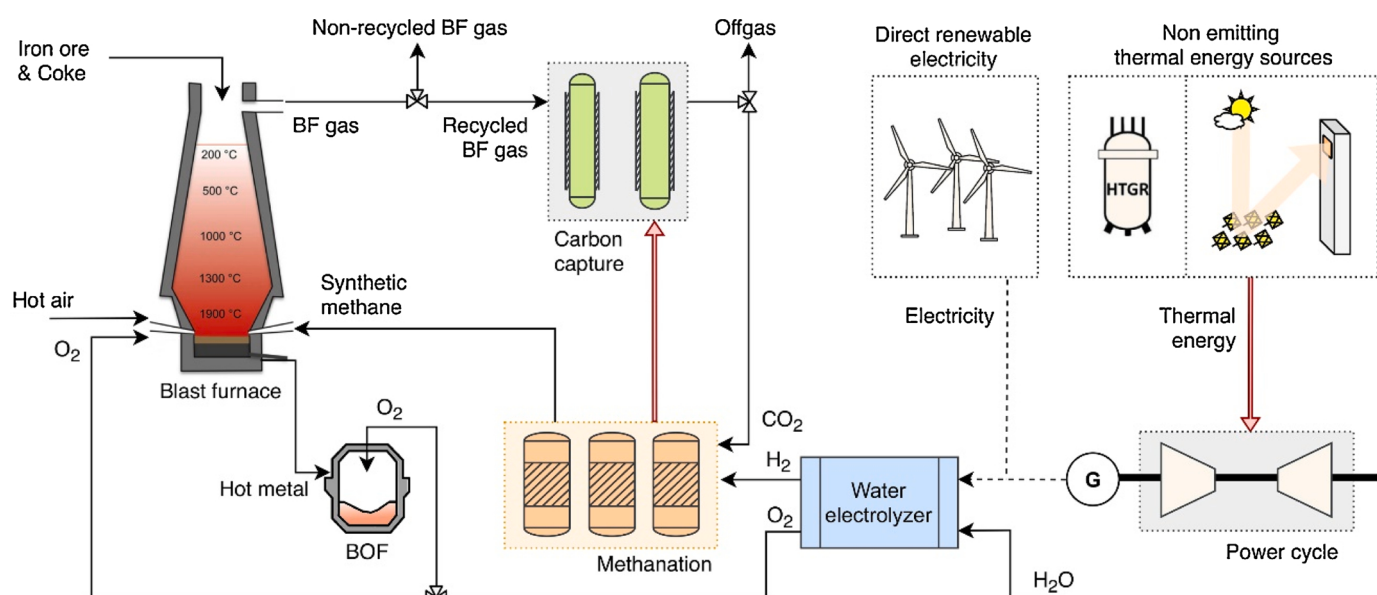
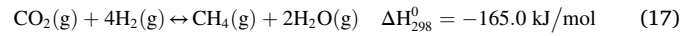


Fig. 12. Conceptual diagram of the integration of Power to Methane in the Iron and Steel industry.

a Power to X process, since it lacks of the initial electrolysis step. Therefore, these studies will not be compared with other research. Nevertheless, as the input energy to the iodine-sulfur may come from non-emitting sources, the main results are briefly commented here. Suzuki et al. [68] concluded that 8.34 % emission reduction compared to conventional system can be achieved when the 30 % of the blast furnace gas is recycled through this route. Moreover, the coke input is reduced a 10.3 %. Hayashi et al. [77] came to a similar result, obtaining a 8.2 % CO₂ emission reduction compared to conventional blast furnace. This abatement is greater than for Power to Syngas based on CO₂ electrolysis and carbon capture, whose reduction ratios are around 3.4 %. The reason is that the H₂ from RWGS ends up acting as reducing agent in the blast furnace, thus additionally reducing the coke input. However, the specific thermal energy consumption of the overall system is four times higher, requiring 9.87 GJt per ton of hot metal.

7. Power to methane

The concept of carbon recycling to regenerate CO₂ to methane, based on the combination of water electrolysis and CO₂ methanation (Eqs. 10 and 17), was firstly proposed by Koji Hashimoto early in 1994 [82]. It was not until 2010 that Kato suggested the possibility of integrating the concept in the Iron and Steel industry [67].



The typical conceptual diagram of integration of Power to Methane and ironmaking is presented in Fig. 12. In this case, the part of the BF gas that is recycled has to pass through a carbon capture stage, in order to avoid excessive nitrogen content in the methanation process. Despite nitrogen does not affect the methanation reaction, if BF gas were directly diverted to the methanator, the required volume of reactor would be unreasonable from an economic point of view. Besides, the exothermal heat from methanation can be used to satisfy the thermal energy requirements in the carbon capture process, so it does not entail a significant energy penalization. The synthetic methane produced is used as reducing agent in the blast furnace, and the oxygen from the electrolyzer can be optionally injected to the blast furnace or the basic oxygen furnace. Thermal energy input for the electrolyzer was not depicted in the diagram, as it was assumed Alkaline or PEM technology because of their higher market maturity compared to SOEC.

7.1. Studies on the concept of Power to Methane

Only a couple of studies have been found in literature about this concept of integration, and both of them have been published recently. The first one belongs to Hisashige et al. [78], who compared the application of Power to Syngas and Power to Methane on a “Packed bed type Partial Smelting Reduction process” (PSR). This process uses scrap steel products and iron ore as raw materials in a shaft furnace for the production of steel. Scrap allows reducing the specific energy consumption and CO₂ emissions of the process (as it is already in a reduced state), while iron ore helps diluting the tramp elements present in scrap. The integrated plant was modelled in Aspen Plus on the basis of the work of Hayashi et al. [77]. The process flow diagram comprises shaft furnace (validated with data from [80]), pressure swing adsorption stages (for carbon capture and CH₄ separation), CH₄ synthesis reactor (at 300 °C and 5.3 bar), and auxiliary systems. The carbon capture stage (80 % recovery) is used on the PSR gas to introduce a pure stream of CO₂ to the methanation stage. Additionally, a CH₄-specific PSA (70 % recovery) is used at the outlet of methanation, in order to blown pure CH₄ into the shaft furnace. The scrap ratio in the PSR was limited to 10 % (percentage of iron from scrap with respect to the total iron) and the gas recirculated in the furnace to 23 % (33 kg_{CH4}/t_{pig} iron). Under this operating conditions, the CO₂ emissions were reduced a 13 % compared with conventional blast furnaces.

Table 12

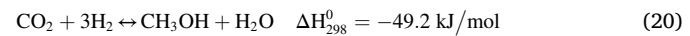
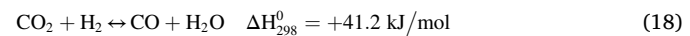
Typical data of steel mill gases [83,86,85,90], and their corresponding ratio R = (H₂ – CO₂)/(CO + CO₂) for methanol production.

	Units	BFG	COG	BOFG
CO	%vol	20 – 25	6 – 7	57 – 64
CO ₂	%vol	22 – 24	2 – 3	14 – 17
CH ₄	%vol	0	22 – 25	0
C _X H _Y	%vol	0	2 – 4	0
H ₂	%vol	3 – 4	61–63	3 – 5
H ₂ O	%vol	0	0	0 – 12
O ₂	%vol	0	0	0 – 1
N ₂	%vol	47 – 53	2 – 6	14 – 16
Ratio R	–	–0.4 – -0.5	6.2 – 7.4	–0.1 – -0.2
Specific volumetric flow	Nm ³ /t _{steel}	1065.8	58.4	51.1
Lower heating value	kWh/Nm ³	0.81 – 0.91	4.78 – 5.02	2.08 – 2.27
Specific emissions	kg _{CO2} /kWh	0.97 – 1.08	0.14 – 0.17	0.66 – 0.68

Rosenfeld et al. [83] analyzed the integration of Power to Methane, together with biomass gasification (mainly for further H₂ supply), in a steel plant. They modelled a theoretical steel plant based on black box models using stream data from public reports from the European Steel Association and the European Commission [84]. The model comprises sinter plant, coke oven, blast furnace (14.5 kt_{pig} iron/day), basic oxygen furnace, hot strip mill, biomass gasification plant, PEM electrolyzer (4.4 kWh/Nm³ H₂) and catalytic methanation plant. The aim of the study was to completely substitute the fossil natural gas consumption of the steel plant (1.9 MJ/kg_{pig} iron) with synthetic natural gas. Assuming that the electrolyzer and the gasification plant provides H₂ in the same proportion, the power capacity required in the electrolyzer and gasification plant would be 273 MWe and 275 MWth, respectively. In this case, the 13.6 % of the emissions from the blast furnace would be recycled in methanation. If the size of the gasification plant is limited to 105 MWth (according to state-of-the-art), the electrolysis capacity should rise to 641 MWe. Since the carbon provided by the gasification gas diminishes in this case, the percentage of blast furnace gas that is recycled increases to 18.6 %. Rosenfeld et al. also quantified the power capacities that would be required to completely recycle the blast furnace gas and the basic oxygen furnace gas. These amount to 2.03 GWe and 2.04 GWth for the electrolyzer and the gasification plant, respectively, assuming equal H₂ contribution [83].

8. Power to methanol

Methanol is one of the most produced organic basic chemicals worldwide (90 Mt/y in 2017). It can be used as energy vector for energy storage, as fuel for transport, or as feedstock for the production of valuable chemicals (olefins, dimethyl ether, etc.) [85]. It is synthesized from a gas mixture of H₂, CO and CO₂ through the combination of three chemical equilibrium reactions (Eqs. 18–20). These take place in catalytic reactors using Cu/Zn/Al₂O₃ catalysts, operating in the range 230–270 °C and 60–100 bar [86].



The idea of producing methanol from blast furnace gas was already studied in 1993 by Akiyama et al. [87,88]. This synthesis process becomes more efficient the closer the reactants ratio R = (H₂ – CO₂)/(CO + CO₂) is to 2 [89]. However, typical compositions of steel mill gases [83] are far from this ratio (Table 12), so their direct use is not suitable. In the case of COG, there is a lack of CO that is typically covered either by reforming the methane present in the gas or by mixing with a supplementary carbon feed (e.g. coal-gasified gas or BOF gas) [89]. On

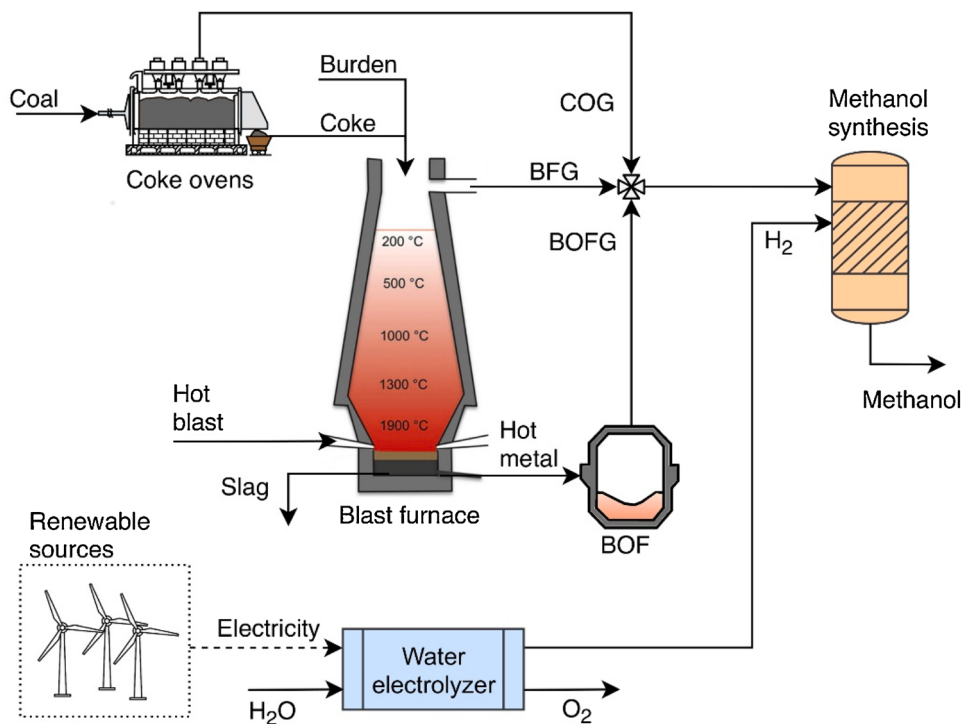


Fig. 13. Conceptual diagram of the integration of Power to Methanol in the Iron and Steel industry.

the other hand, the limiting reactant to use BF and BOF gases in methanol synthesis is H₂, therefore requiring offsite production, which is conventionally based in steam methane reforming (i.e., hydrogen coming from fossil fuel).

Actually, methanol synthesis from steel mill gases can be considered nowadays as a commercial technology, since China already produced in 2011 the 11 % of its total methanol production through these processes [86]. However, none of the mentioned solutions for methanol production can be seen as Power to X concepts since they do not involve the consumption of renewable electricity through an electrolysis process (in fact, they promote the emission of further CO₂). In this section, we focus only on the few research studies that do include H₂ coming from water electrolyzers to properly adjust the reactants ratio and thus perform a sustainable methanol synthesis. The conceptual diagram of Power to Methanol applied to the iron and steel industry is presented in Fig. 13, where there is the possibility of using BFG, COG and BOFG separately or mixed.

8.1. Studies on the concept of Power to Methanol

Among the screened papers in this review, only 5 are actually Power to Methanol concepts, being developed most of them under the framework of the Carbon2Chem® project.

Stießel et al. [91] compared different synthesis routes for the recycling of steel mill gases to valuable products (methanol, OME, urea, polymers and alcohols). These were ranked according to 20 criteria grouped in three categories (technology, economics, and acceptance), following the methodology of weighting factors used by Tremel et al. [92]. Results showed that methanol and urea are the preferred routes for using steel gases because of their technical robustness, and the stability and growth prospects of the market [91]. The methanol synthesis was further analyzed under specific scenario for 2030 (electricity prices, gas volumes, etc.), which was defined through a five-phase model suggested by Kosow et al. [93] and Gausemeier et al. [94]. The plant, assessed with black box models, had 1 GW PEM electrolysis (5.0 kWh/Nm³H₂) and a methanol production of 0.65 kt/day (150 MW). The carbon source was off-gas from a conventional blast furnace. The resulting cost of methanol

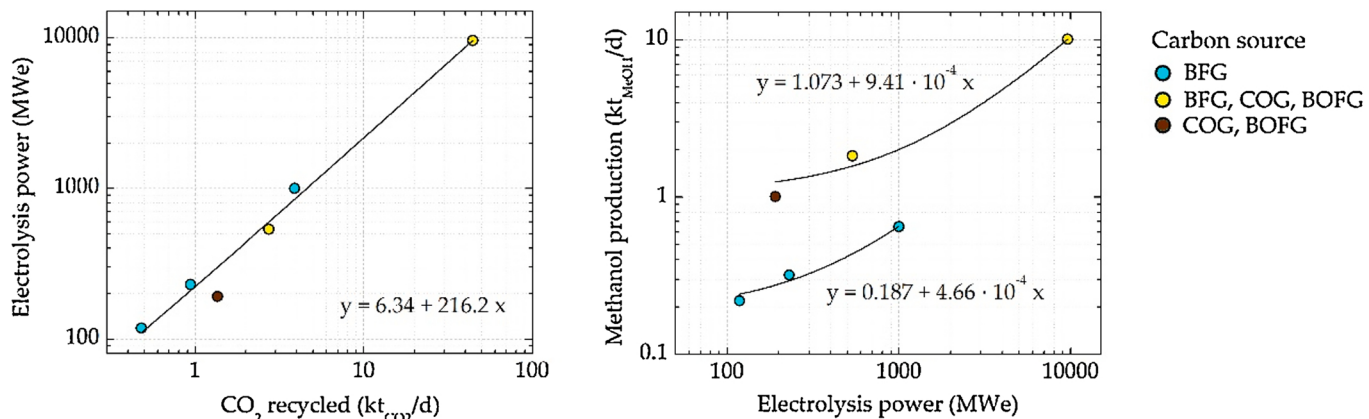
was 760 €/t, and the average share of green electricity consumed by the electrolyzer from the grid was 60 %. Authors stated that there was no CO₂ savings in this case, due to the CO₂ emissions associated to the electricity production. A renewable share of at least 89 % would have been required to achieve a net reduction in CO₂ emissions [91].

Likewise, Bender et al. [95] analyzed different techno-economic scenarios for the production of methanol from steel mill gases, using black box models (overall energy and mass balances) of the Thyssenkrupp steel mill in Duisburg, Germany (31.9 kt_{hot} metal/day, 60 kt_{CO2}/day). One important aspect that Bender et al. took in consideration, as opposed to Stießel et al., is that off-gases are typically used as fuel in integrated power plants for electricity self-consumption, so this energy would no longer be available if gases are used for methanol synthesis. In the analyzed scenarios, this electricity is substituted by renewable electricity purchased from the grid (11.8 GWh/day). Additionally, in those other conventional uses of steel mill gases that cannot be replaced by renewable electricity (i.e., coke plant, rolling trains and steam generation), natural gas is used instead (a total of 14.2 GWh/day). The studied plant had an electrolysis power capacity of 9.6 GW (4.56 kWh/Nm³H₂) that consumes 230 GWh/day of electricity, and a methanol synthesis reactor that produces 10.1 kt/day (2.3 GW). The CO₂ emissions are reduced by 74 % in this case, but the total investment costs (11,374 M€) lead to economic losses (-5672 M€/y). Under this framework, the CO₂ avoidance costs are 352 €/t_{CO2}, which is way beyond the current CO₂ European Emissions Allowances (25 €/t_{CO2}) [14].

Unlike the previous authors, Schlüter et al. [86] did develop a detailed model of methanol synthesis that included kinetics, heat transfer and different boundary conditions depending on the reactor type (tube bundle or quenched bed). For modelling the rest of the plant, they used an engineering model library from Fraunhofer UMSICHT that combines individual models of the different stages (electrolyzer 4.54 kWh/Nm³H₂, buffer tanks, compressors, splitters, etc.), implemented in COMSOL Multiphysics®. The steel mill had a production capacity of 16.4–21.9 kt_{steel}/day, producing a total of 2.74 kt/day of CO₂ equivalent emissions (0.34 kt_{CO2}/day in COG, 1.38 kt_{CO2}/day in BFG and 1.02 kt_{CO2}/day in BOFG). Schlüter et al. compared one scenario in which the three off-gases are diverted to the methanol plant, with other scenario in

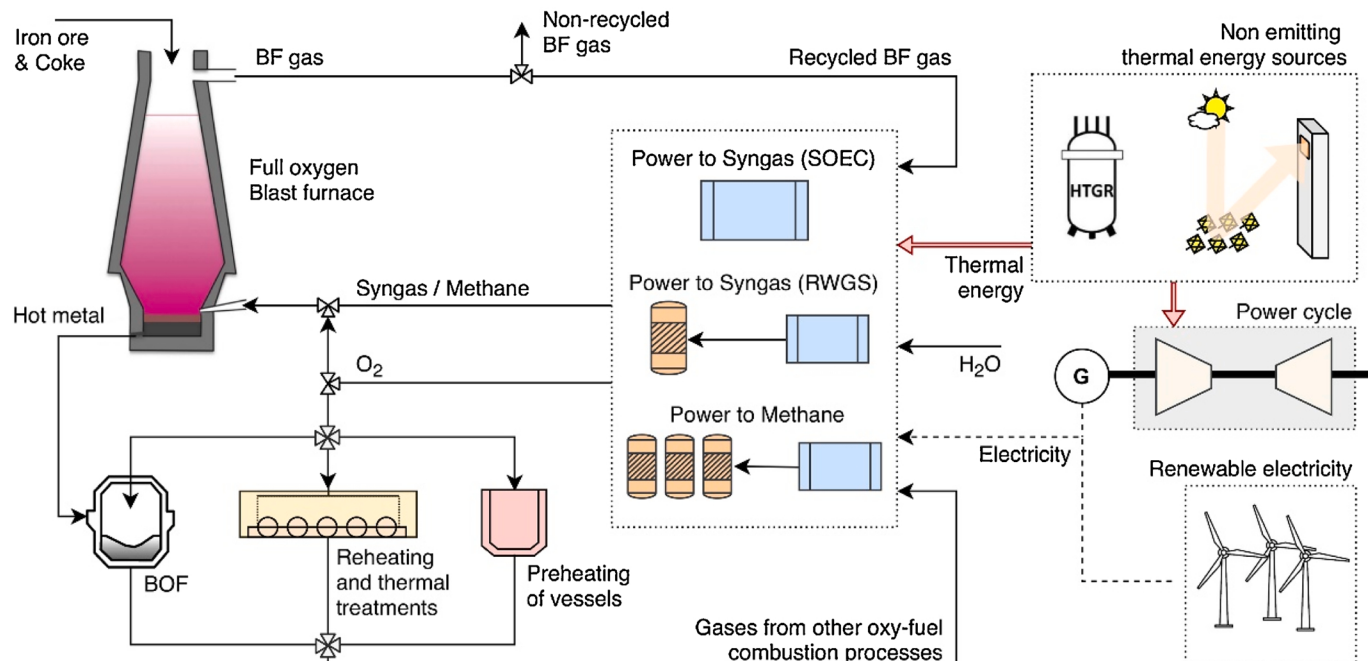
Table 13Studies on Power to Methanol integration in the Iron and Steel industry (ordered by CO₂ source).

Study	CO ₂ source	Equivalent CO ₂ emissions treated (kt _{CO₂} /day)	Electrolysis (MWe)	Specific consumption (MJe/kgCO ₂ recycled)	Methanol production (kt/day)	Specific cost of methanol (€/t _{MeOH})
Stießel et al., 2018 [91]	BFG	3.9	1000	22.1	0.65	760
Kim and Han, 2020 [85]	BFG	0.48 – 0.94	118 – 230	21.2	0.22 – 0.32	880–1140
Bender et al., 2018 [95]	BFG, COG, BOFG	44.4	9600	18.7	10.1	1540
Schlüter et al., 2018 [86]	BFG, COG, BOFG	2.74	536	16.9	1.83	n/a
Schlüter et al., 2018 [86]	COG, BOFG	1.36	191	12.1	1.01	n/a

**Fig. 14.** Electrolysis power capacity vs. CO₂ recycled, and methanol production vs. electrolysis power capacity. Data computed from the papers reviewed concerning Power to Methanol integration.

which BFG is not treated. In the first case, the electrolysis power capacity required is 536 MW, decreasing to 191 MW if BFG is not used in methanol synthesis. The corresponding methanol productions in the plant are 1.83 kt/day (422 MW) and 1.01 kt/day (233 MW), leading to CO₂ emission reduction of 82.5 % and 46.1 %.

Kim and Han [85] also developed a detailed model for the synthesis of methanol in steel plants, comprising kinetics over a commercial Cu/ZnO/Al₂O₃ catalyst, a Lurgi reactor (247 °C, 100 bar), and auxiliary equipment (separators, coolers, compressors, etc.) implemented in Aspen Plus. In this study, the only gas that is diverted from the steel

**Fig. 15.** Conceptual diagram of the integration of Power to Gas and oxy-fuel combustion processes in the Iron and Steel industry.

plant to the methanol plant is BFG (20 %vol CO, 24 %vol CO₂, 3%vol H₂ and 53 %vol N₂). Different scenarios were analyzed, varying the amount of BFG treated from 6.5 to 12.6 Nm³/s (corresponding to 0.48 – 0.94 kt_{CO2}/day). The electrolysis capacity required in the plant (assuming 4.8 kWh/Nm³) varied between 118 MW and 230 MW. The methanol production obtained was 0.22 – 0.32 kt/day (51.6–74.6 MW), and their techno-economic analysis showed that the methanol cost under this scenario would be in the range 880–1140 €/t.

8.2. Discussion on the concept of Power to Methanol

The relevant data of the studies reviewed in this section are summarized in Table 13 for comparison purposes. The order of presentation in the table is in descending order of specific energy consumption, to clearly show the influence of the carbon source on this parameter. It can be seen that the highest energy consumptions take place when the only off-gas treated is BFG (21–22 MJ/kg_{CO2}), because of its low hydrogen content. If blast furnace gas is mixed with COG, the specific consumption is somewhat reduced (17–19 MJ/kg_{CO2}), since coke oven gas has H₂ contents in the range 61–63 %vol. Lastly, when BFG is not used, the efficiency of the overall integrated process remarkably increases (12 MJ/kg_{CO2}). In this case, the H₂ that is present in COG becomes relevant compared to the total inlet gas flow in the methanol synthesis process, because it does not get diluted in BFG.

This effect is also noticeable in the graphs of Fig. 14, when plotting the electrolysis power capacity versus the CO₂ recycled. Those studies that only comprises BFG are slightly above the linear fitting (i.e., more consumption), while those using COG are on or below the curve (i.e., less consumption). Nevertheless, the linear adjustment seems to properly cover all the potential situations, since the adjusted coefficient of determination (R^2) of the linear fitting is above 0.999. Additionally, when plotting the methanol production versus the electrolysis capacity (Fig. 14, right), the effect of the hydrogen content of COG becomes even clearer. For a given electrolysis power capacity, the methanol production will be higher if COG is used. By using these two graphs of Fig. 14, a Power to Methanol system for the Steel industry can be sized as first approach. If the CO₂ recycling aim is decided, the electrolysis capacity required can be then calculated (Fig. 14, left), and with it the corresponding methanol production depending on the carbon source used (Fig. 14, right).

Regarding methanol production costs, the results of the different authors show a potential range of 760–1540 €/t_{MeOH}. Higher costs are found when different carbon sources are used in the plant, mainly because of the requirement of installing multiple gas treatment stages. In any case, the costs are still far from competing with the cost of producing

methanol through conventional processes (210–530 €/t_{MeOH}) [85].

9. Novel proposals based on Power to X and oxy-fuel combustion for the Iron and Steel industry

A novel concept that has not been proposed or studied in literature is the combination of Power to Gas and oxy-fuel carbon capture for CO₂ mitigation in the Iron and Steel industry. Whether by the route of Power to Syngas or Power to Methane, there is available by-product oxygen that can be used in oxy-fuel combustion processes to attain a high concentrated CO₂ stream. This way, the effluent gas can be directly diverted to the recycling process, thus avoiding the energy penalizations of CO₂ separation. The concept is presented in Fig. 15, showing the possibility of integration in different parts of the plant.

In full oxygen blast furnace (FOBF), pure oxygen is used for combustion instead of oxygen-enriched air, thus obtaining a top gas with very little contain of nitrogen. In this type of blast furnaces, it is usual to separate the CO₂ from the top gas for permanent storage, and to recycle the hydrogen and carbon monoxide to act as reducing agents in the furnace (Fig. 16, left). This type of configuration is typically called Top Gas Recycling Blast Furnace (TGRBF) [96]. By integrating Power to Gas (Fig. 16, right), the separation stage and the subsequent sequestration of CO₂ are replaced by the methanation reactor (or SOEC), and CO₂ is converted to methane (or syngas). Therefore, the corresponding energy penalizations and additional costs of carbon capture, transport and underground storage are avoided. Moreover, according to Ariyama et al. [97], FOBF enables injecting large amount of natural gas in addition to pulverized coal, thus making possible to mitigate CO₂ emissions while maintaining the energy supply required in downstream processes (i.e., keeping energy consistency in the integrated steel plant for energy self-sufficiency).

Despite integrating the concept in the blast furnace is the most interesting option in terms of CO₂ mitigation, the FOBF technology is not commercial yet (current TRL is 6–7) [99]. Zuo and Hirsch [100] reported experimental results from a 9 m³ TGRBF, located at LKAB (mining company), Sweden. They used vacuum pressure swing adsorption as carbon capture method for removing CO₂ of the top gas. They found 24 % savings in carbon consumption and 76 % reduction in CO₂ emissions when assuming the underground storage of the corresponding captured CO₂ [101]. On average, the carbon input decreased from 470 kg/t_{hot} metal to 350 kg/t_{hot} metal [99]. It is worth to mention that oxy-fuel combustion could also be applied to the steelmaking route based on Electric arc furnace. In that case, the slag door should be shut during operation, and the furnace operated with a slight overpressure [102].

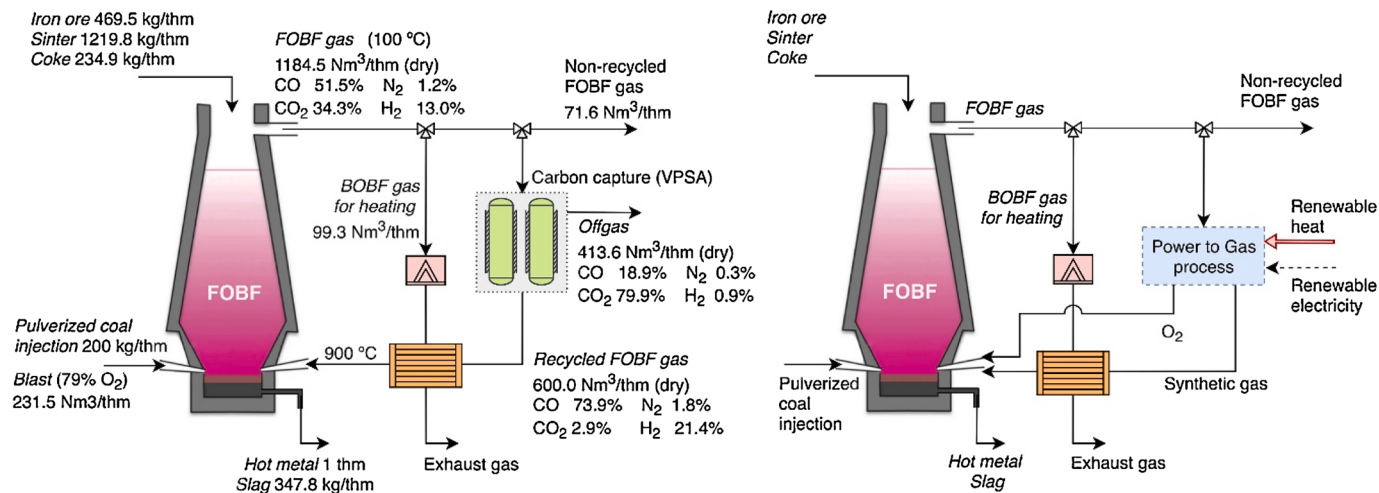


Fig. 16. Conceptual comparison between the standalone full oxygen blast furnace with top gas recycling (TGR-FOBF) and its integration with Power to Gas. Data for TGR-FOBF is taken from [98].

Table 14

Research projects on Power to X processes applied to the Iron and Steel industry.

Route	Project Name	Duration	Location	Abatement potential	TRL	Market entry [139]	Ref.
Power to Steel	SIDERWIN	2017 – 2022	Metz, France	87 %	5–6	2025 – 2030	[105,106]
Power to Hydrogen	SuSteel	2016 – 2023	Leoben, Austria	> 80 %	6	2030 – 2035	[109,112]
Power to Hydrogen	Hybrit	2016 – 2024	Luleå, Sweden	95 %	5 – 7	2025 – 2035	[111,112]
Power to Hydrogen	SALCOS	2017 – 2020	Salzgitter, Germany	60 % – 95 %	7 – 9	2030 – 2035	[112,140]
Power to Hydrogen	H2Future	2017 – 2021	Linz, Austria	> 80 %	7 – 8	2030 – 2035	[116,117]
Power to Hydrogen	Hydrogen path	2019 – 2024	Duisburg, Germany	30 % - 80 %	5–6	2025 – 2050	[119,123]
Power to Methane / Methanol	i3upgrade	2018 – 2021	Leoben, Austria	n/a	4 – 5	n/a	[124,126]
Power to Methanol	FReSMe	2016 – 2020	Luleå, Sweden	25 %	6	n/a	[128,130]
Power to Methanol	Carbon2Chem	2018 – 2025	Duisburg, Germany	60 – 90 %	7 – 8	2025 – 2030	[112,119]
Power to Fuels	eForFuel	2018 – 2022	Postdam, Germany	n/a	4	n/a	[137,138]

Oxy-fuel combustion can also be used during preheating of ladles and converter. Ladles are the vessels used to transport molten metal, while the converter is the vessel used in basic oxygen steelmaking process. This application is already commercial and used by companies like Sandvik, Outokumpu, or Acerinox. Vessels with capacity between 0.5 and 20 tons require thermal powers for preheating in the range 0.15 – 0.5 MW. For large vessels with 90–100 t capacity, the input thermal power increases to 1.4–2.0 MW. The benefits of oxy-fuel preheating compared to air-fired preheating are 50%–55% less fuel consumption and 20%–25% reduction of flue gas produced [103].

Other commercial application of oxy-fuel combustion is steel reheating and heat treatment. These techniques are already used in, for example, soaking pit furnaces, walking beam furnaces, catenary furnaces and rotatory hearth furnaces. Companies such as ArcelorMittal, Ascométal, SSAB or ThyssenKrupp Steel use oxy-fuel furnaces for these processes. The production capacity of the furnaces, compared to conventional air-fired technology, may increase by 30%–50%, while fuel consumption decreases in the range 20%–65%. Typical thermal energy consumptions in oxy-fuel reheating furnaces are 260–270 kWh/t_{cold} metal, plus an additional electricity consumption of 25 kWh/t_{cold} metal for the production of oxygen [104]. Besides, the latter is avoided by using the proposed integration of Power to Gas and oxy-fuel consumption, since the oxygen is available as by-product from the electrolyzer. Therefore, this concept is clearly competitive compared to air-fire reheating, which consumes about 360 kWh/t_{cold} metal [102].

10. Power to X projects in the Iron and Steel industry

In this section, it is presented a non-exhaustive list of research projects concerning Power to X processes that are applied to the iron and steel industry. For the revision, the projects are grouped by technology (i.e., PtSteel, PtH₂, PtSyngas, PtMethane, PtMethanol, and others) and ordered by the starting year of the project (in ascending order). There is a total of 10 projects listed in Table 14, among which 5 are focused in the Power to Hydrogen route. All the projects started within the last five years (from 2016 to 2021) and most of them are developed in Europe.

10.1. SIDERWIN (Power to Steel; 2017–2022)

The SIDERWIN project (Development of new methodologies for industrial CO₂-free steel production by electrowinning) aims at developing an electrolysis process that decomposes iron oxides (e.g., hematite) into iron metal and oxygen gas under mild conditions. The process is based on the ULCOWIN pilot, developed in a previous project [105]. The research is led by ArcelorMittal, which worked for 12 years on the development of this technology from TRL 0 to 4. Currently, the objective is to reach TRL 5–6 [106]. Works for the new building that will locate the SIDERWIN pilot at ArcelorMittal facilities in Maizières-lès-Metz (France) are ongoing [107], but no further information has been released. The overall budget of the project is 6.8 M€, funded by the European Commission through the H2020 programme [106].

10.2. SuSteel (Power to Hydrogen; 2016–2023)

K1-MET GmbH, Voestalpine and Montanuniversität Leoben collaborate in the SuSteel project (Sustainable steel production utilizing hydrogen) aiming for a CO₂-free production of steel through the utilization of hydrogen plasma in a smelting reduction process. The hydrogen acts as reducing agent, while the plasma state offers the thermal energy required for melting the metallurgical iron [108].

First results were obtained at laboratory scale in Montanuniversität Leoben, with iron ore inputs of 50–200 g. Currently, a pilot plant has been erected at the Donawitz site of Voestalpine, able to work in a scale of 50–80 kg of iron ore input. The reactor consists of a conical vessel with refractory. The cathode of the plasma torch is located in the roof of the vessel, and the water cooled anode is placed at the bottom. The fed material is introduced into the plasma through the upper electrode, which is hollow. Different ratios of plasma gas (argon or nitrogen) to reducing gas (hydrogen) are studied to characterize the efficiency of the process [109]. At lab scale, the average degree of hydrogen utilization was 28 %, with runtimes of about 30 min [110].

The production of hydrogen via renewable electricity for this process is studied through the H2Future project, in which K1-MET and Voestalpine also participates. A total capacity of 6 MW of PEM electrolysis was installed in the Voestalpine Linz site [109].

10.3. HYBRIT project (Power to Hydrogen; 2016–2024)

In the HYBRIT project [111], three Swedish companies cooperate to build a pilot plant for fossil-free steel production (LKAB – iron ore producer, SSAB – steel manufacturer, and Vattenfall – power utility). The HYBRIT concept is based on the direct reduction of iron pellets by hydrogen in a shaft furnace, followed by an electric arc furnace. The hydrogen will be produced through water PEM electrolyzer [112], which would consume 15 TW h per year if coal is completely replaced. The project also comprises the development of a hydrogen storage facility and a fossil-free iron pelletizing plant.

According to the feasibility study of the project, this concept would increase the production costs about 20%–30% under current scenario. However, the declining prices in electricity and increasing costs for CO₂ emissions would make the concept able to compete with conventional steelmaking in the mid-term. Thus, the pilot phase is planned to last until 2024, followed by a demonstration phase taking place between 2025 and 2035, expecting for its market entry afterwards.

10.4. SALCOS (Power to Hydrogen; 2017–2020)

The company Salzgitter AG started in 2017 the development of the SALCOS concept (SALzgitter Low CO₂ Steelmaking), aiming for the direct reduction of iron ore by using a mixture of natural gas and hydrogen as reducing agent. Depending on the mixture, the CO₂ emission can be reduced between 60 % (100 % natural gas as reducing agent) and 95 % (100 % hydrogen as reducing agent) compared to conventional ironmaking [112]. The research on this technology is carried out

through the MACOR project, funded by the German government with 1.3 M€, with the collaboration of the Forschung für Nachhaltige Entwicklung (FONA) [113].

To implement the concept, Salzgitter started in 2018 the WindH2 project (Wind Hydrogen Salzgitter) for the construction of an electrolysis plant, together with Linde AG and Avacon Natur GmbH. The budget of this parallel project amounts to 50 M€ [114]. The electrolyzer is developed by Siemens, which was awarded the contract to build a 2.2 MW PEM electrolyzer. The plant will have a hydrogen production capacity of 400 Nm³/h, with an efficiency of 54.5 %_{LHV} (i.e., 5.5 kWh/Nm³). The electrolyzer will be fed by seven wind turbines with a total capacity of 30 MW [115].

10.5. H2Future (Power to Hydrogen; 2017–2021)

The project H2Future is mainly focused in the development and operation of a 6 MW PEM electrolyzer to provide primary control to the grid (frequency containment reserve) and hydrogen to a steelmaking plant. Different load curves will be tested in the electrolyzer to properly match the hydrogen production with the typical demand curve in an electric arc furnace [116]. The electrolysis plant already entered into operation in November 2019 at the voestalpine Linz steel plant in Austria [117], producing 1200 Nm³/h with a 59.9 % efficiency (5 kWh/Nm³). The total capacity of electrolysis was achieved through 12-module PEM. Currently, the hydrogen is blended with the steel plant's coking gas [118]. The partners of the project are Verbund, Voestalpine, Siemens, Austrian Power Grid, K1-MET, and ECN, which received 12 M€ funding from the Fuel Cells and Hydrogen 2 Joint Undertaking (FCH 2 JU) [116,117].

10.6. Hydrogen path (Power to Hydrogen; 2019–2024)

'Hydrogen path' is the climate strategy of Thyssenkrupp for a climate-neutral steelmaking by 2050 [119]. In a first step, it was tested the injection of pure hydrogen into one of the 28 tuyeres on a blast furnace at the Duisburg-Hamborn site. The hydrogen was provided by Air Liquid by road tanker. This phase 1, which took place on November 2019, was funded under the initiative 'IN4climate.NRW' by the state of North Rhine-Westphalia [120]. The budget of the project was 2.7 M€ [121]. The next planned step is to expand the process to all 28 tuyeres of the blast furnace by the end of 2021, supplied from a nearby Air Liquide grid (6.5 km pipeline will have to be laid to the blast furnace) [119]. On June 2020, Thyssenkrupp agreed with RWE Generation to develop large-scale electrolyzers to feed the Duisburg plant. The hydrogen would be produced at the power plant site of Lingen RWE, and transported through the dedicated hydrogen grid mentioned before. According to estimations of RWE, a 100 MW electrolysis capacity would produce 1.7 tons of hydrogen (56.7 % efficiency, and 5.3 kWh/Nm³ specific consumption) [122]. One blast furnace of Thyssenkrupp requires a total injection of 2.25 tons of hydrogen, for all of the tuyeres, to produce 4.6 kt_{pig} iron [121]. Therefore, this electrolysis capacity could satisfy the 75.6 % of the hydrogen demand of one blast furnace. From 2022 onwards, the aims is to gradually convert to hydrogen injection the four existing blast furnaces in Duisburg [119].

Additionally, Thyssenkrupp aims to develop direct reduction plants, starting its operation in 2024 [123]. Thus, it will be produced solid sponge iron (direct reduced iron) instead of molten pig iron. The sponge iron will be melted in the existing blast furnace, which will act only as melting units. By 2030, the objective is to process the sponge iron into crude steel in modern electric arc furnaces powered by renewable energies. Thus, in 2050, Thyssenkrupp will gradually transition all of its facilities to this climate-neutral technology [119].

10.7. i3upgrade (Power to Methane / Methanol; 2018–2021)

The i3upgrade project (Integrated and intelligent upgrade of carbon

sources through hydrogen addition for the steel industry) aims to develop direct methanation and methanol synthesis of by-product gases from integrated steel works under dynamic and transient conditions [124]. They use a methanation plant located at Montanuniversität Leoben, comprising 3 fixed-bed reactors in series. The plant operates at 3 Nm³/h, 1–20 bar, <700 °C and GHSV between 3000 and 5000 h⁻¹. The inlet reactants are hydrogen and real bottled steel mill gases from Voestalpine. A commercial bulk catalyst (Meth 134®) and a honeycomb catalyst have been compared in the experiments, obtaining similar CO₂ conversions [125]. Regarding the methanol unit, they use an industrial pre-pilot unit located at ALFE (Air Liquide Forschung und Entwicklung GmbH) [126].

The total budget of the project is 3.3 M€, of which 2.0 M€ were funded by the Research Fund for Coal and Steel and the European Commission. There are eight participating institutions, which include partners such as Voestalpine, K1-MET, and Air liquid [127].

10.8. FReSMe (Power to Methanol; 2016–2020)

The FReSMe project (From residual steel gasses to methanol) aims to produce methanol by combining CO₂ from an industrial blast furnace and H₂ from electrolysis, in order to use it as fuel in ship transportation [128]. First tests took place on December 2019, at the SWERIM site in Luleå (Sweden) [129]. Then, the pilot plant will run for a total of three months divided over three different runs, producing 50 kg/h of methanol from an input of 800 m³/h of blast furnace gas [130]. Currently, the estimated cost for methanol production based on BFG and BOFG is 530 €/t, which is a 30%–40% higher than the cost of fossil methanol [129, 131]. The total budget of the project was funded by the European Commission, amounting to 11.4 M€. The project, coordinated by I-DEALS, involves partners such as SSAB, Tata Steel and Politecnico di Milano [130].

10.9. Carbon2Chem (Power to Methanol; 2018–2025)

The Carbon2Chem project [90] aims at using emissions from steel production as raw material for base chemicals, consuming renewable electricity during the conversion processes. Base chemicals are later used to make fertilizers, plastics or fuels. First tests took place in September 2018, producing ammonia and methanol at the Thyssenkrupp site in Duisburg, Germany [119]. It was seen that the hydrogen already present in the steel mill gases is sufficient for ammonia synthesis, but additional hydrogen is needed for methanol production [132]. Next step is the industrial pilot phase, which will be focused on the methanol production and it is expected to kick off during 2020 [119]. A total of 240 Nm³/h of gases from the coking plant, blast furnace and converter are diverted to the gas cleaning section of this pilot plant. Hydrogen will be produced by a 2 MW water electrolysis plant, which has been in operation since March 2018 [133]. Since the electrolyzer is fed with renewable electricity, one of the central development tasks is to find catalyst suitable for operating fluctuations in the methanol production process [132]. By 2025, the first industrial-scale plant should be ready [119].

At a lower scale, Carbon2Chem also includes other subprojects oriented toward the production of higher alcohols (used as fuels and chemical intermediates), polymers (for plastics), and oxymethylene ethers (used in diesel and gasoline fuels) [133,134]. A complete Special Issue focused on Carbon2Chem was published on October 2018 in the Chemie Ingenieur Technik journal, presenting results of the different subprojects [135]. In total, the project involves 17 partners, and it is jointly coordinated by Thyssenkrupp, the Max Planck Institute for Chemical Energy Conversion, and the Fraunhofer UMSICHT [134]. The German Federal Ministry of Education and Research funded the project with 60 M€ [119].

10.10. eForFuel (Power to Fuels; 2018–2022)

The eForFuel project (Fuels from electricity) aims at producing hydrocarbon fuels from industrial CO₂ (e.g. steel gases), by combining the electrochemical reduction of CO₂ to formic acid (supplied by renewable electricity) with a subsequent formatrophic microbial culture that consumes the formic acid and produces gaseous propane and isobutene [136]. So far, the research focuses on improving the performance of the individual steps at lab scale (TRL 4). It is not planned to build a prototype combining all stages, either at lab or industrial environment [137]. The project is coordinated by the Max-Planck-Gesellschaft, and was entirely funded by the European Union through the H2020 programme (4.1 M€). There are 14 partners, including entities such as Sintef, ArcelorMittal and the University of Stuttgart [138].

11. Conclusions

In this paper we have presented the first systematic review of Power to X processes applied to the iron and steel industry. These processes convert electricity into valuable chemicals by including an electrolysis stage that yields a necessary intermediate or directly the final product. This kind of solutions allows for substantial CO₂ emission reduction while providing additional benefits compared to conventional carbon capture (e.g., avoidance of CO₂ transport and storage, reutilization of by-products and, in some cases, production of valuable products for selling). We have limited the review to those concepts using renewable electricity in the electrolysis process, establishing a clear classification that comprises five categories: Power to Iron, Power to Hydrogen, Power to Syngas, Power to Methane and Power to Methanol.

Power to Iron produces liquid iron by reducing iron oxides through the application of electricity. This technology is still being researched at lab scale, due to the highly demanding properties required for the materials in the electrolysis cells. So far, there are two main promising technologies, one based in molten oxide electrolytes working at medium (700–800 °C) and high (730–1600 °C) temperature, and the other using alkaline electrolytes at low temperature (110 °C). The molten oxide electrolytes for medium temperature are typically based on Li₂CO₃, while those for high temperature use a mixture of Al₂O₃, MgO, CaO and SiO₂ in different proportions. On the other hand, alkaline electrolytes use 45–50% NaOH solutions. The iron source is in most cases Fe₂O₃ or Fe₃O₄, and experiments have been carried out in a wide range of operating conditions (0.7–12.0 V, 0.02–2 A/cm²). Preliminary results seem to indicate that the potential energy consumption could be in the range 10.8–13.0 GJ/t_{Fe}, which is lower than the average energy consumption in conventional blast furnaces (with the additional advantage of not emitting CO₂). Additionally, some authors have proposed the potential integration of Power to Steel with the partial oxidation of light hydrocarbons in order to produce both iron and organic chemicals in the same process, but it has not been demonstrated technically yet.

Power to H₂ can be integrated in ironmaking in two ways. The first method consists in injecting the H₂ as auxiliary reducing agent in conventional blast furnaces, while the second technique uses the H₂ as reducing agent in combustion-free reactors to directly reduce the iron ore into metallic iron (Direct Reduced Iron, which is later used in electric arc furnaces for steel production). The studies assessing the injection of H₂ in blast furnace show the potential of reducing CO₂ emissions by 21.4 %, barely affecting the overall energy demand of the process. In this case, the injected flow of hydrogen should be around 30.0 kgH₂/t_{HM}, to not modify significantly the operating conditions inside the furnace. Regarding the second method, i.e., the direct reduction of iron, there are different techniques to obtain metallic iron, which differ in the iron source (fine ore or pellets) and the type of reactor (fluidized bed, fixed bed or shaft furnace). Among them, the Energiron and Midrex concepts, which use iron pellets in shaft furnaces with counter-current moving beds, are the best option from an environmental point of view. They lead to the lowest energy consumption (3.5–3.7 MWh/t_{LS}) and CO₂ emission

(0–53 kgCO₂/t_{LS} if carbon-free electricity is used, corresponding to 97–100% emission reduction). Still, to make this route competitive, carbon allowances should reach 62 €/t_{CO₂} and electricity price should be below 40 €/MWh.

Power to Syngas provides a useful fuel to be injected in conventional blast furnace to be used as renewable reducing agent. From the review of the studies found in literature, it seems that CO₂ emission reductions between 11 % and 22 %, with respect to conventional blast furnaces, could be achieved under reasonable scenarios. The required electricity consumption of the overall system, per kilogram of CO₂ recycled, lies in the range 4.8–10.8 MJ/kg_{CO₂}. Moreover, the thermal energy necessities vary from 1 to 2.5 MJ/kg_{CO₂}, increasing to 7.8 MJ/kg_{CO₂} if carbon capture is used. The power capacity of the SOEC may range between 100 MW–900 MW for this type of integration, according to the studies reviewed. It must be noted that only nuclear power has been considered as energy source for the integration so far. There is a lack of studies evaluating the effects of integrating variable renewable electricity (e.g., solar or wind power) in Power to Syngas concepts for ironmaking. Furthermore, detailed analyses using rate-based models, integration of by-product O₂ from SOEC, and optimization of heat exchanger networks could still improve the knowledge on the topic.

Power to Methane, like Power to Syngas, provides a renewable fuel to be injected in conventional blast furnace for iron reduction. The studies about Power to Methane applied on the steel industry are scarce, so only preliminary conclusions can be made on this issue. The CO₂ emissions reduction, compared to conventional ironmaking, are in the range 13.0%–18.6% for the systems studied in literature. Even for this moderate reductions, water electrolysis power capacities of about 880 MW would be required. If there is any other hydrogen source in the Power to Methane plant, like biogas or syngas from gasification, the electrolysis power capacity can be substantially reduced. So far, there are no studies that properly analyze the integration of the different by-product streams, such as heat from methanation or oxygen from electrolysis. Detailed modelling is also necessary to reach reliable results, since assumptions related to black box models may sometimes be unrealistic from a technical or economical point of view (e.g., considering large N₂ input to the methanation process). Lastly, as it occurred in Power to Syngas, the effects of supplying variable renewable electricity to the overall integration of Power to Methane and steelmaking has not been analyzed.

In addition to those Power to X products that can be directly used in ironmaking (H₂, syngas and SNG), there are other valuable chemicals that can be synthetized from steel mill gases (e.g., methanol, OME, urea, polymers). Among them, methanol (Power to Methanol) ranked as the best option according to technologic, economic, and acceptance criteria. Different studies assessed the integration of Power to Methanol in the steel industry, covering together a wide range of electrolysis power capacities (from 0.1 GW to 10 GW). The electricity consumption, per kilogram of CO₂ recycled, is in the range of 21–22 MJe/kg_{CO₂} for BFG, and 12–19 MJe/kg_{CO₂} for gas mixtures containing COG (since it already contains large amounts of H₂). Therefore, the methanol production highly varies depending on the plant configuration and carbon source, ranging from 0.7 to 5.2 t/day per MW of electrolysis power installed, according to the different studies reviewed. However, the techno-economic scenarios that can be found in literature lead to unreasonable costs for methanol production (760–1540 €/t_{MeOH}) and CO₂ avoidance (352 €/t_{CO₂}), compared to current prices (210–530 €/t_{MeOH} for fossil methanol and 25 €/t_{CO₂} for carbon allowances).

In this review paper, we have presented also novel concepts that integrate oxy-fuel ironmaking and Power to Gas for the first time. The by-product oxygen coming from water electrolysis can be used in oxy-fuel combustion processes to obtain off-gases with little N₂ content that can be directly used in the Power to Gas stage. Thus, the energy penalizations in CO₂ separation, transport and storage are avoided. It has been proposed its use in full oxygen blast furnaces (TRL 6–7), during the preheating of ladles, and in the reheating and treatment of steel

(commercial technologies). These options are promising methods to substantially reduce CO₂ emissions, which have to be further analyzed to quantify the potential benefits.

A summary of the most important Power to X projects for the iron and steel industry has been presented to give an overview of the state of experimental research on these integrated concepts. Only those that actually use renewable electricity are included in this review. Power to Hydrogen and Power to Methanol are the most advanced technologies so far, with TRL 7 in average and some initiatives aiming for TRL 8 – 9. These two concepts are mainly being developed in Germany, Sweden and Austria, using electrolysis power capacities in the range 2–6 MW. Regarding Power to Methane, the concept is being researched by Austria within TRL 4 – 5. Additionally, there is other additional initiative not mentioned in the review (DISIPO project, 2021–2023) [141], focused on the combination of Power to Methane with oxy-fuel ironmaking. This is just referred here as it does not comprise the commissioning of a large pilot plant. It aims to reach TRL 2 in this novel concept, involving institutions from Japan, Austria and Spain. All the mentioned projects started within 2016–2021, what gives a clear idea of the increasing interest in the topic.

Funding

This research was funded by the R+D Spanish National Program

Appendix A. – Databases used during the literature search

The following list of databases were used in the search engine of Web of Science:

- Web of Science Core Collection: Science Citation Index Expanded (1900-present)
- Web of Science Core Collection: Conference Proceedings Citation Index- Science (1990-present)
- Web of Science Core Collection: Book Citation Index- Science (2005-present)
- Web of Science Core Collection: Emerging Sources Citation Index (2015-present)
- Web of Science Core Collection: Current Chemical Reactions (1986-present)
- Web of Science Core Collection: Index Chemicus (1993-present)
- Current Contents Connect: Agriculture, Biology & Environmental Sciences (1998–2009)
- Current Contents Connect: Physical, Chemical & Earth Sciences (1998–2009)
- Current Contents Connect: Engineering, Computing & Technology (1998–2009)
- Derwent Innovations Index: Chemical Section (1980–2009)
- Derwent Innovations Index: Electrical and Electronic Section (1980–2009)
- Derwent Innovations Index: Engineering Section (1980–2009)
- KCI-Korean Journal Database (1980-present)
- Russian Science Citation Index (2005-present)
- SciELO Citation Index (2002-present)

Appendix B. – Glossary of involved terms in iron and steelmaking context

Basic oxygen furnace (BOF)

Reactor in which oxygen reduces the carbon content of pig iron in a basic media (burnt lime or dolomite) at high temperatures (~1600 °C). Low-carbon steel is obtained after the oxygen converter process.

Burden

Mixture of sinter, pellets and additives which feed the blast furnace [25].

Electric-steel process

Crude steel production in an electric-arc furnace (EAF). Sponge iron, scrap and pig iron are mixed and heated through the hot arc ignited by electrodes to reach a liquid mixture of steel and slag. Both phases are easily separated by its different density.

Hot-blast

Pre-heated air blown into the blast furnace through nozzles called tuyeres. The preheating up to 1000 °C is performed in specific regenerative heat

from Ministerio de Economía y Competitividad, MINECO (Spanish Ministry of Economy and Competitiveness) and the European Regional Development Funds (European Commission), under project ENE2016–76850-R. This work was also supported by the Government of Aragon and co-financed by FEDER 2014–2020 “Construyendo Europa desde Aragón” (Research Group DGA T46_17R and project LMP134_18). This project received funding from the Khalifa University of Science & Technology by means of Competitive Internal Research Awards 2020 (Ref: CIRA-2020-080).

CRediT authorship contribution statement

Manuel Bailera: Conceptualization, Methodology, Formal analysis, Writing - original draft. **Pilar Lisboa:** Conceptualization, Formal analysis, Writing - original draft. **Begoña Peña:** Formal analysis, Writing - original draft. **Luis M. Romeo:** Writing - original draft.

Declaration of Competing Interest

The authors report no declarations of interest.

exchangers (installed in pairs), called cowper stoves or hot-blast stoves, where waste gases of the blast furnace are usually mixed and burnt with natural gas.

Hot briquetted iron (HBI)

Improved form of direct reduced iron (DRI) after compaction above 650 °C to easy its management. HBI is much less porous and less reactive than DRI. It is mainly used as feedstock of electric arc furnaces, but can be also used in basic oxygen furnaces and blast furnaces.

Iron blast furnace (BF)

Metallurgical furnace to produce pig iron as intermediate product in steelmaking process. Alternating layers of coke and pellets or sinter of iron ore are discharged from the top while the hot blast of air is blown into the lower section of the furnace. The material undergoes different chemical processes as it descends by gravity and heats from 200 to 2000 °C: preheating, indirect reduction, direct reduction, carburization, melting and tapping.

Pig iron

Molten iron with high carbon content, also called ‘crude iron’ or ‘hot metal’, resulting as intermediate product from reduction in blast or electric furnaces. Pig iron is obtained through smelting of iron ore or ilmenite with a high carbon content fuel and a reducing agent, usually coke. It is an old term referred to the ingots’ production process, but currently the majority of pig iron is transferred directly in liquid form to the next stage in the steelmaking process.

Scrap iron

Recycled iron materials.

Shaft furnace

Countercurrent reactor for melting, smelting and calcining or roasting. In the context of iron and steelmaking, the reduction of the descending solid material (iron oxide pellets and lump ores) occurs through an ascending reducing agent, as heat exchange and chemical reactions take place. The blast furnace is also an example of shaft furnace.

Sponge iron (DRI)

Porous solid with high metallized iron content resulting from direct reduction of the iron oxides present in iron ore or steel plant wastes. Direct reduction process takes place in a shaft furnace, rotary kiln, or fluidized beds at typical temperatures of 800–1200 °C through a reducing gas, such as syngas or pure hydrogen. Non-metallic forms of iron, as cementite or wustite, and gangues are present in low fraction [142].

Top gas (TG)

Gas mixture resulting from the partial oxidation of the reducing gas in the blast furnace. Top gas contains mainly nitrogen (if air is used in the blast furnace), carbon dioxide and carbon monoxide.

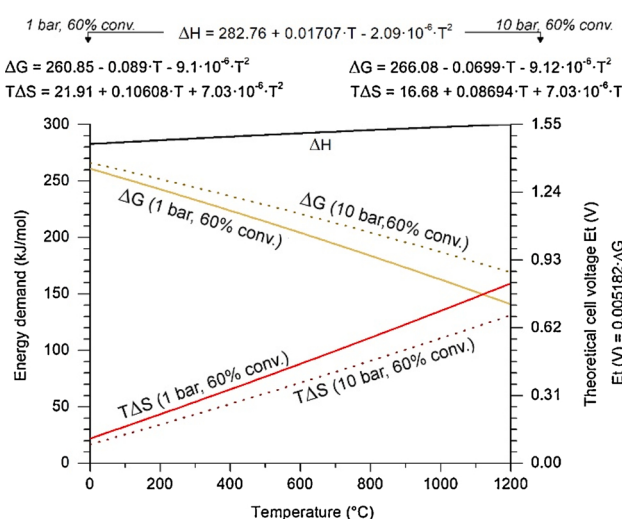


Fig. 17. Enthalpy of reaction, Gibbs energy (with the corresponding theoretical cell voltage) and entropy term for CO₂ electrolysis versus temperature. Conditions: ($p_{CO_2} = 0.4$ bar, $p_{CO} = 0.6$ bar, $p_{O_2} = 1$ bar for the 1 bar and 60 % conversion case, and $p_{CO_2} = 4$ bar, $p_{CO} = 6$ bar, $p_{O_2} = 10$ bar for the 10 bar and 60 % conversion case).

Appendix C. – Thermodynamic analysis of CO₂ electrolysis

To not interrupt the line of review, the thermodynamics of CO₂ electrolysis are explained separately in this Appendix. A comprehension

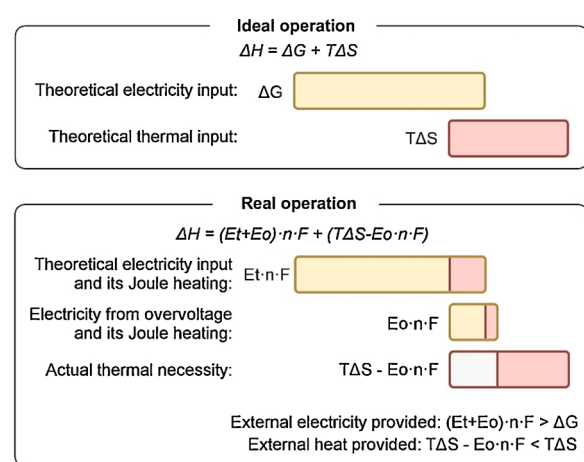


Fig. 18. Schematic illustration comparing the enthalpy change of reaction in SOEC under ideal and real operation (Faradaic losses are not considered).

of this topic is necessary to properly compare the different studies on Power to Syngas concepts. The information presented in Table 11 was calculated from the data of the corresponding references, which in some cases were scarce. Thus, this section aims to shed light on this issue.

The global reaction of CO₂ electrolysis is endothermic, following Eq. 21.



The enthalpy of the reaction (Eq. 22) stands for the minimum energy required to reduce CO₂. This can be provided in form of electricity (ΔG , Gibbs free energy of formation) or heat ($T\Delta S$, entropy term) [69].

$$\Delta H = \Delta G + T\Delta S \quad (22)$$

Both terms are presented versus temperature for specific SOEC configurations in Fig. 17, calculated from data of the Aspen Plus properties database. The cases presented correspond to SOECs with operating pressures of 1 and 10 bar, and CO₂ conversions of 60 %. As it can be seen, the entropy term ($T\Delta S$) increases with temperature, what allows to reduce the necessary electricity consumption (ΔG) to fulfill the enthalpy change of the reaction. Contrarily, high pressures contribute to greater electricity demands.

By knowing the electricity demand, the corresponding voltage required in the electrolyzer cell (voltage difference between the cathode and the anode) can be computed by Eq. 23,

$$E_t [\text{V}] = \frac{\Delta G [\text{J}\cdot\text{mol}^{-1}]}{n [-]\cdot F [\text{C}\cdot\text{mol}^{-1}]} \quad (23)$$

where n is the number of transferred electrons ($n = 2$ in the reduction of CO₂ to CO) and F is the Faraday's constant (96485.34 C/mol). It must be noted that this is the theoretical minimum voltage required in the cell (E_t). However, in practice, part of the electricity consumed by the SOEC will be transformed to heat by the Joule effect. Therefore, it must be applied an over potential (E_o) to ensure that the electricity production reaches ΔG (Eq. 24). Furthermore, as Joule heating becomes available inside the cell, the amount of thermal energy that must be supplied externally diminishes. This drop equals to $E_o \cdot n \cdot F$, as showed graphically in Fig. 18.

$$E = E_t + E_o \quad (24)$$

In addition to the voltage losses caused by Joule heating, it may appear a loss related to non-ideal selectivity. This is known as the Faradaic efficiency, $\eta_F [-]$, which quantifies the fraction of the total electricity that is actually used in the CO₂ reduction process (instead of in other possible side-reactions). In other words, it represents the variation in current due to misdirected electrons. Thus, the final electricity specific consumption (ESC) of the electrolyzer would be given by Eq. 25.

$$ESC [\text{J}\cdot\text{mol}^{-1}] = \frac{(E_t + E_o)[\text{V}] \cdot n [-] \cdot F [\text{C}\cdot\text{mol}^{-1}]}{\eta_F [-]} \quad (25)$$

This kind of analysis is useful to compute the actual electricity and heat consumptions of the SOECs used in the different studies that are compared in section 4.3.1.

References

- [1] T.R. Anderson, E. Hawkins, P.D. Jones, CO₂, the greenhouse effect and global warming: from the pioneering work of Arrhenius and Callendar to today's Earth System Models, *Endeavour* 40 (2016) 178–187, <https://doi.org/10.1016/j.endeavour.2016.07.002>.
- [2] International Energy Agency, CO₂ Emissions from Fuel Combustion, 2015, https://doi.org/10.1787/co2_fuel-2015-en.
- [3] Report from the Commission to the European Parliament, the Council, the European Economic and Social Committee and the Committee of the Regions - Renewable energy progress report, European Commission, 2015.
- [4] European Commission, *A Policy Framework for Climate and Energy in the Period From 2020 to 2030*, 2014.
- [5] K. De Ras, R. Van de Vijver, V.V. Galvita, G.B. Marin, K.M. Van Geem, Carbon capture and utilization in the steel industry: challenges and opportunities for chemical engineering, *Curr. Opin. Chem. Eng.* 26 (2019) 81–87, <https://doi.org/10.1016/j.coche.2019.09.001>.
- [6] M. Abdul Quader, S. Ahmed, S.Z. Dawal, Y. Nukman, Present needs, recent progress and future trends of energy-efficient Ultra-Low Carbon Dioxide (CO₂) Steelmaking (ULCOS) program, Renew. Sustain. Energy Rev. 55 (2016) 537–549, <https://doi.org/10.1016/j.rser.2015.10.101>.
- [7] D. Leeson, N. Mac Dowell, N. Shah, C. Petit, P.S. Fennell, A Techno-economic analysis and systematic review of carbon capture and storage (CCS) applied to the iron and steel, cement, oil refining and pulp and paper industries, as well as other high purity sources, *Int. J. Greenh. Gas Control*. 61 (2017) 71–84, <https://doi.org/10.1016/j.ijggc.2017.03.020>.
- [8] P. Jin, Z. Jiang, C. Bao, S. Hao, X. Zhang, The energy consumption and carbon emission of the integrated steel mill with oxygen blast furnace, *Resour. Conserv. Recycl.* 117 (2017) 58–65, <https://doi.org/10.1016/j.resconrec.2015.07.008>.
- [9] A. Arasto, E. Tsupari, J. Kärki, J. Lilja, M. Sihvonen, Oxygen blast furnace with CO₂ capture and storage at an integrated steel mill-Part I: technical concept analysis, *Int. J. Greenh. Gas Control*. 30 (2014) 140–147, <https://doi.org/10.1016/j.ijggc.2014.09.004>.
- [10] E. Tsupari, J. Kärki, A. Arasto, J. Lilja, K. Kinnunen, M. Sihvonen, Oxygen blast furnace with CO₂ capture and storage at an integrated steel mill - Part II: economic feasibility in comparison with conventional blast furnace highlighting sensitivities, *Int. J. Greenh. Gas Control*. 32 (2015) 189–196, <https://doi.org/10.1016/j.ijggc.2014.11.007>.
- [11] A. Arasto, E. Tsupari, J. Kärki, E. Pisilä, L. Sorsmäki, Post-combustion capture of CO₂ at an integrated steel mill - Part I: technical concept analysis, *Int. J. Greenh. Gas Control*. 16 (2013) 271–277, <https://doi.org/10.1016/j.ijggc.2012.08.018>.
- [12] E. Tsupari, J. Kärki, A. Arasto, E. Pisilä, Post-combustion capture of CO₂ at an integrated steel mill - Part II: economic feasibility, *Int. J. Greenh. Gas Control*. 16 (2013) 278–286, <https://doi.org/10.1016/j.ijggc.2012.08.017>.
- [13] A. Berrio, Oxícombustión: Una Alternativa Para La Captura De CO₂ Y La Transformación Del Proceso Productivo Del Cemento, 2012.
- [14] K. W. H. J., Carbon Capture, Storage and Use. Technical, Economic, Environmental and Societal Perspectives, Springer, 2015.
- [15] M. Bailera, P. Lisboa, L.M. Romeo, S. Espatolero, Power to gas projects review: lab, pilot and demo plants for storing renewable energy and CO₂, *Renew. Sustain. Energy Rev.* 69 (2017) 292–312, <https://doi.org/10.1016/j.rser.2016.11.130>.
- [16] O. Strohbach, Audi e-gas plant stabilizes electrical grid, Press Release - Audi MediaInfo, Technol. Innov. Commun. (2015) (Accessed January 21, 2016), <http://www.audi-mediacenter.com/en/press-releases/4499>.
- [17] K. Kuparinen, Transforming the Chemical Pulp Industry - From an Emitter to a Source of Negative CO₂ Emissions, 2019, LUT University Press, 2019. <http://urn.fi/URN:ISBN:978-952-335-423-4>.
- [18] M. Bailera, S. Espatolero, P. Lisboa, L.M. Romeo, Power to gas-electrochemical industry hybrid systems: a case study, *Appl. Energy* 202 (2017) 435–446, <https://doi.org/10.1016/j.apenergy.2017.05.177>.
- [19] T. Ariyama, K. Takahashi, Y. Kawashiri, T. Nouchi, Diversification of the ironmaking process toward the long-term global goal for carbon dioxide mitigation, *J. Sustain. Metall.* 5 (2019) 276–294, <https://doi.org/10.1007/s40831-019-00219-9>.
- [20] T. Ariyama, 鉄鋼における二酸化炭素削減長期目標達成に向けた技術展望 (Technological prospects for achieving long-term carbon dioxide reduction goals for steel), *Tetsu-to-Hagané* 105 (2019) 567–586, <https://doi.org/10.2355/tetsutohagané.TETSU-2019-008>.
- [21] International Energy Agency, Iron and Steel Technology Roadmap, 2020.
- [22] IEA, Tracking Industry 2019, Paris, 2019.
- [23] M.D. Fenton, C.A. Tuck, *Iron and Steel. 2016 Minerals Yearbook*, US Geological Survey, 2019.

- [24] Q. Wang, Y. Zhu, Q. Wu, E. Gratz, Y. Wang, Low temperature electrolysis for iron production via conductive colloidal electrode, RSC Adv. 5 (2015) 5501–5507, <https://doi.org/10.1039/C4RA14576C>.
- [25] A. Otto, M. Robinius, T. Grube, S. Schiebahn, A. Praktiknjo, D. Stolten, Power-to-Steel : Reducing CO₂ through the Integration of Renewable Energy and Hydrogen into the German Steel Industry, (n.d.). doi:10.3390/en10040451.
- [26] H. Hamadeh, O. Mirgaux, F. Patisson, Detailed modeling of the direct reduction of iron ore in a shaft furnace, Materials (Basel) 11 (2018), <https://doi.org/10.3390/mal1101865>.
- [27] A. Shams, F. Moazeni, Modeling and simulation of the MIDREX shaft furnace: reduction, transition and cooling zones, JOM 67 (2015) 2681–2689, <https://doi.org/10.1007/s11837-015-1588-0>.
- [28] C. Yilmaz, T. Turek, Modeling and simulation of the use of direct reduced iron in a blast furnace to reduce carbon dioxide emissions, J. Clean. Prod. 164 (2017) 1519–1530, <https://doi.org/10.1016/j.jclepro.2017.07.043>.
- [29] C. Ramakgala, G. Danha, A review of ironmaking by direct reduction processes: quality requirements and sustainability, Procedia Manuf. 35 (2019) 242–245, <https://doi.org/10.1016/j.promfg.2019.05.034>.
- [30] Environmental Protection Agency, Available and Emerging Technologies for Reducing Greenhouse Gas Emissions from the Iron and Steel Industry, 2012.
- [31] V. Feynerol, H.L.P. Marlier, M.N.P.F. Lapicque, Reactivity of suspended iron oxide particles in low temperature alkaline electrolysis, J. Appl. Electrochem. 4 (2017) 1–12, <https://doi.org/10.1007/s10800-017-1127-5>.
- [32] E. Kvalheim, G.M. Haarberg, A.M. Martinez, S. Rosseth, K.S. Olsen, H. Gudbrandsen, High temperature electrolysis for liquid iron production, ECS Trans. 50 (2013) 63–72, <https://doi.org/10.1149/05044.0063ecst>.
- [33] W.D. Judge, A. Allanore, D.R. Sadoway, G. Azimi, E-logQ2 diagrams for ironmaking by molten oxide electrolysis, Electrochim. Acta 247 (2017) 1088–1094, <https://doi.org/10.1016/j.electacta.2017.07.059>.
- [34] J. Wiencke, H. Lavelaine, P. Jean, P. Carine, P. Christophe, Electrolysis of iron in a molten oxide electrolyte, J. Appl. Electrochem. 48 (2018) 115–126, <https://doi.org/10.1007/s10800-017-1143-5>.
- [35] A. Allanore, L. Yin, D.R. Sadoway, A new anode material for oxygen evolution in molten oxide electrolysis, Nature 497 (2013) 353–356, <https://doi.org/10.1038/nature12134>.
- [36] H. Kim, J. Paramore, A. Allanore, D.R. Sadoway, Electrolysis of molten Iron oxide with an iridium anode : the role of electrolyte basicity, J. Electrochem. Soc. 158 (2011) 101–105, <https://doi.org/10.1149/1.3623446>.
- [37] Y. Gao, C. Yang, C. Zhang, Q. Qin, G.Z. Chen, Magnesia-stabilised zirconia solid electrolyte assisted electrochemical investigation of iron ions in a SiO₂-CaO-MgO-Al2O₃ molten slag at 1723 K, Phys. Chem. Chem. Phys. 19 (2017) 15876–15890, <https://doi.org/10.1039/C7CP01945A>.
- [38] S. Licht, B. Wang, High solubility pathway for the carbon dioxide free production of iron, Chem. Commun. (Camb.) 46 (2010) 7004–7006, <https://doi.org/10.1039/C0CC01594F>.
- [39] S. Licht, H. Wu, Z. Zhang, H. Ayub, Chemical mechanism of the high solubility pathway for the carbon dioxide free production of iron w, Chem. Commun. (Camb.) 47 (2011) 3081–3083, <https://doi.org/10.1039/c0cc05581f>.
- [40] S. Licht, H. Wu, S.T.E.P. Iron, a Chemistry of Iron Formation without CO₂ Emission: Molten Carbonate Solubility and Electrochemistry of Iron Ore Impurities, J. Phys. Chem. C. 115 (2011) 25138–25147, <https://doi.org/10.1021/jp2078715>.
- [41] F.-F. Li, B. Wang, S. Licht, Sustainable electrochemical synthesis of large grain- or catalyst-sized Iron, J. Sustain. Metall. 2 (2016) 405–415, <https://doi.org/10.1007/s40831-016-0062-8>.
- [42] A. Allanore, H. Lavelaine, J. Birat, G. Valentin, F. Lapicque, Experimental investigation of cell design for the electrolysis of iron oxide suspensions in alkaline electrolyte, J. Appl. Electrochem. 40 (2010) 1957–1966, <https://doi.org/10.1007/s10800-010-0172-0>.
- [43] B. Parkinson, C. Greig, E. Mcfarland, S. Smart, Techno-economic analysis of a process for CO₂-free coproduction of iron and hydrocarbon chemical products, Chem. Eng. J. 313 (2017) 136–143, <https://doi.org/10.1016/j.cej.2016.12.059>.
- [44] M. Fischbeck, J. Marzinkowski, P. Winzer, M. Weigel, Techno-economic evaluation of innovative steel production technologies, J. Clean. Prod. 84 (2014) 563–580, <https://doi.org/10.1016/j.jclepro.2014.05.063>.
- [45] M. Weigel, M. Fischbeck, J. Marzinkowski, P. Winzer, Multicriteria analysis of primary steelmaking technologies, J. Clean. Prod. 112 (2016) 1064–1076, <https://doi.org/10.1016/j.jclepro.2015.07.132>.
- [46] J.K. Ahmad, Using water hydrogen instead of reducing gas in the production of direct reduced iron (DRI), J. Adv. Oxid. Technol. 13 (2010) 124–129.
- [47] A. Ranzani Da Costa, D. Wagner, F. Patisson, Modelling a new, low CO₂ emissions, hydrogen steelmaking process, J. Clean. Prod. 46 (2013) 27–35, <https://doi.org/10.1016/j.jclepro.2012.07.045>.
- [48] V. Vogl, M. Ahman, L.J. Nilsson, Assessment of hydrogen direct reduction for fossil-free steelmaking, J. Clean. Prod. 203 (2018) 736–745, <https://doi.org/10.1016/j.jclepro.2018.08.279>.
- [49] A. Bhaskar, M. Assadi, H.N. Somehsaraei, Decarbonization of the iron and steel industry with direct reduction of iron ore with green hydrogen, Energies 13 (2020) 1–23, <https://doi.org/10.3390/en13030758>.
- [50] D.A. Sortwell, Sohn Michael, Boy H.Y. George, Green, Ed, and Li, a Novel Flash Ironmaking Process, Washington, D.C. (United States), 2018, <https://doi.org/10.2172/1485414>.
- [51] C. Yilmaz, J. Wendelstorff, T. Turek, Modeling and simulation of hydrogen injection into a blast furnace to reduce carbon dioxide emissions, J. Clean. Prod. 154 (2017) 488–501, <https://doi.org/10.1016/j.jclepro.2017.03.162>.
- [52] D. Nuber, H. Eichberger, B. Rollinger, Circored fine ore direct reduction, Raw Mater. Ironmak. (2006) 37–40.
- [53] Midrex, Direct from Midrex, News + Resoruces. First Quart. 2020. (2020). www.midrex.com/wp-content/uploads/Midrex-2020-DFM1QTR-Final.pdf.
- [54] P. Duarte, Hydrogen-based steelmaking, Millennium Steel. (2019) 18–22.
- [55] ArcelorMittal, ArcelorMittal Commissions Midrex to Design Demonstration Plant for Hydrogen Steel Production in Hamburg, News Release, 2019, <https://bit.ly/32rVhMA>.
- [56] M. Hölling, S. Gellert, Direct reduction: transition from natural gas to hydrogen? ICSTI Conf. (2018).
- [57] SDR Platform, Start of Initiative for Construction of 1 GW Electrolysis Plant for Green Hydrogen in Zeeland, 2019. <https://www.smartdeltaresources.com/en/news/start-of-initiative-for-construction-of-1-gw-electrolysis-plant-for-green-hydrogen-in-zeeland>.
- [58] M. Bailera, P. Lisboa, B. Peña, L.M. Romeo, Energy Storage, Springer International Publishing, Cham, 2020, <https://doi.org/10.1007/978-3-030-46527-8>.
- [59] W.H. Chen, M.R. Lin, A.B. Yu, S.W. Du, T.S. Leu, Hydrogen production from steam reforming of coke oven gas and its utility for indirect reduction of iron oxides in blast furnace, Int. J. Hydrogen Energy 37 (2012) 11748–11758, <https://doi.org/10.1016/j.ijhydene.2012.05.021>.
- [60] J. Astier, J. Krug, Y. Depressigny, Technico-economic potentialities of hydrogen utilization for steel production, Int. J. Hydrogen Energy 7 (1982) 671–679, [https://doi.org/10.1016/0360-3199\(82\)90192-6](https://doi.org/10.1016/0360-3199(82)90192-6).
- [61] H. Nogami, Y. Kashiiwaya, D. Yamada, Simulation of blast furnace operation with intensive hydrogen injection, ISIJ Int. 52 (2012) 1523–1527, <https://doi.org/10.2355/isijinternational.52.1523>.
- [62] European Environmental Agency, CO₂ Emission Intensity, 2016.
- [63] F. Patisson, O. Mirgaux, Hydrogen ironmaking: how it works, Metals (Basel) 10 (2020) 1–15, <https://doi.org/10.3390/met10070922>.
- [64] K. Huitu, M. Helle, H. Helle, M. Kekkonen, H. Saxén, Optimization of midrex direct reduced iron use in ore-based steelmaking, Steel Res. Int. 86 (2015) 456–465, <https://doi.org/10.1002/srin.201400091>.
- [65] H. He, H. Guan, X. Zhu, H. Lee, Assessment on the energy flow and carbon emissions of integrated steelmaking plants, Energy Rep. 3 (2017) 29–36, <https://doi.org/10.1016/j.egyr.2017.01.001>.
- [66] Y. Kato, Hydrogen utilization for carbon recycling iron making system, ISIJ Int. 52 (2012) 1433–1438, <https://doi.org/10.2355/isijinternational.52.1433>.
- [67] Y. Kato, Carbon recycling for reduction of carbon dioxide emission from iron-Making process, ISIJ Int. 50 (2010) 181–185, <https://doi.org/10.2355/isijinternational.50.181>.
- [68] K. Suzuki, K. Hayashi, K. Kuribara, T. Nakagaki, S. Kasahara, Quantitative evaluation of CO₂ emission reduction of active carbon recycling energy system for ironmaking by modeling with aspen plus, ISIJ Int. 55 (2015) 340–347, <https://doi.org/10.2355/isijinternational.55.340>.
- [69] R. Küngas, Review—electrochemical CO₂ reduction for CO production: comparison of low- and high-temperature electrolysis technologies, J. Electrochem. Soc. 167 (2020), 044508, <https://doi.org/10.1149/1945-7111/ab7099>.
- [70] A.L. Dipu, J. Ryu, Y. Kato, Carbon dioxide electrolysis for a carbon-recycling iron-making system, ISIJ Int. 52 (2012) 1427–1432, <https://doi.org/10.2355/isijinternational.52.1427>.
- [71] Y. Kato, T. Obara, I. Yamanaka, S. Mori, A. Lambertus Dipu, J. Ryu, Y. Ujisawa, M. Suzuki, Performance analysis of active carbon recycling energy system, Biol. Sci. 53 (2011) 1017–1021, <https://doi.org/10.1016/j.pnucene.2011.04.024>.
- [72] A.L. Dipu, Y. Ujisawa, J. Ryu, Y. Kato, Carbon dioxide reduction in a tubular solid oxide electrolysis cell for a carbon recycling energy system, Nucl. Eng. Des. 271 (2014) 30–35, <https://doi.org/10.1016/j.nucengdes.2013.11.004>.
- [73] G. Fujii, J. Ryu, K. Yoshida, T. Yano, Y. Kato, Possibility of application of solid oxide electrolysis cell on a smart iron-making process based on an active carbon recycling energy system, ISIJ Int. 55 (2015) 387–391, <https://doi.org/10.2355/isijinternational.55.387>.
- [74] Y. Numata, K. Nakajima, H. Takasu, Y. Kato, Carbon dioxide reduction on a metal-supported solid oxide electrolysis cell, ISIJ Int. 59 (2019) 628–633, <https://doi.org/10.2355/isijinternational.ISIJINT-2018-430>.
- [75] 鉄鋼プロセスにおける次世代CO₂削減技術調査・検討, Research and Study of Future Technology for Reducing CO₂ Emission in Iron and Steel Manufacturing Process, ISIJ, Tokyo, 2007. [#7B%22category%22%3A%220%22%22C%22keyword%22%3A%225%22%22N%220080860%5C%22%22%227D](https://jglobal.jst.go.jp/en/detail?JGLOBAL_ID=200909059573597186&rel=1).
- [76] S. Wang, A. Inoishi, J.E. Hong, Y.W. Ju, H. Hagiwara, S. Ida, T. Ishihara, Ni-Fe bimetallic cathodes for intermediate temperature CO₂ electrolyzers using a La_{0.9}Sr_{0.1}Ga_{0.8}Mg_{0.2}O₃ electrolyte, J. Mater. Chem. A Mater. Energy Sustain. 1 (2013) 12455–12461, <https://doi.org/10.1039/c3ta11863k>.
- [77] K. Hayashi, S. Kasahara, K. Kuribara, T. Nakagaki, X.L. Yan, Y. Inagaki, M. Ogawa, Process evaluation of use of high temperature gas-cooled reactors to an ironmaking system based on active carbon recycling energy system, ISIJ Int. 55 (2015) 348–358, <https://doi.org/10.2355/isijinternational.55.348>.
- [78] S. Hisashige, T. Nakagaki, T. Yamamoto, CO₂ emission reduction and exergy analysis of smart steelmaking system adaptive for flexible operating conditions, ISIJ Int. 59 (2019) 598–606, <https://doi.org/10.2355/isijinternational.ISIJINT-2018-355>.
- [79] A. Rist, N. Meysson, A dual graphic representation of the blast-furnace mass and heat balances, JOM 19 (1967) 50–59, <https://doi.org/10.1007/bf03378564>.
- [80] T. Yamamoto, 充填層型スクラップ溶解および部分溶融還元プロセスの開発に関する研究 (Research on Packed Layer Scrap Melting and Partial Melting Reduction

- Process Development), Tohoku University, 2004. <http://hdl.handle.net/10097/8487>.
- [81] Y. Kato, Utilization of HTGR on active carbon recycling energy system, *Nucl. Eng. Des.* 271 (2014) 79–83, <https://doi.org/10.1016/j.nucengdes.2013.11.014>.
- [82] K. Hashimoto, Metastable metals for “green” materials for global atmosphere conservation and abundant energy supply, *Mater. Sci. Eng. A* 179–180 (1994) 27–30.
- [83] D.C. Rosenfeld, H. Böhm, J. Lindorfer, M. Lehner, Scenario analysis of implementing a power-to-gas and biomass gasification system in an integrated steel plant: a techno-economic and environmental study, *Renew. Energy* 147 (2020) 1511–1524, <https://doi.org/10.1016/j.renene.2019.09.053>.
- [84] R. Remus, S. Roudier, M.A. Aguado, L.D. Sancho, Best Available Techniques (BAT) Reference Document for Iron and Steel Production, Publications Office of the European Union, 2013, <https://doi.org/10.2791/97469>.
- [85] D. Kim, J. Han, Techno-economic and climate impact analysis of carbon utilization process for methanol production from blast furnace gas over Cu/ZnO/Al2O3 catalyst, *Energy* 198 (2020), 117355, <https://doi.org/10.1016/j.energy.2020.117355>.
- [86] S. Schlüter, T. Hennig, Modeling the catalytic conversion of steel mill gases using the example of methanol synthesis, *Chemic-Ingenieur-Technik* 90 (2018) 1541–1558, <https://doi.org/10.1002/cite.201800021>.
- [87] T. Akiyama, H. Sato, A. Muramatsu, J.I. Yagi, Feasibility study on blast furnace ironmaking system integrated with methanol synthesis for reduction of carbon dioxide emission and effective use of exergy, *ISIJ Int.* 33 (1994) 1136–1143, <https://doi.org/10.2355/isijinternational.33.1136>.
- [88] A. Muramatsu, H. Sato, T. Akiyama, J.I. Yagi, Methanol synthesis from blast furnace off gas, *ISIJ Int.* 33 (1993) 1144–1149, <https://doi.org/10.2355/isijinternational.33.1144>.
- [89] S. Shin, J.K. Lee, I.B. Lee, Development and techno-economic study of methanol production from coke-oven gas blended with Linz Donawitz gas, *Energy*. 200 (2020), 117506, <https://doi.org/10.1016/j.energy.2020.117506>.
- [90] G. Deerberg, M. Oles, R. Schlägl, The project Carbon2Chem®, *Chemic-Ingenieur-Technik* 90 (2018) 1365–1368, <https://doi.org/10.1002/cite.201800060>.
- [91] S. Stießel, A. Berger, E.M. Fernández Sanchis, M. Ziegmann, Methodology for the evaluation of CO₂-Based syntheses by coupling steel industry with chemical industry, *Chemic-Ingenieur-Technik* 90 (2018) 1392–1408, <https://doi.org/10.1002/cite.201800030>.
- [92] A. Tremel, P. Wasserscheid, M. Baldauf, T. Hammer, Techno-economic analysis for the synthesis of liquid and gaseous fuels based on hydrogen production via electrolysis, *Int. J. Hydrogen Energy* 40 (2015) 11457–11464, <https://doi.org/10.1016/j.ijhydene.2015.01.097>.
- [93] H. Kosow, R. Gaßner, Methods of Future and Scenario Analysis - Overview, Assessment, and Selection Criteria, German Development Institute, 2008. http://edoc.vifapol.de/opus/volltexte/2013/4381/pdf/Studies_39.2008.pdf.
- [94] J. Gausemeier, A. Fink, O. Schlake, Szenario-Management: Planen Und Führen Mit Szenarien, 1995.
- [95] M. Bender, T. Roussiere, H. Schelling, S. Schuster, E. Schwab, Coupled production of steel and chemicals, *Chemic-Ingenieur-Technik* 90 (2018) 1782–1805, <https://doi.org/10.1002/cite.201800048>.
- [96] P. Cavaliere, Clean Ironmaking and Steelmaking Processes – Efficient Technologies for Greenhouse Emissions Abatement, 2019, Springer Nature Switzerland AG, 2019, <https://doi.org/10.1080/03019233.2019.1703500>.
- [97] T. Ariyama, M. Sato, T. Nouchi, K. Takahashi, Evolution of blast furnace process toward reductant flexibility and carbon dioxide mitigation in steel works, *ISIJ Int.* 56 (2016) 1681–1696, <https://doi.org/10.2355/isijinternational.ISIJINT-2016-210>.
- [98] R.K. Sahu, S.K. Roy, P.K. Sen, Applicability of top gas recycle blast furnace with downstream integration and sequestration in an integrated steel plant, *Steel Res. Int.* 86 (2015) 502–516, <https://doi.org/10.1002/srin.201400196>.
- [99] A. Keys, M. van Hout, B. Daniels, Decarbonisation Options for the Dutch Steel Industry, 2019. <https://www.pbl.nl/en/publications/decarbonisation-options-for-the-dutch-steel-industry>.
- [100] G. Zuo, A. Hirsch, The trial of the top gas recycling blast furnace at LKAB’s EBF and Scale-up, *La Rev. Métallurgie* 106 (2009) 387–392, <https://doi.org/10.1051/metal/2009067>.
- [101] G. Danloy, A. Berthelemot, M. Grant, J. Borlée, D. Sert, J. van der Stel, H. Jak, V. Dimastromatteo, M. Hallin, N. Eklund, N. Edberg, L. Sundqvist, B.E. Sköld, R. Lin, A. Feiterne, R. Korthas, A. Müller, R. Feilmayr, A. Habermann, ULCOS - Pilot testing of the Low-CO₂ Blast Furnace process at the experimental BF in Luleå, *Rev. Metall. Cah. D’Informations Tech.* 106 (2009) 1–8, <https://doi.org/10.1051/metal/2009008>.
- [102] J. Von Scheele, Oxyfuel combustion in the steel industry: energy efficiency and decrease of CO₂ emissions, in: J. Palm (Ed.), *Energy Effic.*, InTech, 2010.
- [103] J. von Scheele, Creating customer value as a solutions provider to leading stainless and Special steel producers, in: 10th Int. Stainl. Spec. Steel Summit, Metalbulletin, Munich, Germany, 2011. <https://www.metalbulletin.com/events/presentations/6505/10th-international-stainless-and-special-steel-summit/a0ID000000X0jyMAJ/20-joachim-von-scheelepdf.html>.
- [104] J. von Scheele, Technologies for energy and operation efficiency in stainless steel production, in: INDINOX Stainl. Steel Conf. 2015, Metalbulletin, Ahmedabad, Gujarat, India, 2015. <https://www.metalbulletin.com/events/presentations/7807/indinox-stainless-steel-conference-2015/a0ID000000X0kE8MAJ/13-joac-him-von-scheele-lindepdf.html>.
- [105] SIDERWIN - Objectives (Project Web Page), (2019). <https://www.siderwin-spire.eu/content/objectives> (accessed July 29, 2020).
- [106] CORDIS, Development of New Methodologies for Industrial CO₂-free Steel Production by Electrowinning, 2020. <https://cordis.europa.eu/project/id/768788>.
- [107] Pilot Plant Building Construction, Newsl. SIDERWIN No. 2, (2019), https://www.siderwin-spire.eu/sites/siderwin.drupal.pulsartecnalia.com/files/document/s/Newsletter_SIDERWIN_2019_02.pdf (accessed July 29, 2020).
- [108] K1-MET, Project SuSteel - Sustainable Steel Production Utilising Hydrogen (Project Web Page), 2016. https://www.k1-met.com/en/research_programme/susteel/.
- [109] A. Sormann, J. Schenk, M. NAseri Seftejani, M.A. Zarl, D. Spreitzer, The Way to a carbon free steelmaking, in: ADMET 2018, Lviv, Ukraine, 2018. <https://www.researchgate.net/publication/328075380>.
- [110] M.N. Seftejani, J. Schenk, D. Spreitzer, M.A. Zarl, Slag formation during reduction of Iron oxide using hydrogen plasma smelting reduction, *Materials* (Basel) 13 (2020) 935, <https://doi.org/10.3390/ma13040935>.
- [111] SAAB-LKAB-Vattenfall, Three HYBRIT Pilot Projects - Towards Fossil Free Iron and Steel, 2018. <http://www.hybritdevelopment.com/articles/three-hybrit-pilot-projects>.
- [112] European commission, strengthening strategic value chains for a future-ready EU industry, Report of the Strategic Forum for Important Projects Fo Common European Interest. Annex II Key Strategic Value Chains – Detailed Recommendations, 2019. <https://ec.europa.eu/docsroom/documents/37824>.
- [113] Forschung für Nachhaltige Entwicklung (FONA), MACOR: Machbarkeitsstudie Zur Reduzierung Der CO₂-Emissionen Im Hüttenwerk (Project Web Page), 2017. <https://www.fona.de/de/massnahmen/foerdermassnahmen/machbarkeitsstudie-zur-reduzierung-co2-emission.php>.
- [114] Into the Future with Hydrogen - Salzgitter AG Is Pioneering low-CO₂ Steel Production, Salzgitter AG Mag., 2018, pp. 10–14. https://www.salzgitter-ag.com/fileadmin/footage/MEDIA/SZAG_microsites/salcos/STIL-02-19-SpecialPrint-Salcos-Hydrogen-en.pdf.
- [115] PEM electrolyser from Siemens for Salzgitter steelmaking hydrogen, *Fuel Cells Bull.* 2019 (2019) 10, [https://doi.org/10.1016/S1464-2859\(19\)30520-6](https://doi.org/10.1016/S1464-2859(19)30520-6).
- [116] H2Future (Project web page), (n.d.). www.h2future-project.eu (accessed July 29, 2020).
- [117] P. Felsbach, H2FUTURE: World’s Largest “green” Hydrogen Pilot Facility Successfully Commences Operation, Press Release - Voestalpine, 2019. <https://www.voestalpine.com/group/static/sites/group/downloads/de/presse/2019-11-11-h2future-worlds-largest-green-hydrogen-pilot-facility-successfully-commences-operation.pdf>.
- [118] M. Leithinger, The Run-up for a High Performance Facility, 2020. <https://www.voestalpine.com/blog/en/innovation-en/the-run-up-for-a-high-performance-facility/>.
- [119] ThyssenKrupp, Our Climate Strategy for Sustainable Steel, 2020. <https://www.thyssenkrupp-steel.com/en/company/sustainability/climate-strategy/>.
- [120] M. Stagge, Hydrogen instead of coal. Thyssenkrupp Steel Launches Pioneering Project for Climate-friendly Steel Production at Its Duisburg Site, 2019 (Accessed July 29, 2020), https://www.thyssenkrupp-steel.com/media/content_1/presse/dokumente/2019_2/april_1/april_en/hydrogen_instead_of_coal_1_english.pdf.
- [121] ThyssenKrupp, Graphic: Hydrogen for the Blast Furnace, 2019. https://www.thyssenkrupp-steel.com/media/content_1/presse/dokumente/2019_2/april_1/april_en/grafikchart_a4_l04_en.pdf.
- [122] M. Stagge, O. Winter, Green Hydrogen for Steel Production: RWE and Thyssenkrupp Plan Partnership, 2020. https://www.thyssenkrupp-steel.com/media/content_1/presse/dokumente/2020_1/juni_2/20200610_pm_thyssenkrupp_stahl_loi_rwe_pre-final_en.pdf.
- [123] Infographics: two. Technological paths, one goal, Thyssenkrupp Steel Mag. (2019) (Accessed July 29, 2020), https://www.thyssenkrupp-steel.com/media/content_1/unternehmen_3/nachhaltigkeit/hydrogen2steel/thyssenkrupp_steele_1_infographics_climate_strategy.pdf.
- [124] i3upgrade project web page, (2018). www.i3upgrade.eu (accessed June 25, 2020).
- [125] P. Wolf-Zöllner, A. Medved, A. Krammer, K. Salbrechter, M. Lehner, Dynamic methanation of by-product gases from integrated steelworks, in: Int. Conf. Polygeneration Strateg., Vienna, 2019. https://www.i3upgrade.eu/files/2020/02/Dynamic-Methanation-of-By-product-Gases-from-Integrated-Steelworks_ICPS2019_Wolf-Zoellner.pdf.
- [126] K1-MET, Projekt i3Upgrade - Intelligent Integrated Industries (Web Page), 2020. <https://www.k1-met.com/forschungsprogramm/i3upgrade/>.
- [127] European Union, Synopsis of RFCS Projects 2015 - 2018, Projects Co-financed by the European Union Research Fund for Coal and Steel, 2018. http://ec.europa.eu/research/industrial_technologies/pdf/rfcs/synopsis_projects_2015-18.pdf.
- [128] FReSMe project web page, (2017). www.fresme.eu (accessed June 25, 2020).
- [129] FReSMe: From residual steel gases to methanol, Aportando Valor al CO₂ (2019). http://www.fresme.eu/events/pdf/FReSMe%20Aportando%20Valor%20al%20CO2_vdef.pdf.
- [130] CORDIS, From Residual Steel Gasses to Methanol, 2019. <https://cordis.europa.eu/project/id/727504/es>.
- [131] D.C. Pardo, FReSMe: CCUS Para La Descarbonización Del Sector Del Acero (TRL 6), Aportando Valor Al CO₂, 2019, pp. 50–52 (Accessed July 30, 2020), http://www.fresme.eu/events/pdf/Libro_Ponentes_III_Aportando_Vvalor.pdf.
- [132] ThyssenKrupp, Carbon2Chem (Project web page), (2020). <https://www.thyssenkrupp.com/en/newsroom/content-page-162.html> (accessed July 31, 2020).
- [133] T. Wich, W. Lüke, K. Büker, O. von Morstein, R. Kleinschmidt, M. Oles, R. Achatz, Carbon2Chem® – technical center in Duisburg, *Chemic-Ingenieur-Technik*. 90 (2018) 1369–1374, <https://doi.org/10.1002/cite.201800067>.

- [134] Fraunhofer UMSICHT, Carbon2Chem® joint project, (2020). <https://www.umsicht.fraunhofer.de/en/strategic-lines-of-research/carbon-cycle.html> (accessed July 31, 2020).
- [135] Special issue: Carbon2Chem®, Chemie Ing. Tech. 90 (2018) 1349–1599. <https://onlinelibrary.wiley.com/toc/15222640/2018/90/10>.
- [136] INEA, eForFuel, (2020). https://ec.europa.eu/inea/en/horizon-2020/projects/h2_020-energy/biomass-biofuels-alternative-fuels/eфорfuel (accessed August 3, 2020).
- [137] eForFuel (Project web page), (2020). <https://www.eforfuel.eu/> (accessed August 3, 2020).
- [138] CORDIS, Fuels From Electricity: De Novo Metabolic Conversion of Electrochemically Produced Formate Into Hydrocarbons, 2019. <https://cordis.europa.eu/project/id/763911/es>.
- [139] European Commission, In-Depth Analysis in Support of the Commission Communication COM(2018), 773, 2018. https://ec.europa.eu/clima/sites/clima/files/docs/pages/com_2018_733_analysis_in_support_en_0.pdf.
- [140] Salzgitter A.G., SALCOS Project, (2020). <https://salcos.salzgitter-ag.com/en/>.
- [141] DISIPO, Decarbonisation of Carbon-intensive Industries (Iron and Steel Industries) Through Power to Gas and Oxy-fuel Combustion, 2020. <https://cordis.europa.eu/project/id/887077>.
- [142] M. Barati, Application of slag engineering fundamentals to continuous steelmaking. Treatise Process Metall, Elsevier, 2014, pp. 305–357, <https://doi.org/10.1016/B978-0-08-096984-8.00015-X>.